Journal of Medicinal Chemistry

Article

Cite This: J. Med. Chem. XXXX, XXX, XXX−XXX

pubs.acs.org/jmc

Discovery of (*S*)-3-(3-(3,5-Dimethyl-1*H*-pyrazol-1-yl)phenyl)-4-((*R*)-3-(2-(5,6,7,8-tetrahydro-1,8-naphthyridin-2-yl)ethyl)pyrrolidin-1-yl)butanoic Acid, a Nonpeptidic $\alpha_v\beta_6$ Integrin Inhibitor for the Inhaled Treatment of Idiopathic Pulmonary Fibrosis

Panayiotis A. Procopiou,[†] Niall A. Anderson,[†] John Barrett,[‡] Tim N. Barrett,[†] Matthew H. J. Crawford,[†] Brendan J. Fallon,[†] Ashley P. Hancock,[†] Joelle Le,[§] Seble Lemma,[†] Richard P. Marshall,[#] Josie Morrell,[‡] John M. Pritchard,[†] James E. Rowedder,[∥] Paula Saklatvala,[⊥] Robert J. Slack,[#] Steven L. Sollis,[†] Colin J. Suckling,[▽] Lee R. Thorp,[†] Giovanni Vitulli,[‡] and Simon J. F. Macdonald*[,†]

[†]Medicinal Chemistry, Fibrosis and Lung Injury DPU, Respiratory Therapeutic Area, [‡]Drug Metabolism & Pharmacokinetics, Fibrosis and Lung Injury DPU, Respiratory Therapeutic Area, [§]Drug Design and Selection—Molecular Design, Platform Technology & Science, [∥]Biological Sciences, Platform Technology & Science, [⊥]Pharmacy, Platform Technology & Science, and [#]Translational Biology, Fibrosis and Lung Injury DPU, Respiratory Therapeutic Area, GlaxoSmithKline Medicines Research Centre, Gunnels Wood Road, Stevenage, SG1 2NY, United Kingdom

[▽]Department of Pure & Applied Chemistry, University of Strathclyde, 295 Cathedral Street, Glasgow G1 1XL, Scotland, U.K.

Supporting Information

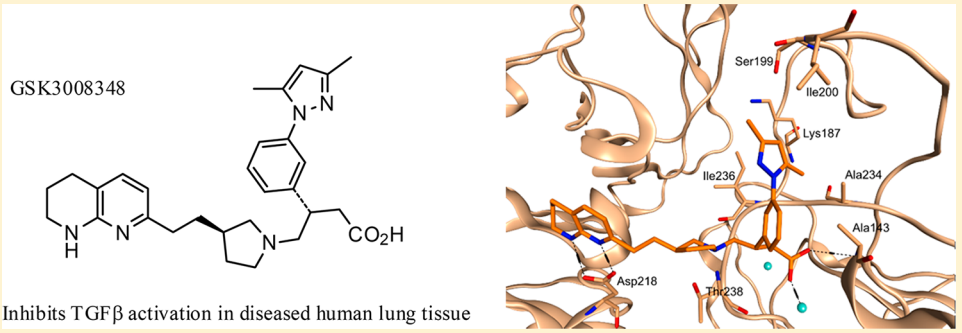

ABSTRACT: A series of 3-aryl(pyrrolidin-1-yl)butanoic acids were synthesized using a diastereoselective route, via a rhodium catalyzed asymmetric 1,4-addition of arylboronic acids in the presence of (*R*)-BINAP to a crotonate ester to provide the (*S*) absolute configuration for the major product. A variety of aryl substituents including morpholine, pyrazole, triazole, imidazole, and cyclic ether were screened in cell adhesion assays for affinity against $\alpha_v\beta_1$, $\alpha_v\beta_3$, $\alpha_v\beta_5$, $\alpha_v\beta_6$, and $\alpha_v\beta_8$ integrins. Numerous analogs with high affinity and selectivity for the $\alpha_v\beta_6$ integrin were identified. The analog (*S*)-3-(3-(3,5-dimethyl-1*H*-pyrazol-1-yl)phenyl)-4-((*R*)-3-(2-(5,6,7,8-tetrahydro-1,8-naphthyridin-2-yl)ethyl)pyrrolidin-1-yl)butanoic acid hydrochloride salt was found to have very high affinity for $\alpha_v\beta_6$ integrin in a radioligand binding assay (pK_i = 11), a long dissociation half-life (7 h), very high solubility in saline at pH 7 (>71 mg/mL), and pharmacokinetic properties commensurate with inhaled dosing by nebulization. It was selected for further clinical investigation as a potential therapeutic agent for the treatment of idiopathic pulmonary fibrosis.

INTRODUCTION

Idiopathic pulmonary fibrosis (IPF) is a chronic lung disease of unknown etiology, which is characterized by progressive loss of lung function due to deposition of collagen within the lungs resulting from an aberrant wound healing response. The symptoms of IPF include cough and dyspnoea, and diagnosis is achieved either by high-resolution computed tomography or histology.[1] The incidence of IPF in North America and Europe is estimated to be up to 18 cases per 100 000 people per year; incidence might be lower in South America and Asia.[2] The prevalence of the disease increases with age (median age at diagnosis is 65 years) and is more common in men. It is rare in people younger than 50 years old. Average life expectancy from the time of diagnosis is less than 3 years, reflecting the lack of any effective treatment and that early diagnosis is not straightforward.[3,4] It is currently poorly treated, and we describe here the discovery of a small molecule $\alpha_v\beta_6$ inhibitor (GSK3008348) which is undergoing clinical evaluation for treating this disease. To the best of our knowledge this is the

Received: June 15, 2018

DOI: 10.1021/acs.jmedchem.8b00959
J. Med. Chem. XXXX, XXX, XXX−XXX

first highly selective, highly potent small molecule $\alpha_v\beta_6$ inhibitor to be described. Current therapies for IPF emerged from the repositioning of clinical assets originally designed for treating other conditions. In contrast, the work described here is one of very few approaches designed from the outset to treat IPF based on robust in-house studies from target validation to pharmacokinetic and pharmacodynamic effects in human IPF tissue.

While international guidelines recommend consideration of lung transplantation for certain patient populations,[5] pirfenidone **1** and nintedanib **2**, a multiple tyrosine-kinase inhibitor, have been reported to slow disease progression and have thus recently been approved for use in patients with IPF (Figure 1).[6] Both compounds are administered orally with pirfenidone

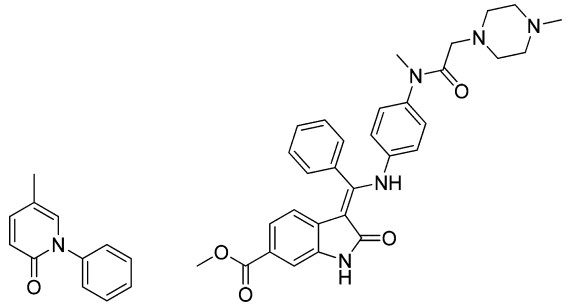

Figure 1. Structures of pirfenidone and nintedanib.

dosed at 801 mg three times a day and nintedanib 150 mg twice a day. Side effects with pirfenidone include gastrointestinal issues and phototoxicity inter alia and requires dose titration, whereas nintedanib may require dose reduction to 100 mg due to adverse events.[7] Effective novel therapies for the treatment of IPF are therefore still needed.[8]

Integrins are a family of transmembrane, heterodimeric cell adhesion receptors that connect cell-surface ligands to the extracellular matrix and play a pivotal role in signaling between the extracellular and intracellular environments.[9] In vertebrates, there are 24 known integrins each comprising one of 18 α subunits and one of eight β subunits, which are noncovalently associated. Integrin-based therapeutic agents have recently been reviewed.[10−12] The integrin superfamily can be divided into several subfamilies, including the collagen, laminin, leukocyte-specific families, and of specific interest here, the arginyl−glycinyl−aspartic acid (RGD) receptor family. In this family, eight integrins recognize the tripeptide RGD sequence in extracellular matrix proteins and include the α_v subset of integrin receptors $\alpha_v\beta_1$, $\alpha_v\beta_3$, $\alpha_v\beta_5$, $\alpha_v\beta_6$, and $\alpha_v\beta_8$.

So far, no therapeutic agent that targets the α_v RGD integrin subfamily has received regulatory approval, although several compounds have been widely explored clinically. Modulation of the integrin $\alpha_v\beta_3$ has perhaps been most examined for over 30 years primarily for cancer but also other diseases such as inflammation, multiple sclerosis, osteoporosis, and organ fibrosis, although clinical success has been limited.[13]

Some of the α_v inhibitors that have progressed furthest clinically include a peptide and nonpeptidic small molecules. The cyclic peptide cilengitide **3** (Figure 2) is a potent inhibitor of both the $\alpha_v\beta_3$ and $\alpha_v\beta_5$ integrins and has been extensively studied in numerous clinical trials for the treatment of cancer.[14]

A nonpeptidic nonselective pan α_v integrin inhibitor **4** (GLPG0187, Figure 2) has also been investigated in the clinic for the treatment of bone metastasis in breast and prostate cancer.[15,16]

Another potent, nonpeptidic, small-molecule dual $\alpha_v\beta_3$ and $\alpha_v\beta_5$ integrin inhibitor, and also progressed to clinical trials for

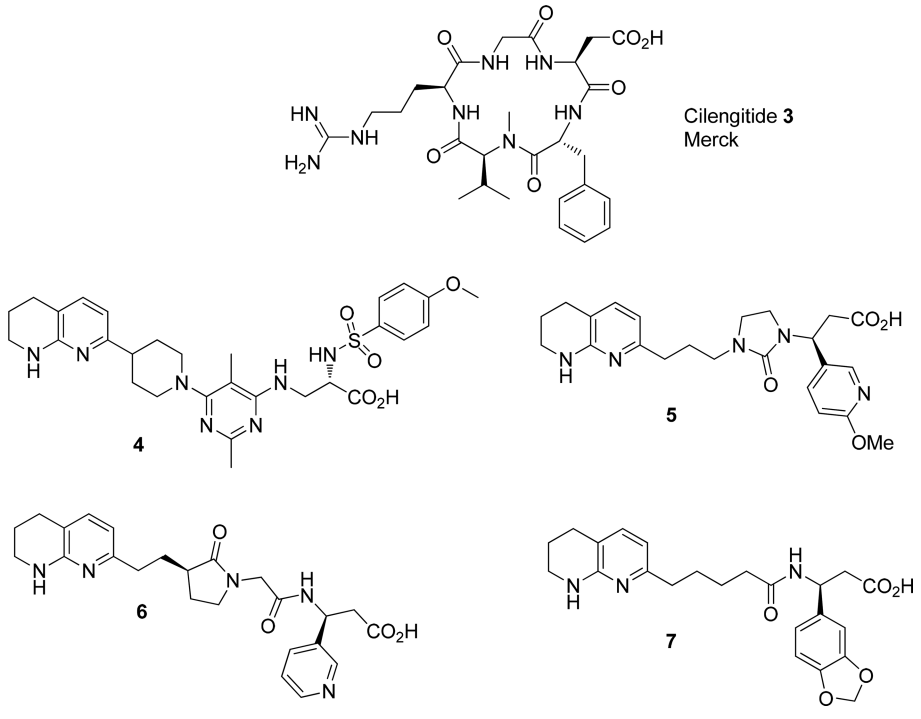

Figure 2. Structures for cilengitide **3**, Galapagos' pan α_v candidate (GLPG0187) **4**, and various Merck's $\alpha_v\beta_3/\alpha_v\beta_5$ integrin antagonists **5**−**7**.

DOI: 10.1021/acs.jmedchem.8b00959
J. Med. Chem. XXXX, XXX, XXX−XXX

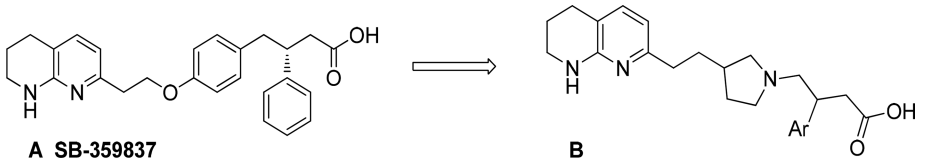

Figure 3. Changes in the overall template as a result of lead optimization from an exemplar hit identified in cross screening (A) to the template in clinical candidate (B).

Scheme 1[a]

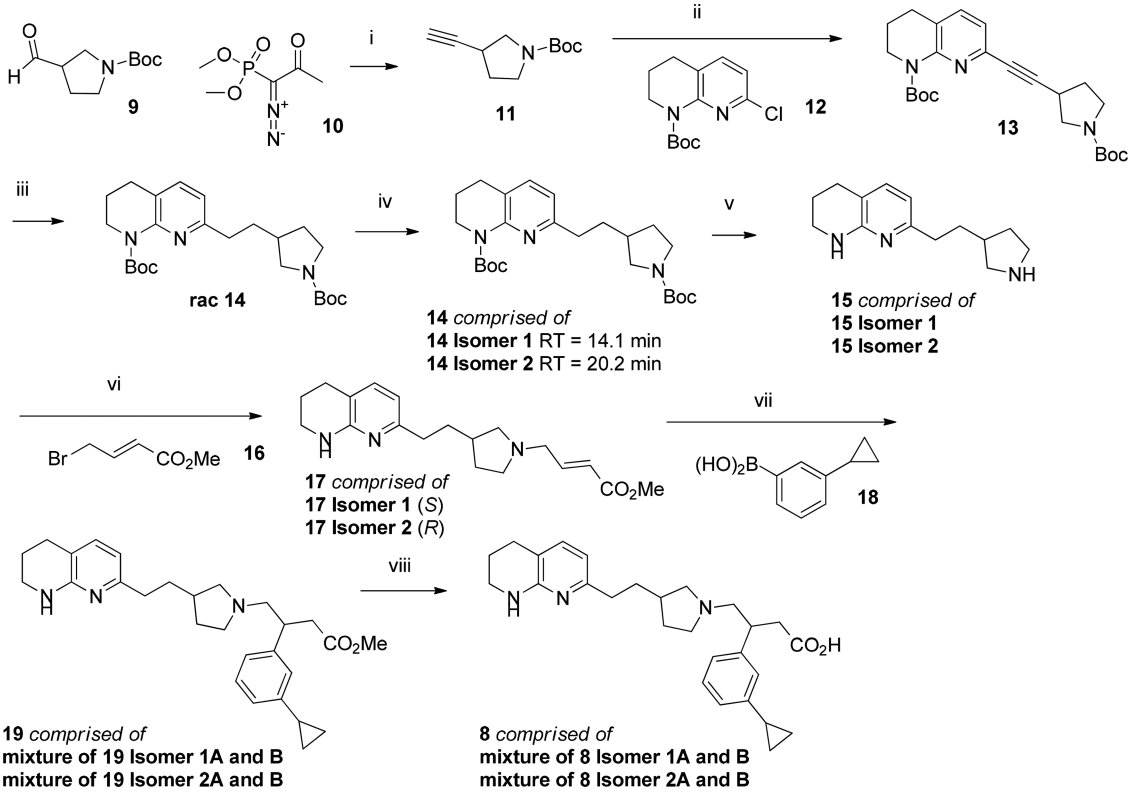

[a]Reagents and conditions (see Experimental Section for full chemical names): (i) K_2CO_3, MeOH, 20°C, 89%; (ii) K_2CO_3, XPhos, $Pd_2(dba)_3$, DMA, 100°C, 45%; (iii) H_2, Pd/C, EtOH, 85%; (iv) Chiralpak OJ, column 250 mm id × 4.6 mm, heptane−IPA, 98:2, flow rate = 1 mL/min, 47% for Isomer 1, 45% for Isomer 2; (v) 4 M HCl in 1,4-dioxane, DCM, 71%; (vi) DIPEA, **16**, DCM, 38% for Isomer 1; (vii) **17**, $[Rh(COD)Cl]_2$, aq KOH, 1,4-dioxane, 95°C, 26% from **17 Isomer 1**; (viii) 4 M HCl in 1,4-dioxane, DCM, water.

the treatment of osteoporosis and prostate cancer, is the imidazolidinone **5**.[17] This compound (derived from the Arg-Gly-Asp tripeptide) was discovered by the Merck group in a series of elegant lead optimization studies. The guanidine group of the arginine was replaced with the tetrahydronaphthyridine group, while the γ-lactam scaffold was used as a conformational constraint for glycine leading to analogs such as **6**.[18] This was followed by removal of one of the two remaining peptide bonds and shortening the chain length to provide **7**, which possessed improved binding affinity and oral bioavailability.[19] The last peptide bond was then replaced by the cyclic urea isostere, and optimization of the aryl group substitution provided the clinical candidate **5**.

Several seminal publications in the past decade have described the role of the $\alpha_v\beta_6$ integrin in the activation of transforming growth factor $\beta1$ (TGF$\beta1$).[20−22] The $\alpha_v\beta_6$ integrin is induced on damaged epithelium where it binds the latency-associated protein (LAP) of TGF$\beta1$ resulting in the release of the active form of the growth factor. Active TGF$\beta1$ induces myofibroblast differentiation, proliferation, and collagen synthesis.[15] In mouse models of fibrosis,[20] overexpression of TGF$\beta1$ causes progressive fibrosis which can be reduced by inhibition of $\alpha_v\beta_6$. Consequently, several ways of inhibiting TGF$\beta1$ signaling or blockading its activation have been examined including development of a specific $\alpha_v\beta_6$ humanized monoclonal antibody BG00011, also known as STX-100 by Sheppard et al. which is currently undergoing clinical trials for the treatment of IPF.[23]

On the basis of these and our own target validation studies, we became interested in identifying novel, selective, and high affinity small-molecule $\alpha_v\beta_6$ integrin inhibitors for the treatment of IPF. Given IPF is a respiratory disease and our in-house expertise in developing inhaled medicines, we chose an inhaled nebulized route of administration. This requires high aqueous solubility, and we envisaged this could be one beneficial consequence of optimizing mimetics of the polar RGD peptide sequence.

To identify leads, we cross-screened RGD mimetics from a historic $\alpha_v\beta_3$ integrin program that had previously been run at GSK[24] for $\alpha_v\beta_6$ activity and, based on these (Figure 3),

DOI: 10.1021/acs.jmedchem.8b00959
J. Med. Chem. XXXX, XXX, XXX−XXX

initiated lead optimization. A more detailed description of this early work which led to the template B will be described elsewhere as we focus here on the late lead optimization. However, some key structure−activity relationships (SARs) for $\alpha_v\beta_6$ potency and selectivity in identifying template B are summarized here.

- The tetrahydronaphthyridine of **A** (Figure 3) remained optimal for $\alpha_v\beta_6$ potency and selectivity despite extensive exploration of substituted tetrahydronaphthyridines and alternative guanidine mimetics, most of which lose activity.
- Modifications to the carboxylic acid (which binds to a metal ion in the metal ion dependent adhesion site (MIDAS)) are not tolerated.
- The spatial distance between the tetrahydronaphthyridine and the acid is important for potency and selectivity, with a slightly shorter distance being preferred for $\alpha_v\beta_6$ compared to $\alpha_v\beta_3$ (see later).
- Significant studies around the linker (the replacement for the central aromatic ring in **A** for the pyrrolidine in **B** (Figure 3)) were carried out. Both the position and the physicochemical properties of the heterocycle are important.
- Finally the aryl group in B (Figure 3) and its substituent are major contributors. The *meta* position is especially preferred for $\alpha_v\beta_6$,[25] and some of the studies that led to the inhaled clinical candidate are described here.

Alongside these studies, a summary of the profile of the clinical candidate GSK3008348 is described including its pharmacokinetic, pharmacological, and physicochemical properties. The safety, tolerability, and pharmacokinetics of GSK3008348 in healthy subjects have also recently been described.[26]

CHEMISTRY

The first synthetic route used for the preparation of **8** (see Scheme 1) was nonstereoselective providing mixtures of isomers which were separated by HPLC on a chiral stationary phase (Scheme 1). Reaction of the commercially available racemic *tert*-butyl carbamate protected pyrrolidine-3-carbaldehyde **9** with the Bestmann−Ohira reagent[27] **10** provided acetylene **11** in 89% yield. This was coupled with the tetrahydronaphthyridine chloride **12**[28] by a Sonogashira reaction to provide the disubstituted acetylene **13** (45% yield) which was then hydrogenated over 10% palladium on carbon to give **14** (85% yield). Pyrrolidine **14** was resolved by HPLC on a chiral support to provide the two enantiomers whose absolute configuration were unknown at this stage and were therefore labeled as **14 Isomer 1** (retention time = 14.1 min) and **14 Isomer 2** (retention time = 20.2 min). Each enantiomer was individually treated with 4 M hydrogen chloride in dioxane to remove the *tert*-butyl carbamate protecting groups to give **15** (71% for Isomer 1 and 74% yield for Isomer 2) which were then selectively alkylated with commercially available (*E*)-methyl 4-bromocrotonate (**16**) to provide the *α*, *β*-unsaturated esters **17 Isomer 1** and **17 Isomer 2** (38% yield for each isomer) (Scheme 1). In the absence of any chiral ligand, rhodium catalyzed 1,4-addition of 3-cyclopropylphenylboronic acid **18**[29] to each enantiomer of **17** gave 1:1 mixtures of diastereomers at the benzylic asymmetric center, namely, **19 Isomer 1A** and **19 Isomer 1B** and similarly **19 Isomer 2A** and **19 Isomer 2B**. Hydrolysis of these provided the two diastereomeric acids **8 Isomer 1A** and **8 Isomer 1B** and similarly **8 Isomer 2A** and **8 Isomer 2B**. The mixture of acids **8** that was derived from **14 Isomer 1** was subsequently found to be the more active acid when it was screened in the $\alpha_v\beta_6$ cell adhesion assay.

While the route in Scheme 1 delivered the target compounds, a route that provided predominantly the most preferred isomer would obviously be more efficient. To achieve this, the identity of the absolute configuration of the pyrrolidine asymmetric center of **8** was required. Consequently, both enantiomers of **20** were prepared using our published procedure for the synthesis of the (*R*) enantiomer.[30] Each enantiomer was hydrogenated over 10% palladium on carbon to give **21**. The *tert*-butyl carbamate group cleaved with hydrogen chloride in dioxane to provide **15** and finally each enantiomer alkylated with (*E*)-methyl 4-bromocrotonate **16** to yield (*R*)-**17** and (*S*)-**17** (Scheme 2). Comparison of the

Scheme 2[a]

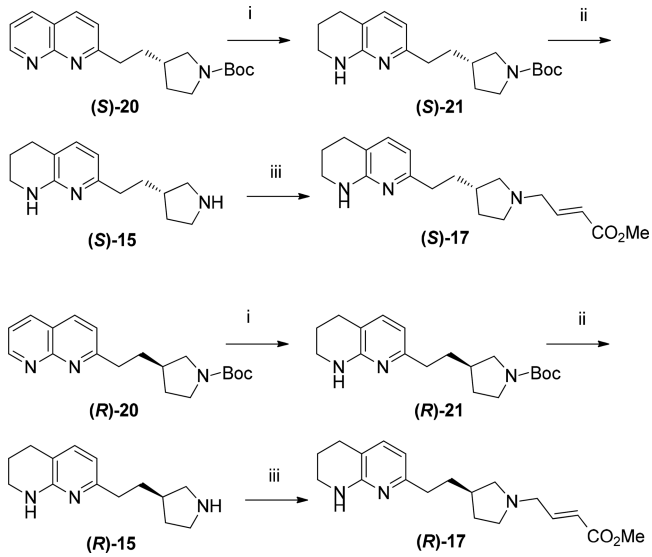

[a]Reagents and conditions: (i) H_2, 10% Pd/C, EtOH, 62% for (*S*)-**21**; (ii) 4 M HCl in 1,4-dioxane, DCM, 93% for (*S*)-**15** and 94% for (*R*)-**15**; (iii) (*E*)-methyl 4-bromocrotonate **16**, DIPEA, DCM, 30% for (*S*)-**17**.

HPLC retention times (RT) of **17 Isomer 1** (RT = 21.2 min), **17 Isomer 2** (RT = 29.4 min) on a Chiralpak AD-H column eluting with 15% ethanol−heptane containing 0.2% isopropylamine with authentic (*S*)-**17** (RT = 22 min) identified the first peak to elute off the column **17 Isomer 1** as the (*S*)-enantiomer. Since **17 Isomer 2** was the enantiomer that provided the more potent diastereoisomer of **8**, it was therefore concluded its configuration at the pyrrolidine asymmetric center is (*R*).

The diastereomers **19** derived from the (*R*) pyrrolidine (**Isomer 2**) were then separated by HPLC on Chiralcel OJ (analytical chiral HPLC RT = 9.0 and 16.3 min), and the diastereomeric esters were hydrolyzed to give two diastereomeric acids **8 Isomer 2A** and **8 Isomer 2B**. The diastereomer of **8**, derived from **19 Isomer 2** (RT = 16.3 min), provided the most active isomer of **8 Isomer 2B**. Having traced the most active isomer of **8** as **Isomer 2B**, a stereoselective asymmetric synthesis was then sought.[31] This involved a Hayashi asymmetric 1,4-addition of boronic acid **18** to (*R*)-**17** utilizing

DOI: 10.1021/acs.jmedchem.8b00959
J. Med. Chem. XXXX, XXX, XXX−XXX

Scheme 3[a]

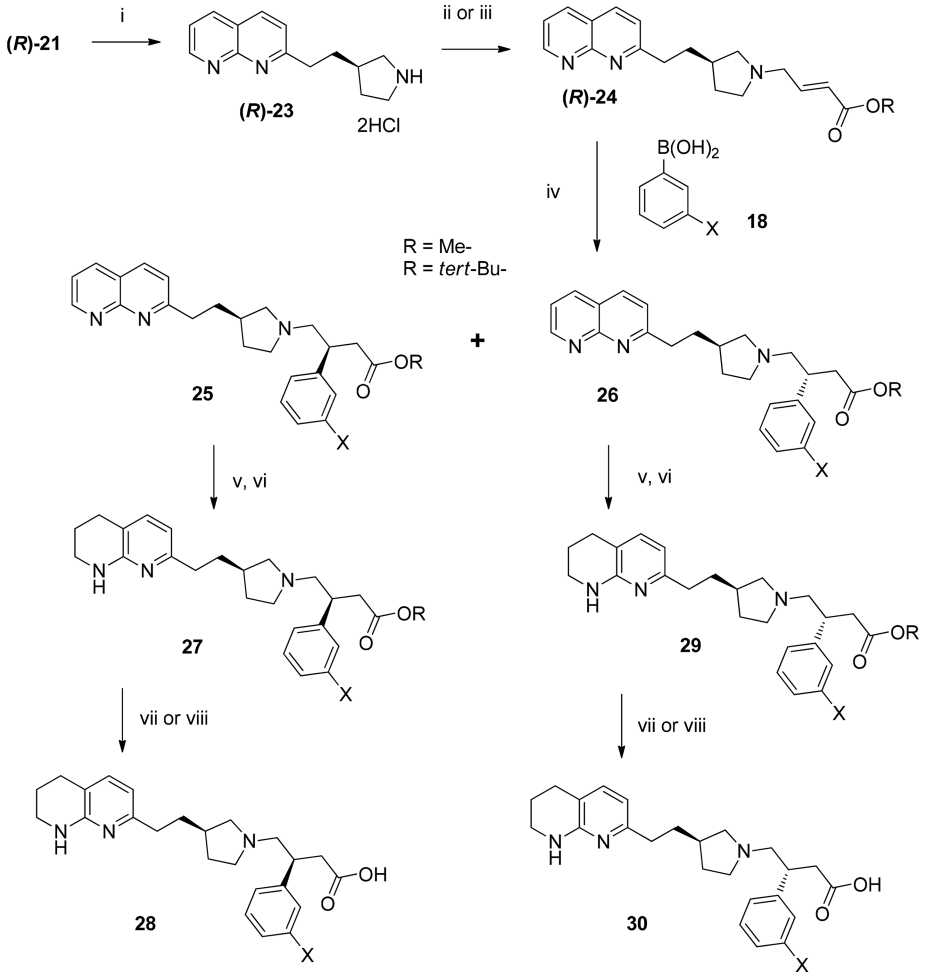

[a]Reagents and conditions: (i) 4 M HCl in dioxane, 93%; (ii) (*E*)-methyl 4-bromocrotonate **16**, base, DCM, 20°C or (iii) methyl or *tert*-butyl 4-acetoxycrotonate, iso-Pr_2NEt, 1,1′-bis(diphenylphosphino)ferrocene]dichloropalladium(II) [$Pd(dppf)Cl_2$], DCM, 20°C, 85%; (iv) aq KOH, $[Rh(COD)Cl]_2$, (*R*)-BINAP, 1,4-dioxane, 90 °C, 1 h, varying yields; see Experimental Section; (v−viii) for reagents, see experimental details.

Scheme 4[a]

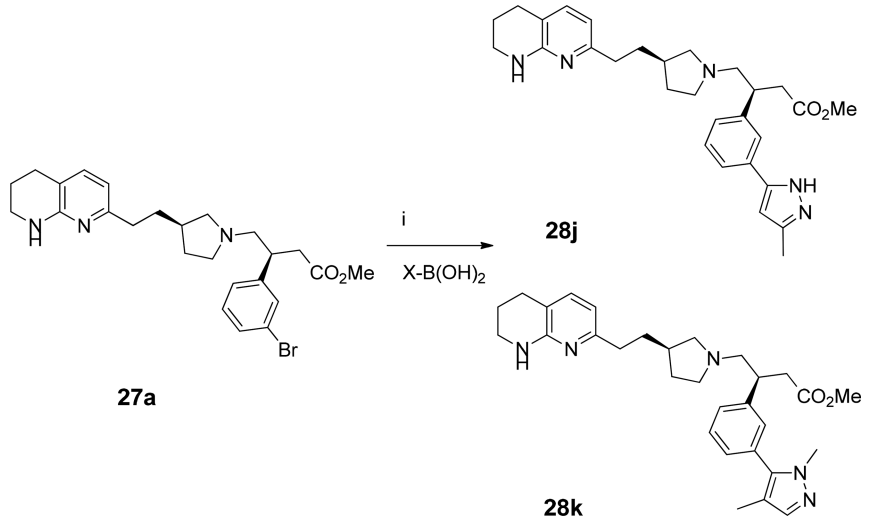

[a]Reagents and conditions: (i) [X-$B(OH)_2$] from 3-methyl-5-(4,4,5,5-tetramethyl-1,3,2-dioxaborolan-2-yl)-1*H*-pyrazole or 1,4-dimethyl-5-(4,4,5,5-tetramethyl-1,3,2-dioxaborolan-2-yl)-1*H*-pyrazole, K_3PO_4, chloro(dinorbonylphosphino)(2′-dimethylamino-1,1′-biphenyl-2-yl)palladium(II), aq EtOH, 130 °C, 30 min, microwave irradiation, 32% for **28j**, 13% for **28k**.

DOI: 10.1021/acs.jmedchem.8b00959
J. Med. Chem. XXXX, XXX, XXX−XXX

Table 1. Cell Adhesion Assay at $\alpha_v\beta_6$, $\alpha_v\beta_1$, $\alpha_v\beta_3$, $\alpha_v\beta_5$, and $\alpha_v\beta_8$ Integrins, Radioligand Binding at $\alpha_v\beta_6$, hERG Inhibition in Barracuda and Q Patch Assays, and Lipophilicity (chromLogD) Values[a]

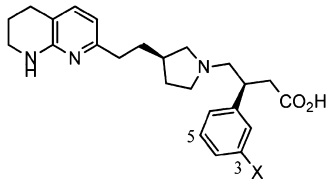

Cmpd	X	$\alpha_v\beta_6$ pIC_{50}	$\alpha_v\beta_1$ pIC_{50}	$\alpha_v\beta_3$ pIC_{50}	$\alpha_v\beta_5$ pIC_{50}	$\alpha_v\beta_8$ pIC_{50}	pK_i[b] (n)	hERG Barracuda	hERG QPatch	Chrom $logD_{7.4}$
28a	Br	8.4	6.7	7.3	8.5	8.5	-	5.9	-	3.15
28b		8.4	6.8	6.8	8.1	8.2	10.1	5.3	5.7	3.34
30b[c,d]		7.3	5.4	5.4	6.6	6.9	-	-	-	3.21
28c	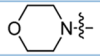	8.4	6.6	6.2	7.3	7.8	10.2	<4.2	<4.5	2.27
30c[c]	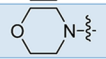	5.2	6.1	5.0	5.0	5.0	-	-	-	1.99
28d	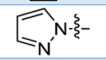	8.6	6.9*[e]	6.8	7.7	8.0	10.0	<4.3	6.1	2.40
28e	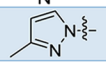	8.4	6.8*	6.7	7.6	7.5	10.1	4.4	5.0	2.79
28f	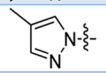	7.4	5.7*	5.7	6.7	7.4	-	5.0	-	3.01
28g	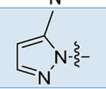	8.8	7.3	6.3	6.8	8.0	10.2	<4.2	4.6	2.55
28h	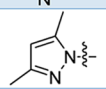	8.4	7.3	6.0	6.9	7.8	10.4	4.5	4.9	2.82
30h[c]	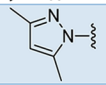	6.8	-	5.2	5.6	6.4	-	-	-	2.88
28j	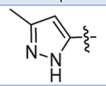	8.6	7.2*	7.3	8.2	8.4	-	<4.3	4.6	2.53
28k	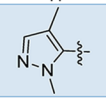	8.1	7.4*	6.0	7.4	8.1	-	4.5	4.9	2.72
28l	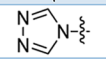	8.8	7.2	6.3	7.7	8.2	-	<4.3	<4.5	1.05
28m	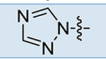	8.8	7.0	6.7	7.7	8.2	-	<4.3	<4.5	1.95
28n	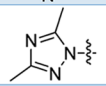	8.4	7.3	6.0	7.1	8.0	10.2	<4.3	<4.5	1.66
28o	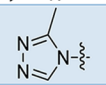	8.4	7.0	6.6	7.8	8.0	10.3	<4.3	<4.5	1.77
28p	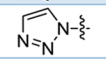	8.5	7.2	6.6	7.5	8.3	10.4	<4.3	<4.5	1.75
28q[f]	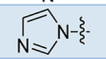	8.2	-	5.9	7.3	7.6	-	<4.3	<4.5	1.97
28r	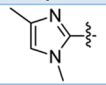	8.7	7.0*	6.1	7.2	8.1	-	<4.3	<4.5	2.09
28s	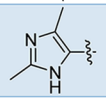	8.6	7.0	6.5	7.0	8.0	10.4	<4.3	<4.5	1.77
28t	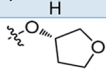	8.8	7.3	6.8	7.7	8.2	10.4	4.5	4.8	2.51

DOI: 10.1021/acs.jmedchem.8b00959
J. Med. Chem. XXXX, XXX, XXX−XXX

Table 1. continued

Cmpd	X	$\alpha_v\beta_6$ pIC_{50}	$\alpha_v\beta_1$ pIC_{50}	$\alpha_v\beta_3$ pIC_{50}	$\alpha_v\beta_5$ pIC_{50}	$\alpha_v\beta_8$ pIC_{50}	pK_i^b (n)	hERG Barracuda	hERG QPatch	Chrom $logD_{7.4}$
28u	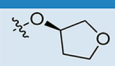	8.6	6.9	6.6	7.6	8.0	10.2	4.4	4.5	2.32
28v	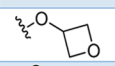	9.0	7.0	6.8	8.3	8.6	-	<4.3	<4.5	2.07
28w	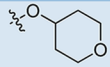	8.6	7.0	6.8	7.9	8.2	-	<4.3	5.1	2.75
28xI1	 Isomer 1	8.7	7.2	6.7	7.4	8.1	-	4.4	4.9	2.56
28xI2	 Isomer 2	8.7	7.2	6.6	7.3	8.0	10.7	4.4	4.5	2.58
28y		7.9	-	6.4	-	-	-	-	-	2.62
28bc	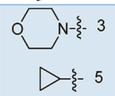	8.4	7.2*	5.7	6.7	7.8	10.1	<4.2	-	3.07
28ch	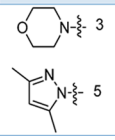	8.1	7.0*	5.5	5.7	8.0	10.5	<4.2	<4.5	2.73

[a]Standard deviations and n numbers are detailed in the Supporting Information. Dashes indicate compounds were not tested in the assay. [b]Measured at an $\alpha_v\beta_6$ integrin protein concentration of 0.3 nM. [c]Stereochemistry *R* at the benzylic center. [d]This is the same compound as compound **8 Isomer 2 Isomer A**. [e]Asterisks (∗) indicate these values are $n = 1$. [f]This is a 63:37 mixture of diastereomers.

Scheme 5[a]

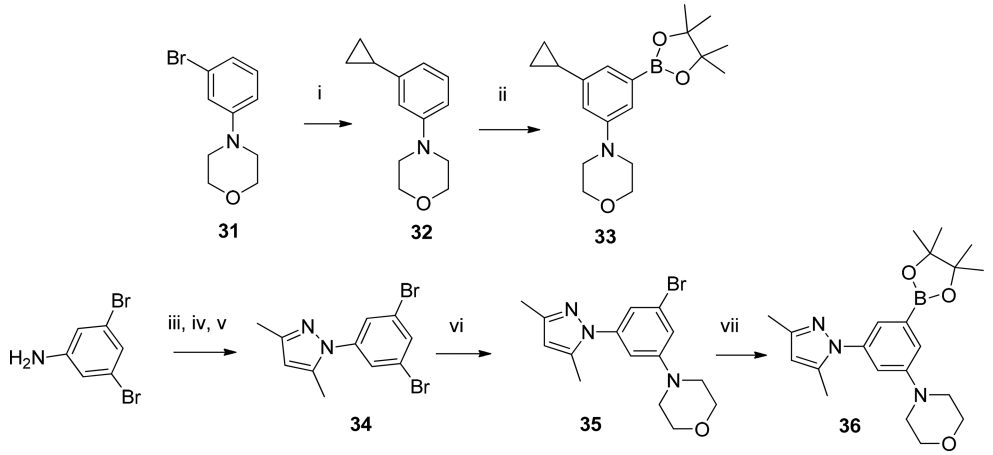

[a]Reagents and conditions (see Experimental Section for full chemical names): (i) cyclopropylmagnesium bromide, $PdCl_2(dppf)-CH_2Cl_2$ adduct, THF, 60°C, 3 h, 88%; (ii) bis(pinacolato)diboron, $[Ir(COD)OMe]_2$, 4,4′-di-*tert*-butyl-2,2′-bipyridine, TBME, 80 °C, 1 h, 52%; (iii) H_2SO_4, $NaNO_2$, H_2O, MeCN, 0°C; (iv) L-ascorbic acid; (v) pentane-2,4-dione 62% (for three steps); (vi) morpholine, BINAP, NaO^tBu, $Pd_2(dba)_3$, PhMe, 80°C, 2 h, 33%; (vii) bis(pinacolato)diboron, KOAc, XPhos, $Pd_2(dba)_3$ 1,4-dioxane, 110°C, 1 h, 36%.

chloro(1,5-cyclooctadiene)rhodium(I) dimer {$[Rh(COD)Cl]_2$} as a catalyst, with (*R*)-BINAP ((*R*)-(+)-2,2′-bis-(diphenylphosphino)-1,1′-binaphthyl) as the chiral ligand. These conditions provided a 77:23 diastereomeric mixture of esters **18**, the major isomer of which provided the required more active isomer of **8 Isomer 2B**.

Analogs of **8** possessing a variety of cyclic aryl substituents such as morpholine, pyrazoles, triazoles, imidazoles, and cyclic ethers were made in the pyrrolidine (*R*)-series starting from either (*R*)-**17** or the route shown in Scheme 3. The latter route is essentially the same route as before, apart from the stage at which the naphthyridine ring is selectively hydrogenated. This sequence involves deprotection of (*R*)-**21**, followed by alkylation to give the *α,β*-unsaturated ester (*R*)-**24** prepared as recently reported (Scheme 3).[30] Both methyl and *tert*-butyl esters were used and the alkylation was achieved using the appropriate 4-bromocrotonate ester, which gave low yields due to bis-alkylation. The alkylation can be carried out in higher

DOI: 10.1021/acs.jmedchem.8b00959
J. Med. Chem. XXXX, XXX, XXX−XXX

yields by using (*E*)-4-acetoxycrotonate ester instead of the corresponding bromide following the Tsuji–Trost procedure[32] and Pd(dppf)Cl_2 (1,1′-bis(diphenylphosphino)ferrocene]-dichloropalladium(II)) catalysis, as already reported.[30] The α, β-unsaturated ester (*R*)-**24** was then reacted with a series of arylboronic acids **18** using [Rh(COD)Cl]$_2$ catalysis and in the presence of (*R*)-BINAP to provide a mixture of diastereomers, with the diastereomeric ratio for the preferred isomer usually being at least 70:30. The isomers were separated by HPLC on a chiral support to give **25** and **26**, the absolute configuration of which was established by alternative asymmetric synthesis.[30] The naphthyridine ring of **25** was hydrogenated over 10% palladium on charcoal to provide **27** and finally converted to the required carboxylic acids **28** for screening. The minor isomer **26** was similarly hydrogenated to **29** and then deprotected to give acid **30**.

For two analogs of **28** where the X group is C-linked, a different synthetic route was used (Scheme 4). In this case (*R*)-**17** was treated with commercially available (3-bromophenyl)boronic acid, in the presence of [Rh(COD)Cl]$_2$, (*R*)-BINAP, and aqueous KOH solution to provide the bromophenyl ester **27a**. Suzuki couplings of **27a** were carried out with the appropriate boronic acids [X-B(OH)$_2$] which were generated in situ from the pinacol boronic acid esters 3-methyl-5-(4,4,5,5-tetramethyl-1,3,2-dioxaborolan-2-yl)-1*H*-pyrazole and 1,4-dimethyl-5-(4,4,5,5-tetramethyl-1,3,2-dioxaborolan-2-yl)-1*H*-pyrazole catalyzed by chloro(dinorbonylphosphino)(2′-dimethylamino-1,1′-biphenyl-2-yl)palladium(II).,[33] These basic conditions simultaneously hydrolyze the methyl esters to give **28j** and **28k**.

The various arylboronic acids **18** used for the preparation of acids **28a-ch** (shown in Table 1) either were commercially available or were prepared according to published procedures. In general, they were prepared from aryl bromides via lithiation, reaction with tri(isopropyl) borate, and hydrolysis, as already described for **18b**[29] and **18h**.[30] Alternatively, aryl bromides were converted to pinacol esters of the boronic acids using palladium catalysis and bis(pinacolato)diboron (see Supporting Information). The more complex 3,5-disubstituted arylboronic acids **33** and **36** were prepared as follows (Scheme 5). Coupling of the commercially available 4-(3-bromophenyl)morpholine **31** with cyclopropylmagnesium bromide using palladium catalysis gave **32** in 88% yield. This was converted into the boronic ester via an iridium catalyzed C–H insertion reaction using bis(pinacolato)diboron in the presence of 4,4′-di-*tert*-butyl-2,2′-bipyridine in *tert*-butyl methyl ether (TBME) to provide the boronic ester **33** in 52% yield. This steric control C–H activation–borylation of arenes containg *ortho*- and *para*-directing substituents is a modification of the published procedure of Maleczka for the synthesis of phenols bypassing the oxidation step.[34]

The synthesis of the boronic acid **36** started from 3,5-dibromoaniline, which was diazotized, reduced with L-ascorbic acid to the hydrazine and then reacted with pentane-2,4-dione to give the pyrazole **34** in 62% yield for the three steps. Sequential palladium catalyzed reactions first with morpholine gave **35** (33% yield) and then with bis(pinacolato)diboron gave the pinacol boronate **36** in 36% yield.

RESULTS AND DISCUSSION

Molecules can be nebulized as a solution or a suspension, and it has been shown[35] that there is a more consistent delivery of drug substance (especially at high concentrations) via solution nebulization compared to suspension nebulization. This and the desire to minimize the time needed for the patient to inhale the necessary dose led to the requirement for a highly soluble molecule. This had a significant influence on the design of $\alpha_v\beta_6$ inhibitors. One question that arises, for example, is whether a highly soluble molecule might be rapidly cleared from the lung, meaning prolonged integrin inhibition in the lung to deliver the desired pharmacodynamic effect might be challenging. However, as will be described later, binding of the inhibitor to $\alpha_v\beta_6$ causes receptor internalization, thus preventing activation of TGFβ. Re-expression of the receptor on the cell surface takes hours, and this strategy is used to drive duration of effect.

Inhaled delivery can be used to minimize systemic exposure and reduce side effects[36,37] while maximizing the concentration in the lung which in the case of IPF is also the site of action. This has been achieved by designing molecules with limited oral absorption of any swallowed compound coupled with higher metabolic clearance of compound reaching the circulatory system. The safety profile of an $\alpha_v\beta_6$ inhibitor was unknown (although there are α_v and $\alpha_v\beta_6$ antibodies in the clinic[12]), so molecules were not specifically optimized for low oral bioavailability and high clearance in this case.

To help minimize the clinical dose, a high intrinsic affinity of an $\alpha_v\beta_6$ inhibitor was targeted; this is also likely to improve the binding kinetics and particularly ligand dissociation. Our primary goal therefore was to identify highly potent and selective inhibitors initially determined through cell adhesion assays.

Assays. Integrin cell adhesion assays were primarily used to assess potency and selectivity against all five α_v integrins ($\alpha_v\beta_1$, $\alpha_v\beta_3$, $\alpha_v\beta_5$, $\alpha_v\beta_6$, and $\alpha_v\beta_8$). These assays[38] measure the ability of compounds to inhibit the binding of the integrin expressed on the surface of cells to the endogenous peptide ligand coated to a 96-well plate. On the basis of the configuration of the assay, the upper limit of potency for $\alpha_v\beta_6$ is $pIC_{50} \approx 9$ with a difference of around 0.4 log units and above required for any difference in potency between compounds to be regarded as significant reflecting the variation observed in such data (mean SD for all compounds tested is 0.2).[39]

Compounds of further interest were also examined in a radioligand assay to determine accurate p*Ki*'s and to definitively rank compounds based on potency. These competition binding experiments were performed with $\alpha_v\beta_6$ integrin protein concentration of 0.3 nM and are regarded as a more accurate representation of affinity than cell adhesion potencies. Differences in activity of around 0.2 are regarded as significant in competition binding assays that use 0.3 nM $\alpha_v\beta_6$ protein, again reflecting the variation in data (mean SD for all compounds tested 0.1).

Cardiovascular safety was assessed in two hERG channel assays: the IonWorks Barracuda automated patch clamp (a high throughput assay)[40] and QPatch (a lower throughput assay).[41]

Lipophilicity was determined by measuring the log *D* of the compounds at pH 7.4 chromatographically ($chromLogD_{7.4}$).[42]

High-throughput solubility of analogs was routinely measured; aqueous solubility is uniformly excellent (>1 mg/mL) due to the presence of three ionizable centers (the tetrahydronaphthyridine, pyrrolidine, and carboxylic acid), and so the data are not presented.

A number of factors need to be taken into account in the design of inhaled drugs. The dose size (likely to be small (<10

DOI: 10.1021/acs.jmedchem.8b00959
J. Med. Chem. XXXX, XXX, XXX–XXX

mg)), the method of delivery (dry powder or nebulized), and whether systemic exposure will cause unacceptable side effects all need to be determined alongside the frequency of dosing. At the start of the project it was decided that nebulized dosing would maximize the likelihood of the drug reaching the fibrotic areas of the lung of IPF patients where normal lung function is usually compromised. It was also thought that developing a molecule for nebulization would be quicker than formulation of a crystalline, micronized powder for dry powder administration and consequently would shorten the timelines to phase II studies.

Selection of the Clinical Candidate. As mentioned earlier, preliminary SAR studies (data not shown) indicated that *meta* substitution of the benzene ring is preferred for both $\alpha_v\beta_6$ potency and selectivity over related integrins such as $\alpha_v\beta_3$. This is in general agreement with aryl substituent effects described in the literature[25] and also from the numerous reported studies on $\alpha_v\beta_3$ inhibitors.[17−19] Initially the *m*-bromo **28a** and *m*-cyclopropyl analogs **28b** were attractive for their high potency, both having pIC_{50} = 8.4 in the $\alpha_v\beta_6$ cell adhesion assay and ease of synthesis although the latter also has significant $\alpha_v\beta_5$ activity (pIC_{50} = 8.1) (Table 1). In broader profiling, however, both proved to have unacceptably high hERG activity with pIC_{50} > 5. (Although the hERG risk from inhaled delivery of a compound might in general be thought to be lower due to the smaller dose size, heart exposure can still be relatively high for a compound rapidly absorbed from the lung, as a result of the intimate connection of cardiopulmonary circulation). To check whether the in vitro hERG assays were predictive of effects in tissue in this series of compounds, **28b** was also assessed in the rabbit cardiac ventricular wedge assay, which allows a direct measurement of drug effects on the QT interval. It showed significant concentration dependent increases in QT interval prolongation at concentrations of 1 and 3 μM (data not shown), thus confirming the in vitro hERG data. **28b** has moderate lipophilicity ($chromLogD_{7.4}$ = 3.3), and so to reduce the risk of hERG inhibition, a lipophilicity threshold of around $chromLogD_{7.4}$ = 3 was introduced to ideally avoid or at least reduce this liability.[43]

Consequently, a range *meta* substituents of **28** were prepared with a focus on heteroaromatic and heteroaliphatic rings which allowed a wide exploration of substitution in this position while also controlling lipophilicity (Table 1).

The morpholine **28c** reduces lipophilicity ($chromLogD_{7.4}$ = 2.27) while increasing polarity (and solubility), and gratifyingly hERG inhibition is much lower (pIC_{50} < 4.5 in both assays). It is a potent $\alpha_v\beta_6$ inhibitor with a pIC_{50} of 8.4 (cell adhesion) and a pK_i of 10.2 in the $\alpha_v\beta_6$ radioligand binding assays, although its off-rate ultimately proved to be faster than **28h** (see later).

A wide variety of heteroaromatic substituents **28d−s** in the *meta* position were designed and prepared including a series of pyrazoles **28d−k** (a preferred heteroaromatic from a developability perspective[44]) with lipophilicity ranging from $chromLogD_{7.4}$ of 2.40 (**28d**) up to 3.23 (**28i**). Careful selection of the number of heteroatoms in the ring alongside any substituents on the heteroaromatic ring itself meant the $chromLogD_{7.4}$ could be adjusted appropriately given concerns about hERG liabilities.

The parent pyrazole **28d** has high affinity for the $\alpha_v\beta_6$ integrin (pIC_{50} = 8.6) in the cell adhesion assay and good affinity in the binding assay (pK_i = 10.0) but unexpectedly high hERG activity (pIC_{50} = 6.1) given the lipophilicity ($chromLogD_{7.4}$ = 2.40). Introduction of a single methyl group at the C3-, C4-, or C5-pyrazole position demonstrates that substitution is tolerated at the C3- and C5 positions (**28e** and **28g** pIC_{50} of 8.4 and 8.8, respectively) and reduces hERG activity 10-fold compared to **28d**. **28e** and **28g** have good $\alpha_v\beta_6$ binding affinity in the radioligand assay (pK_i of 10.1 and 10.2, respectively). In contrast, methylation is less tolerated at the C4-position of the pyrazole (**28f** pIC_{50} = 7.4). Introduction of two methyl groups in the C3- and C5- positions that tolerate substitution provided **28h**. It has high affinity for $\alpha_v\beta_6$ in both the cell adhesion (pIC_{50} = 8.4) and the $\alpha_v\beta_6$ radioligand assay (pK_i = 10.4). In a more sensitive version of the radioligand assay with a lower protein concentration (75 pM) and therefore increased sensitivity, **28h** demonstrates an even higher affinity with a pK_i = 11.0. While **28h** has weak activity in the in vitro hERG assays, both pIC_{50} values are <5 and the safety risk was regarded as manageable given the rest of the compound's profile. Additionally, as the compound is developed, further in vitro and in vivo assessments would be carried out and good safety multiples to predicted human exposures were anticipated (data not shown). **28h** has modest to excellent selectivity over the other α_v integrins in cell adhesion assays for $\alpha_v\beta_6$ (see later). Two C-linked pyrazoles **28j** and **28k** were prepared; the NH analog **28j** has high affinity for $\alpha_v\beta_6$ (pIC_{50} = 8.6) but reduced selectivity, whereas the demethylated analog **28k** is a little less potent (pIC_{50} = 8.1).

From this work, the very potent and $\alpha_v\beta_6$ selective dimethylpyrazolo analog **28h** was selected for further profiling (see later) and ultimately became the clinical candidate.[45] This decision was supported by further pharmacological studies including some with IPF human tissue; detailed studies to check the pharmacokinetic profile are commensurate with inhaled dosing and activity in various animal models (see later). However, to understand the SAR around **28h** more fully, we continued to explore analogs from both this and related series[46,47] and the profile of these are now described. Some of these analogs have comparable profiles to **28h** but were in fact identified and profiled considerably later. At the time, in the judgment of the project team, these did not offer any significant advantage to **28h** which by that point was progressing through expensive and resource intensive development processes.

Five N-linked triazole analogs **28l−p** were prepared differing in terms of regiochemistry, linking position, and substitution pattern. The addition of an extra nitrogen into the heteroaromatic over the pyrazole analog reduces the lipophilicity typically by at least a log unit; compare the matched pair dimethylpyrazole **28h** having a $chromLogD_{7.4}$ of 2.82 with the dimethyltriazole **28n** having a $chromLogD_{7.4}$ of 1.66. All the triazoles have high affinity for the $\alpha_v\beta_6$ integrin in the cell and in radioligand binding assays although some have less selectivity over some of the other α_v integrins compared to **28h**. None of them show hERG activity perhaps due to the reduced lipophilicity.

Continuing the exploration of various azole analogs, three imidazoles (both C- and N-linked) **28q−s** were made based on the ready availability of the building blocks. Despite their isomeric similarity, the matched pair imidazole analogs of the corresponding pyrazoles have reduced lipophilicity, reflecting the obvious differences in basicity; compare dimethylpyrazole **28h** having a $chromLogD_{7.4}$ of 2.82 with the dimethylimidazole **28r** having a $chromLogD_{7.4}$ of 2.09. These changes in

DOI: 10.1021/acs.jmedchem.8b00959
J. Med. Chem. XXXX, XXX, XXX−XXX

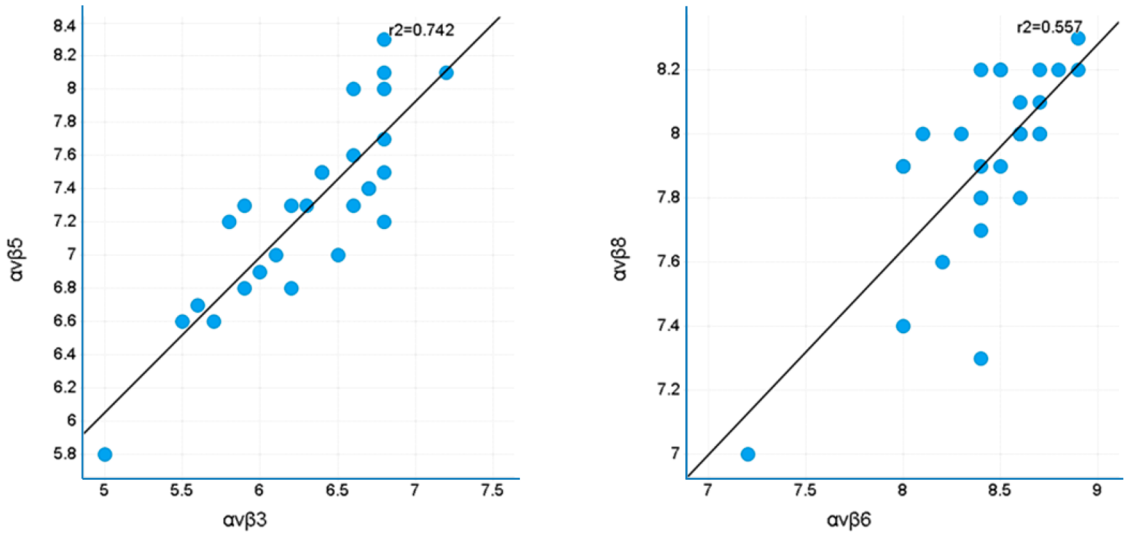

Figure 4. Plots of $\alpha_v\beta_3$ vs $\alpha_v\beta_5$ (left panel) and $\alpha_v\beta_6$ vs $\alpha_v\beta_8$ (right panel) cell adhesion values for the compounds described in Table 1 with r^2 correlations of 0.74 and 0.56, respectively.

lipophilicity between azole matched pairs and isomeric azole matched pairs are in agreement with some of our previous work exploring these effects more generally.[44] Like the triazoles, the imidazoles show no hERG activity in the in vitro assays and have high potency against $\alpha_v\beta_6$ in the cell adhesion and binding assays with **28r** having a similar potency and selectivity profile to **28h**. **28q** is a little less potent with a pIC_{50} of 8.2 in the $\alpha_v\beta_6$ cell adhesion assay but may have a CYP p450 inhibition risk.[48]

The last group to be examined was a range of cyclic ether analogs **28t−z**,[47] which are linked to the phenyl ring either via oxygen or carbon atoms. These compounds typically have slightly lower lipophilicity compared to **28h** ranging from $chromLogD_{7.4}$ = 2.75 for **28w** to $chromLogD_{7.4}$ = 2.07 for **28v**. Little or no hERG activity is seen in the Barracuda assay, although several have increased activity in the Qpatch assay (see for example the tetrahydropyran **28w**, pIC_{50} < 4.3 in Barracuda but pIC_{50} = 5.1 in Qpatch). The C4-linked tetrahydropyran **28y** ($\alpha_v\beta_6$ pIC_{50} = 7.9) has lower affinity in the cell adhesion assay, whereas **28t−w** have excellent $\alpha_v\beta_6$ activity but are typically less selective especially against the $\alpha_v\beta_5$ integrin having 10-fold more activity against this integrin in comparison to **28h**; see for example the O-linked oxetane **28v** with $\alpha_v\beta_6$ pIC_{50} = 9.0 (cell adhesion) but $\alpha_v\beta_5$ pIC_{50} = 8.3. The C3-linked tetrahydrofuran **28x** isomers (described in Table 1 as **28xI1** and **28xI2**) are also very potent against $\alpha_v\beta_6$ (with **28x Isomer 2** (listed in Table 1 as **28xI2**) having a pK_i of 10.7 in the radioligand binding assay) but a slightly better selectivity profile (almost comparable to **28h**). The introduction of a third asymmetric center as in the O- and C-linked tetrahydrofuran-3-yl analogs **28t**, **28u**, and **28x** (isomers 1 and 2) has little effect on the $\alpha_v\beta_6$ integrin affinity or α_v selectivity profile.

Finally, several 3,5-disubstituted phenyl analogs were prepared. Adding a 5-cyclopropyl or a 5-(3,5-dimethyl)-pyrazolo substituent to the 3-morpholino analog **28c** provided compounds **28bc** and **28ch**, respectively. Both have comparable $\alpha_v\beta_6$ potency to **28h** in the radioligand binding assay but show improved selectivity particularly **28ch**; compare **28h** and **28ch** $\alpha_v\beta_3$ pIC_{50} of 6.0 and 5.5, respectively, and $\alpha_v\beta_5$ pIC_{50} of 6.9 and 5.7, respectively. It is clear the space in the specificity defining loop (SDL) where these substituents bind is more restricted in $\alpha_v\beta_3$ and $\alpha_v\beta_5$ compared to $\alpha_v\beta_6$ (see later). Neither **28bc** nor **28ch** has any activity in the in vitro hERG assays.

Inverting the configuration at the benzylic asymmetric center reduces $\alpha_v\beta_6$ affinity considerably as illustrated by the cyclopropyl substituent **30b** (1.1 log drop to $\alpha_v\beta_6$ pIC_{50} = 7.3), the morpholine substituent **30c** (3.2 log drop to pIC_{50} = 5.2) and the dimethylpyrazolo substituent **30h** (1.6 log drop to pIC_{50} = 6.8). Inversion of the pyrrolidine asymmetric center has much less or minimal effect on $\alpha_v\beta_6$ affinity (data not shown).

Comparison of the α_v integrin selectivity profiles for the series (Figure 4) highlights the pronounced effects of substitution on the different α_v integrin activities. There is a good correlation in the cell adhesion activity of substituents for $\alpha_v\beta_3$ and $\alpha_v\beta_5$ (r^2 = 0.74) and a moderate correlation for $\alpha_v\beta_6$ and $\alpha_v\beta_8$ (r^2 = 0.56), which agrees with correlations described elsewhere[12] and reflects similarities/differences in the SDL as described later.

In general, the substituents described inherently have at least around a log unit selectivity in cell adhesion for $\alpha_v\beta_6$ over $\alpha_v\beta_3$ (with a range of 1.1−2.7 log difference) and $\alpha_v\beta_1$ (with a range of 0.7−1.8 log difference) (Figure 5). There is a wider variation for selectivity for $\alpha_v\beta_6$ over $\alpha_v\beta_5$ from no selectivity to 2.4 logs. Among the α_v integrins, there is least selectivity for $\alpha_v\beta_6$ over $\alpha_v\beta_8$ from no selectivity to 0.9 logs. Compounds with the greatest selectivity over $\alpha_v\beta_3$ also tend to be highly selective over $\alpha_v\beta_5$ (and vice versa as might be expected from the correlation already mentioned) but are less so for $\alpha_v\beta_1$ or $\alpha_v\beta_8$. Overall, consideration of the α_v selectivity profile played a role in picking **28h** as the clinical candidate and is one of the most selective compounds (Figure 5). Radioligand binding data (see later) confirms **28h** has high selectivity for $\alpha_v\beta_6$ over the other α_v integrins.

Protein Binding. An understanding of plasma protein or blood binding values is helpful in interpreting data from in vivo experiments and in the prediction of clinical dose. Human blood binding data on selected analogs were therefore generated (Table 2) which can be compared with the measured $chromLogD_{7.4}$ lipophilicity values. The free unbound

DOI: 10.1021/acs.jmedchem.8b00959
J. Med. Chem. XXXX, XXX, XXX−XXX

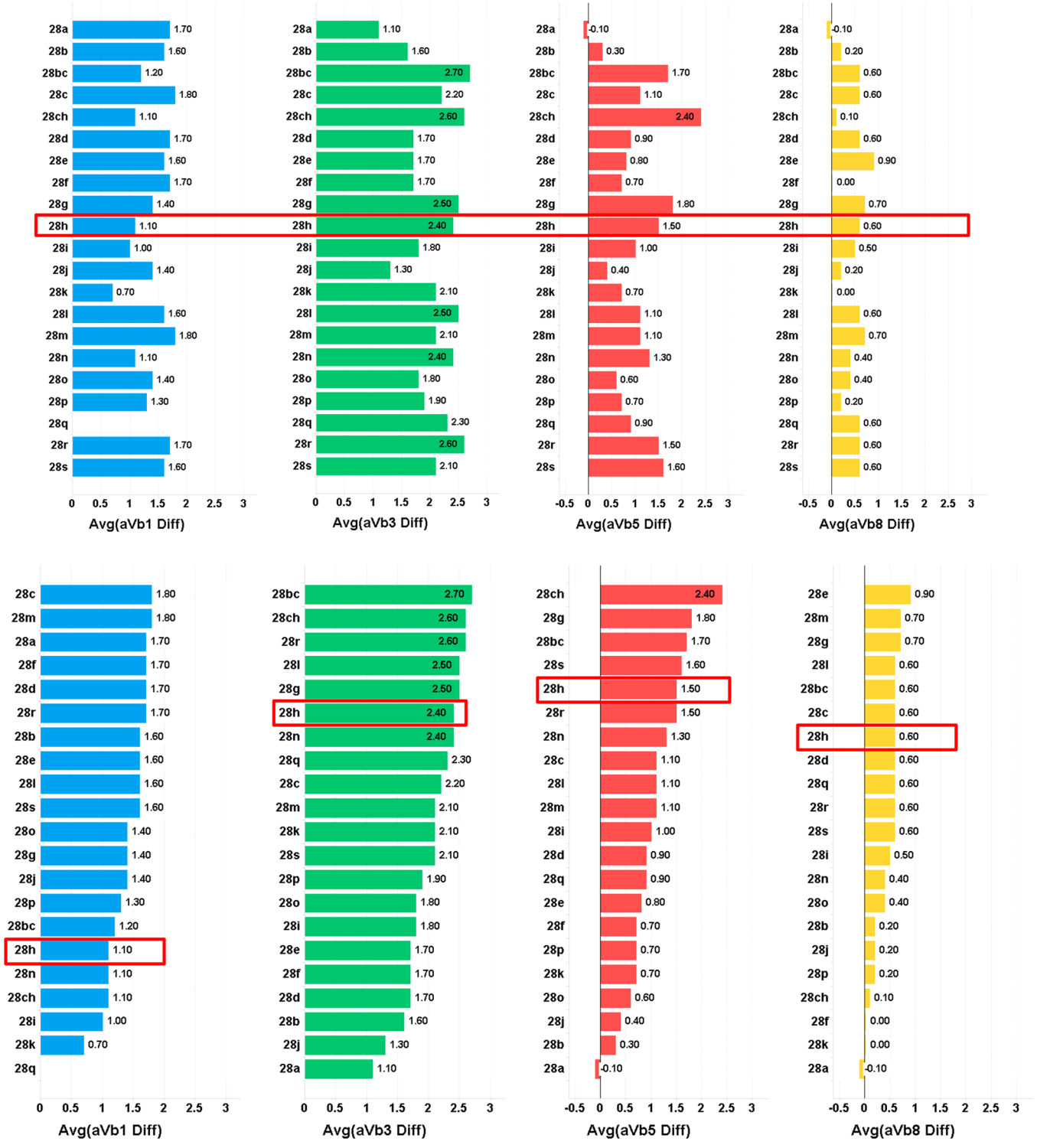

Figure 5. Pictorial representation of the cell adhesion selectivity for selected compounds in Table 1. Each bar is the average log difference between the cell adhesion potency for $\alpha_v\beta_6$ and $\alpha_v\beta_1$ (blue bars), $\alpha_v\beta_3$ (green bars), $\alpha_v\beta_5$ (red bars), and $\alpha_v\beta_8$ (yellow bars). The red boxes highlight the cell adhesion selectivity profile for the clinical candidate **28h**. In the top panel the compounds are ordered according to compound number, and in the lower panel, the compounds are ordered separately for each integrin from most to least selective.

fractions are moderately high to very high, and there is a reasonable correlation between blood binding and molecular lipophilicity (r^2 = 0.72, graph not shown) for the compounds shown with the more lipophilic compounds exhibiting higher levels of compound bound in blood.

Higher free unbound fractions in blood build confidence that the unbound fraction in the lung (the site of action) may also be higher (see later). Higher free fractions may also translate into a lower dose medicine which can offer the added benefits of an improved safety profile, lower cost of manufacturing drug substance, and better compatibility with inhaled delivery platforms (as development of bespoke platforms can be prohibitively expensive).

DOI: 10.1021/acs.jmedchem.8b00959
J. Med. Chem. XXXX, XXX, XXX−XXX

Table 2. Human Blood Binding Measured by Equilibrium Dialysis at 37°C and Measured Chromatographic log *D* at pH 7.4 for Selected Analogs

compd	human blood binding (%)	measured chromLogD$_{7.4}$
28s	47	1.77
28l	54	1.05
28m	60	1.95
28p	72	1.75
28x Isomer 2	83	2.58
28g	90	2.55
28h	92	2.82

Modeling Considerations. Despite considerable modeling and docking efforts aimed at understanding the SAR of the aryl substituents in the SDL (see later), we were unable to consistently predict or design specific integrin profiles. Relatively subtle changes in structure can have a profound effect on $\alpha_v\beta_6$ potency and selectivity as described here and elsewhere.[45] Thus, while specific SAR can be rationalized through modeling, once data are available, compounds were principally designed empirically. Given the conformational changes in the active site that occur through binding, activation, and signaling, this may be unsurprising.[49]

Given the liabilities with complete TGFβ inhibition[8] and the excellent preclinical target validation studies for $\alpha_v\beta_6$[21] at the outset of this work, our aim was for the clinical candidate to have high $\alpha_v\beta_6$ selectivity. Since an $\alpha_v\beta_6$ crystal structure was not available during lead optimization, a homology model based on the $\alpha_v\beta_3$ crystal structure 1L5G[50] was developed in an attempt to facilitate structure-based design and aid the rationalization of series SAR. Modeling of $\alpha_v\beta_3$ antagonists and comparison with $\alpha_v\beta_6$ lead optimization compounds (such as those described here) were used to rationalize differences in aV integrin selectivity profiles.

Docking into the $\alpha_v\beta_6$ homology model was used to generate binding poses for lead optimization compounds such as **28h** (Figure 6). The tetrahydronaphthyridine binds to the α_v subunit and the substituted aryl acid to the β_6 subunit.

Comparison of the $\alpha_v\beta_3$ X-ray crystal structure 1L5G and $\alpha_v\beta_6$ homology model revealed key differences in the β-subunit whereby selectivity for $\alpha_v\beta_6$ might be obtained (Table 3).

Table 3. β-Subunit Residue Differences between $\alpha_v\beta_3$ Crystal Structure and $\alpha_v\beta_6$ Homology Model Identified Regions To Target for Selectivity

$\alpha_v\beta_3$	$\alpha_v\beta_6$
Tyr122	Ala143
Tyr166	Lys187
Asp179	Ser199
Met180	Ile200
Arg214	Ala234
Arg216	Ile236
Ala218	Thr238

Notably, differences in residue composition of the SDL suggested that bulky *meta*-substituted groups on the aryl ring would be more favorable in the larger $\alpha_v\beta_6$ pocket. In $\alpha_v\beta_3$, this subpocket is more enclosed due to the Tyr166 ($\alpha_v\beta_6$ = Lys187) side chain directed into the pocket and the salt-bridge between Asp179 ($\alpha_v\beta_6$ = Ser199) and Arg214 ($\alpha_v\beta_6$ = Ala234) side chains, which is absent in $\alpha_v\beta_6$. The central linker group (connecting the 1,8-tetrahydronapthyridine and carboxylic acid) is positioned proximal to Ala218 in $\alpha_v\beta_3$, which is replaced by the larger and more polar Thr238 residue in $\alpha_v\beta_6$, providing a further region to exploit for optimization of $\alpha_v\beta_6$ selectivity. These observations are echoed when the $\alpha_v\beta_3$ crystal structure 1L5G (Figure 7) is compared to the $\alpha_v\beta_6$

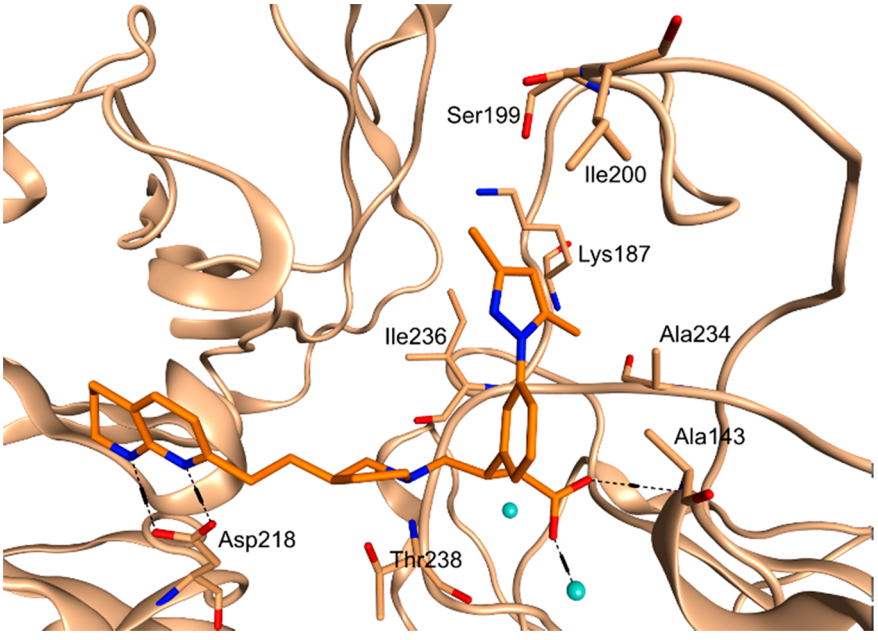

Figure 6. Docked pose of **28h** in the $\alpha_v\beta_6$ homology model. Hydrogen bonds are displayed as dashed lines between the 1,8-tetrahydronaphthyridine and α_v-Asp218, and the carboxylate is coordinated with the metal ion (cyan sphere) in the metal ion dependent adhesion site (MIDAS) and Ala143 in the β-subunit. An additional hydrogen bond (not shown) between the protonated pyrrolidine cation and the Thr238 side chain is predicted. The *meta*-substituted aryl group is positioned in the β-subunit in proximity to the specificity determining loop (SDL).

DOI: 10.1021/acs.jmedchem.8b00959
J. Med. Chem. XXXX, XXX, XXX−XXX

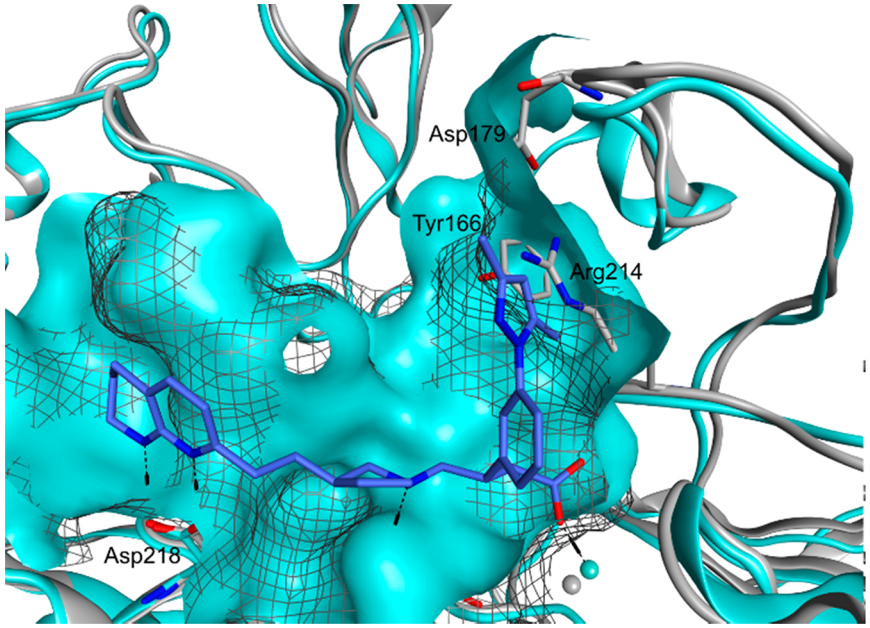

Figure 7. Comparison of binding site surfaces between an $\alpha_v\beta_6$ crystal structure 4UM9 (blue) and an $\alpha_v\beta_3$ crystal structure 1L5G (gray). The $\alpha_v\beta_6$ site provides a pocket into which bulky *meta*-substituted aryl substituents can bind (solid blue surface). In comparison, the $\alpha_v\beta_3$ Tyr166 side chain and the salt-bridge between Asp179 and Arg214 side chains result in a more enclosed pocket which is less favorable for these groups (gray mesh and residue labeling).

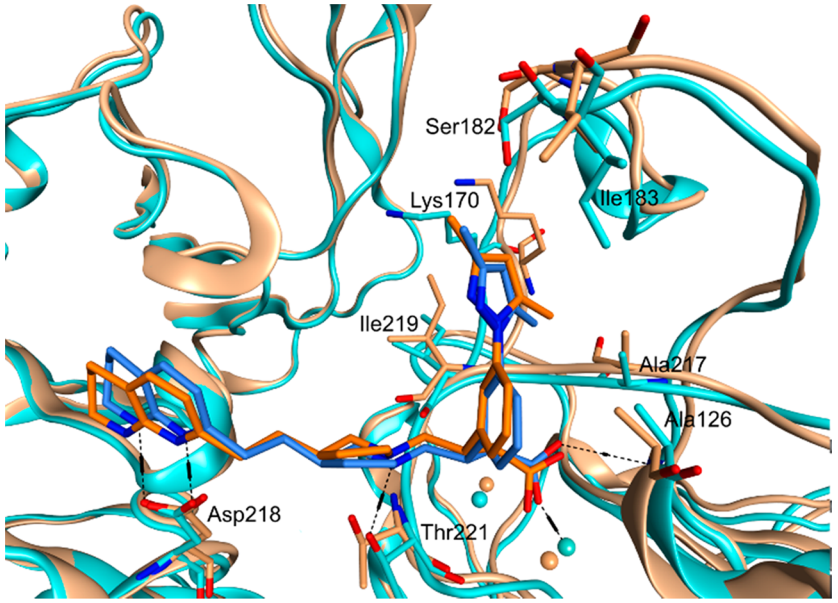

Figure 8. Docked pose of **28h** in the $\alpha_v\beta_6$ X-ray crystal structure 4UM9 (blue with residue labeling). Key protein−ligand interactions are between the 1,8-tetrahydronaphthyridine and α_v-Asp218, the pyrrolidine and Thr221 and the carboxylate coordinated with the MIDAS. This binding mode and protein−ligand interactions are consistent with those proposed by the $\alpha_v\beta_6$ homology model (light orange colored residues) with docked **28h** (superimposed in orange), although note the differences in the β-subunit SDL (upper right quartile of figure).

crystal structure 4UM9 which also displays a larger aryl group binding region.

The predicted binding mode and key protein−ligand interactions of **28h** in the $\alpha_v\beta_6$ homology model were found to be consistent with modeling in the subsequently published $\alpha_v\beta_6$ X-ray crystal structures.[49,51] Comparison of docked poses reveals there is some translation of the ligand due to conformational differences between the $\alpha_v\beta_6$ 4UM9 crystal structure[51] and $\alpha_v\beta_6$ homology model in the highly flexible SDL (Figure 8).

Profile of the Clinical Candidate 28h. Described here are the in vitro pharmacology, pharmacokinetic profile and other properties of **28h**. The translational studies supporting the clinical candidate will be published elsewhere shortly.

Pharmacology Profile. *Affinity and Selectivity.* The first steps were to confirm the potency, affinity, and selectivity of **28h** particularly against the other RGD-binding integrins. As described above (Table 1), the 2,5-dimethylpyrazole analog has high affinity for $\alpha_v\beta_6$. In saturation binding experiments, which provides a more accurate indication of selectivity than

DOI: 10.1021/acs.jmedchem.8b00959
J. Med. Chem. XXXX, XXX, XXX−XXX

the cell adhesion assays, tritiated **28h** has a pK_D of 10.8 with between 17-fold ($\alpha_8\beta_1$) and 6667-fold ($\alpha_5\beta_1$) selectivity against other RGD binding integrins (Table 4).[52] On the basis of these

Table 4. Saturation binding pK_D's for tritiated 28h[38]

RGD integrin	[^{3}H]**28h**, pK_D	[^{3}H]**28h**, K_D (nM)	$\alpha_v\beta_6$ fold selectivity
$\alpha_v\beta_6$	10.80	0.02	1
$\alpha_v\beta_1$	8.59	2.60	173
$\alpha_v\beta_3$	7.74	18.40	1227
$\alpha_v\beta_5$	7.68	21.00	1400
$\alpha_v\beta_8$	8.56	2.74	183
$\alpha_5\beta_1$	7.00	100.00	6667
$\alpha_8\beta_1$	9.59	0.26	17

data, **28h** is at least 170-fold selective over the other α_v integrins. Importantly minimal activity is seen against $\alpha_{IIb}\beta_3$ integrin (the only other RGD binding integrin) up to 10 μM (data not shown) inhibitors of which are used clinically as platelet aggregation inhibitors.[12] While not at antibody selectivity levels (such as the $\alpha_v\beta_6$ antibody STX-100 in clinical trials),[21] **28h** is clearly highly selective and was therefore deemed suitable to test the hypothesis that $\alpha_v\beta_6$ inhibition might be beneficial in treating IPF.

28h was cross-screened against a panel of more than 50 enzymes and receptors for off-target activity and showed excellent selectivity (data not shown).

Off-Rate. It is important to understand the dissociation of **28h** from $\alpha_v\beta_6$ because this contributes to estimating the likely size and frequency of clinical dosing. Thus, dissociation binding kinetics of **28h** were determined against the $\alpha_v\beta_6$ protein and compared with those for **28c** and a pan α_v inhibitor from the literature SC-68448 (Figure 9).[38] Dissociation half-lives of $t_{1/2}$ ~ 7 h, 2 h, and 5 min, respectively, were obtained. The half-lives correlate with the affinity of the compounds (Figure 9); the higher is the affinity of the compound, the slower is the dissociation half-life. **28h** is clearly superior and therefore more likely to increase duration of action in vivo and minimize clinical dose.

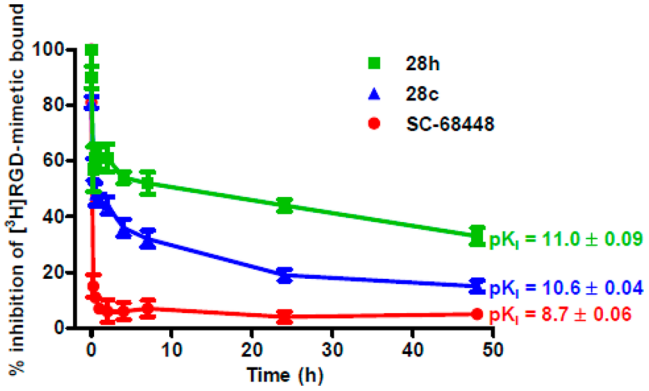

Figure 9. Dissociation binding kinetics for **28h**, **28c**, and SC-68448 (a pan α_v integrin inhibitor literature standard[38]). The pK_i values shown are from the 0.075 nM radioligand binding assay format. Experimental details are provided in the reference cited.

Receptor Internalization. As has been described elsewhere with the cell surface $\alpha_v\beta_6$ integrin,[53] ligand binding induces rapid receptor internalization (within minutes) and in so doing prevents activation of TGFβ. Having determined the affinity and off-rate for **28h**, it was next important to characterize its effect on receptor internalization as this also contributes to estimating the size and frequency of the clinical dose. Thus, in primary lung epithelial cells, **28h** causes internalization with a pEC_{50} of 9.8,[54] and at a concentration of 250 nM, around 80% of the receptor is internalized after 1 h with a $t_{1/2}$ of 2.6 min.[54,55] Recycling or re-expression of the receptor is slow with a $t_{1/2}$ of 11.0 h. This has been shown to be driven by the high affinity engagement of $\alpha_v\beta_6$ and subsequent slow dissociation of **28h** that induces degradation followed by new synthesis of the integrin.[56] As described elsewhere, this internalization translates into a duration of action in vivo. While perhaps unsurprising, it is also encouraging that by substantially removing the $\alpha_v\beta_6$ driven activation of TGFβ, some reduction in collagen formation is seen in animal models.[54]

Human Tissue Data. While these results are promising, it is also important to build confidence that similar effects will be observed in the human disease prior to expensive clinical trials. Thus, in precision cut tissue lung slices derived from IPF patients, 1 μM **28h** decreases TGFβ levels to those seen with healthy lung slices. It also inhibits phosphoSMAD2 (phosphorylated intracellular signaling molecule Mothers Against Decapentaplegic homolog 2, a marker for TGFβ activation) in a dose dependent manner with an approximate IC_{50} of 1 nM.[54]

Summary. These data (together with other pharmacological data published elsewhere[54]) provide confidence **28h** has potential clinically with the diseased human tissue in particular providing reassurance that in vitro assays and in vivo models may be predictive of inhibition of $\alpha_v\beta_6$ in humans and reduce the effects of TGFβ activation. Given both the usual rate of attrition of clinical candidates and in particular those for IPF, the linking of the target validation, data in vitro assays and in vivo models[54] to efficacy in ex vivo human tissue increases confidence in carrying out clinical studies.

Pharmacokinetic Profile. In order to predict its pharmacokinetic (PK) profile in human, evaluate its tractability as an inhaled drug candidate, and assist with the interpretation of pharmacokinetic/pharmacodynamic studies, **28h** was profiled in a range of in vivo studies in preclinical species (Table 5). In particular, intravenous (iv) studies in rat and dog were conducted to support allometric scaling and predictions of clearance and volume of distribution in human, while characterization of oral pharmacokinetics is essential to predict the fate of the fraction of an inhaled dose in human that is swallowed into the gastrointestinal tract. The pharmacokinetic parameters obtained for rat and dog contributed to the prediction of the clinical PK for **28h**, which is described elsewhere.[26]

Intravenous/Oral PK in Rat and Dog. The selection of rat and dog as main species for testing the preclinical safety of **28h** was driven by (a) knowledge that the pharmacological target is actively expressed in these two species and (b) the considerable in-house knowledge of the general pathology in these species and their response to a wide variety of drugs developed by the inhaled route. In terms of ADME properties, metabolic stability data in hepatocytes and liver microsomes were generated across species, and the results are described later.

In a crossover iv infusion/oral PK study in male Wistar Han rat, the pyrazole **28h** showed moderate−high blood clearance (56 mL min^{-1} kg^{-1}, ~70% liver blood flow (LBF)), moderate volume of distribution (2.1 L/kg), short terminal half-life (0.8 h), and negligible oral bioavailability (<2%). In a crossover iv

DOI: 10.1021/acs.jmedchem.8b00959
J. Med. Chem. XXXX, XXX, XXX−XXX

Table 5. Pharmacokinetic Parameters for 28h in Rat and Dog[a]

parameter	species		
	male Wistar Han rat[b] (n = 3 iv, n = 3 po, crossover)	female Wistar Han rat[c] (topical, n = 4)	male Beagle dog[d] (n = 3 iv, n = 3 po, crossover)
Clb (mL min^{-1} kg^{-1})	51−60		25−33
V_{ss} (L/kg)	1.8−2.3		2.6−4.7
$T_{1/2}$ (h) (iv)	0.8−0.9		1.2−5.4
oral or nebulized C_{max} (ng/mL)	3−9	30−53	55−76
T_{max} (h)	0.5−2	0.2	0.25−0.5
oral or nebulized bioavailability (%)	<2	40−63	27−34

[a]All animal studies were ethically reviewed and carried out in accordance with Animals (Scientific Procedures) Act 1986 and the GSK Policy on the Care, Welfare and Treatment of Animals. [b]Dosed at 1 mg/kg (iv, 30 min infusion) and 3 mg/kg (oral). [c]Nebulized with a dose level of 0.227 mg/kg. [d]Dosed at 1 mg/kg (iv, 60 min infusion) and 1 mg/kg (oral).

infusion/oral PK study in male Beagle dog, **28h** showed moderate−high blood clearance (28 mL min^{-1} kg^{-1}, ∼50% LBF), moderate volume of distribution (3.6 L/kg), moderate terminal half-life (3.6 h), and moderate oral bioavailability (30%). In preliminary studies (n = 1 animal/species) to investigate the routes of elimination in vivo, after intravenous administration at 1 mg/kg, **28h** showed a low−moderate renal clearance (15% and 21% of the total blood clearance in rat and dog, respectively). **28h** also showed moderate biliary clearance (as unchanged parent) in the rat (24% of the total blood clearance). The unaccounted fraction of the total clearance (∼55% in the rat) is likely to be due to metabolism as the chemical structure of **28h** offers several potential sites for both phase I (oxidation) and phase II (conjugation) metabolism. However, a formal metabolite identification study has not yet been conducted.

Pulmonary Delivery in Rat. Additional in vivo studies were conducted on **28h** in order to characterize its pharmacokinetics with pulmonary delivery, to understand any partitioning into lung tissue, and for integration with pharmacodynamic and in vivo efficacy data. Thus, studies conducted in Wistar Han rats by the pulmonary route of administration (by intratracheal instillation and nebulization) suggested a very rapid absorption into the systemic circulation. The observed bioavailability from the pulmonary route was ∼21% from the intratracheal study and ∼54% from the nebulized administration. The lack of complete bioavailability is attributed to the uncertainty regarding the actual dose delivered to the lung in both studies and not to any hypothetical lung retention properties of **28h**, as demonstrated by the time-course of lung tissue concentration in the nebulized study.

After administration by the nebulized route at 0.227 mg/kg, concentrations of **28h** in rat lung peaked immediately at the end of the nebulization (716 ng/g), rapidly declined in a biexponential manner, and fell below the limit of quantification (10 ng/lung) at 7 h, suggesting a very low risk of accumulation in the lung upon repeated administration (Figure 10).

The distribution of **28h** in rat lung after nebulized inhalation (60 min exposure time) at a dose level of 6.23 mg/kg was investigated by MALDI-MS imaging (Figure 11). **28h** was detected evenly throughout the lung immediately after the inhalation period. One hour after completion of the inhalation period, levels of **28h** were barely detectable in the lung, confirming the rapid absorption from the pulmonary route observed in in vivo studies.

Lung Tissue Partitioning in Mouse. An important aspect of inhaled drug discovery is understanding the lung tissue

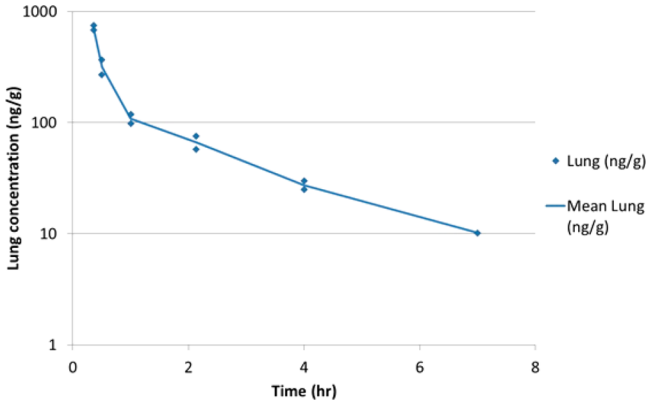

Figure 10. Lung concentration of **28h** following nebulized solution administration to rat at 0.227 mg/kg. All animal studies were ethically reviewed and carried out in accordance with Animals (Scientific Procedures) Act 1986 and the GSK Policy on the Care, Welfare and Treatment of Animals.

partitioning of the candidate regardless of any specific route of administration. The pulmonary uptake of **28h** was therefore investigated in the mouse by the subcutaneous route of administration. A steady state was achieved within 24 h by continuous infusion of **28h** using osmotic minipumps at 1.5 and 15 mg kg^{-1} day^{-1} which showed linear increase in exposure in the dose range investigated. Lung to blood ratios of 8:1 (15 mg kg^{-1} day^{-1}) to 11:1 (1.5 mg kg^{-1} day^{-1}) were measured in the mouse at steady state (96 h) indicating favorable distribution to the site of action irrespective of the route of administration. As no intravenous PK study was conducted in the mouse, the high lung-to-blood partition measured in this species cannot be related to the observed volume of distribution in the same species. Nonetheless the data suggest the findings are not specific to the mouse. In a preliminary (n = 1) distribution and elimination study conducted in the rat after a 30 min intravenous infusion of **28h** at 1 mg/kg, a lung-to-blood ratio of 12 was measured at 7 h. Other studies (e.g., toxicokinetics from early safety investigations) also confirm the favorable lung distribution.

The high values of the lung to blood partition coefficients might be explained by **28h** having higher affinity for lung tissue proteins compared to plasma proteins or by association to cell membrane phospholipids or intracellular uptake. However, when the unbound concentrations of **28h** at steady state in lung tissue and blood were compared, values within 2-fold were obtained, suggesting there is no active uptake mechanism in the lung that could subvert the "free fraction hypothesis".[57]

DOI: 10.1021/acs.jmedchem.8b00959
J. Med. Chem. XXXX, XXX, XXX−XXX

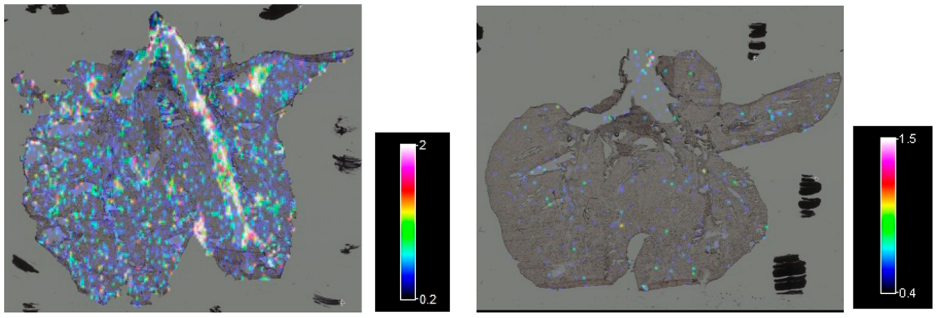

Figure 11. Distribution of **28h** by MALDI-MS imaging in rat lung after inhalation at a dose level of 6.23 mg/kg (left panel, immediately after dosing; right panel, 1 h after dosing). The color scale represents the signal intensity for the predominant fragment ion of **28h** with the images having 200 μM spatial resolution. All animal studies were ethically reviewed and carried out in accordance with Animals (Scientific Procedures) Act 1986 and the GSK Policy on the Care, Welfare and Treatment of Animals.

Table 6. In Vitro Pharmacokinetic Properties of 28h[58]

In Vitro Binding and Blood Distribution Studies				
	mouse	rat	dog	human
blood (% bound)	78.9	70.6	77.2	91.7
plasma (% bound)	not available	71.8	60.0	96.4
blood-to-plasma ratio	not available	0.82	0.69	0.61
lung (% bound)	90.0	not available	not available	89.2
liver (% bound)	not available	91.5	not available	not available
kidney (% bound)	not available	97.3	not available	not available
In Vitro Metabolic Clearance ((mL/min)/g Liver)				
	mouse	rat	dog	human
liver microsomes	3.0	0.55	<0.53	0.58
hepatocytes	15.3	9.45	<1.73	<0.86
In Vitro Passive Permeability and P-gp Assessment on MDR1-MDCK Cells				
in vitro passive permeability			20 nM/s	
efflux ratio (−/+ GF120918)			145/5.6	
P-gp substrate?			yes	

Although the high tissue partitioning observed with total drug concentrations was not confirmed by the unbound drug ratio, the partitioning is still a favorable condition in terms of PK/PD modeling, as it suggests that the easily measurable systemic unbound drug levels are representative of free drug at the site of action.

Supporting in Vitro Studies. To complete the characterization as an inhaled drug candidate, assist with the interpretation of PK/PD results (reported elsewhere), help building relevant physiologically based PK models, characterize the safety margins, and enable the pharmacokinetic scaling to human, in vitro studies on **28h** were also conducted. These included in vitro metabolic stability in hepatocytes and liver microsomes, in vitro blood, plasma and tissue binding, in vitro blood distribution, in vitro passive permeability, and preliminary assessment of P-glycoprotein. The results are summarized in Table 6.

Summary. Overall, **28h** displays a favorable pharmacokinetic profile in preclinical species, which (combined with its excellent physicochemical properties) suggests full suitability for progression and development as an inhaled medicine. In particular, the likely clinical dose (to be described elsewhere), together with other factors that potentially limit systemic availability, and the anticipated involvement of multiple routes of elimination (metabolic, biliary, and renal) indicate low potential for drug−drug interactions. More specifically for the inhaled route of administration, the combination of high solubility and rapid pulmonary absorption completely minimizes the risk of excessive lung retention or potential for accumulation upon repeated administration.

Physicochemical and in Vitro Safety Profile of 28h. *Physicochemical Properties of* ***28h.*** The measured pK_a's of **28h** are 4.1, 7.4, and 9.5 for the carboxylic acid, the tetrahydronaphthyridine, and pyrrolidine, respectively. The zwitterionic form of **28h** is an amorphous solid, whereas the corresponding monohydrochloride is crystalline.[30] The hydrochloride is stable in the solid state for 4 weeks at a range of elevated temperatures and relative humidity. The solubility of free base **28h** in saline (pH 7) and simulated lung fluid (SLF) at pH 6.9 is >71 and >34 mg/mL, respectively. The solubility of hydrochloride **28h** in saline at pH 4, 5, 6, and 7 is >55 mg/mL in all cases. In saline at pH 7.5 the solubility is 31 mg/mL and in SLF at pH 6.6 is >55 mg/mL. Compound **28h** thus demonstrated acceptable solubility for inhaled dosing by nebulization. **28h** at a concentration of 1 mg/mL is stable in saline at pH 4 at 50 °C for up to 6 weeks, while solutions prepared at pH 5, 6, and 7 are stable for 6 weeks when refrigerated.

In Vitro Safety Profile. The in silico assessment of direct acting mutagenicity was conducted according to the guidelines of ICH M7[59] and included the expert rule-based structure−activity relationship model Derek Nexus version 4.0.5 (KB

DOI: 10.1021/acs.jmedchem.8b00959
J. Med. Chem. XXXX, XXX, XXX−XXX

version 2014 1.0) developed by Lhasa Ltd. and the statistical based SAR model Leadscope version 1.8 (Salmonella version 3, E. coli-Sal 102 version 1) developed by Leadscope Inc. **28h** was not predicted to be mutagenic in Derek Nexus, version 4.0.5, but was out of the domain of applicability of the Leadscope model. The mutagenic and clastogenic potential of **28h** hydrochloride was assessed in the AMES and mouse lymphoma screening assays[60] and was not genotoxic in these assays up to the recommended maximum concentrations tested.

CONCLUSION

Described here is the discovery and profile of an $\alpha_v\beta_6$ inhibitor clinical candidate **28h**. The candidate came from lead optimization of a series of novel RGD $\alpha_v\beta_6$ integrin inhibitors possessing the 1,8-tetrahydronaphthyridine guanidine isostere as a replacement of arginine, a pyrrolidine ring as a constrained glycine replacement, and 3-arylbutanoic acid as a replacement of aspartic acid. Compounds were synthesized using a diastereoselective route that involved rhodium catalyzed asymmetric 1,4-addition of arylboronic acids. Thus, a variety of aryl substituents including cycloalkyl, heterocyclic, heteroaryl, and cyclic ether were screened in cell adhesion assays for affinity against $\alpha_v\beta_1$, $\alpha_v\beta_3$, $\alpha_v\beta_5$, $\alpha_v\beta_6$, and $\alpha_v\beta_8$ integrins, and several analogs with high aqueous solubility, high affinity, and selectivity for the $\alpha_v\beta_6$ integrin (over the other α_v integrins) were identified. (*S*)-3-(3-(3,5-Dimethyl-1*H*-pyrazol-1-yl)-phenyl)-4-((*R*)-3-(2-(5,6,7,8-tetrahydro-1,8-naphthyridin-2-yl)ethyl)pyrrolidin-1-yl)butanoic acid hydrochloride salt (**28h**) has physicochemical properties commensurate with nebulized delivery (71 mg/mL saline solubility at pH 7), a molecular weight of 487, and moderate lipophilicity (chromLogD$_{7.4}$ = 2.77). The measured pK_a for the carboxylic acid group was 4.07, for the tetrahydronaphthyridine 7.38, and for the pyrrolidine 9.50. **28h** is exceptionally potent with a pK_i of 11 for $\alpha_v\beta_6$ integrin in a radioligand binding assay and a long dissociation half-life (7 h). It inhibits the release of active TGFβ in primary human cellular assays and exhibits a long duration of action as a result of rapid induction of $\alpha_v\beta_6$ endocytosis (internalization), which occurs in minutes, and subsequent slow recycling (over hours). The high solubility of **28h** and overall pharmacokinetic properties including the rapid pulmonary absorption, multiple routes of elimination, and potentially limited systemic availability are commensurate with inhaled administration. The hydrochloride salt of **28h** was therefore selected for further investigation as a potential therapeutic agent for the treatment of idiopathic pulmonary fibrosis and is currently undergoing clinical investigations.

EXPERIMENTAL SECTION

TLC was performed on Merck 0.25 mm Kieselgel 60 F_{254} plates. Products were visualized under UV light and/or by staining with aqueous $KMnO_4$ solution. LCMS analysis was conducted on one of the following four systems. System A an Acquity UPLC BEH or CSH C18 column (2.1 mm × 50 mm i.d., 1.7 μm packing diameter) eluting with 10 mM NH_4HCO_3 in water adjusted to pH 10 with aqueous ammonia (solvent A) and acetonitrile (solvent B), using the following elution gradient for BEH column: 0.0−1.5 min 1−97% B, 1.5−1.9 min 97% B, 1.9−2.0 min 97−1% B. For CSH column: 0.0−1.5 min 3−95% B, 1.5−1.9 min 95% B, 1.9−2.0 min 95−3% B, at a flow rate of 1 mL min^{-1} at 40 °C. The UV detection was an averaged signal from wavelength of 210−350 nm, and mass spectra were recorded on a mass spectrometer using alternate-scan electrospray positive and negative mode ionization (ES+ve and ES−ve). System B an Acquity UPLC BEH C18 column (2.1 mm × 50 mm i.d., 1.7 μm packing diameter)) eluting with 0.1% trifluoroacetic acid in water (solvent A) and 0.1% trifluoroacetic acid in MeCN (solvent B) using the following elution gradient 0.0−1.5 min 3−100% B, 1.5−1.9 min 100% B, 1.9−2.0 min 100−3% B at a flow rate of 1 mL min^{-1} at 40 °C. System C an Acquity UPLC BEH or CSH C18 column (2.1 mm × 50 mm i.d., 1.7 μm packing diameter) eluting with 0.1% formic acid in water (solvent A) and 0.1% formic acid in acetonitrile (solvent B), using the following elution gradient 0.0−1.5 min 3−100% B, 1.5−1.9 min 100% B, 1.9−2.0 min 100−3% B, at a flow rate of 1 mL min^{-1} at 40 °C. System D an Acquity UPLC BEH C18 column (2.1 mm × 50 mm i.d., 1.7 μm packing diameter) eluting with 0.1% formic acid in water (solvent A) and 0.1% formic acid in acetonitrile (solvent B), using the following elution gradient 0.0−0.4 min 3% B, 0.4−3.2 min 3−98% B, 3.2−3.8 min 98% B, 3.8−4.2 min 98−3% B, 4.2−4.5 min, 3% B at a flow rate of 0.6 mL min^{-1} at 35 °C. These systems were used to demonstrate the purity of the final compounds to be ≥95% purity (see Supporting Information for a table of purities for the final compounds). Column chromatography was performed on disposable, normal phase SPE cartridges (2−100 g). Mass-directed autopreparative HPLC (MDAP) for method A was conducted on a Xbridge C18 column (100 mm × 30 mm i.d., 5 μm packing diameter) at ambient temperature eluting with 10 mM NH_4HCO_3 in water adjusted to pH 10 with ammonia (solvent A) and acetonitrile (solvent B), using an appropriate elution gradient over 10 min at a flow rate of 40 mL min^{-1} and detecting at 210−350 nm at room temperature. Method B was conducted on a Sunfire C18 column (150 mm × 30 mm i.d., 5 μm packing diameter) at ambient temperature eluting with aqueous 0.1% HCO_2H solution (solvent A) and 0.1% HCO_2H solution in acetonitrile (solvent B), using an appropriate elution gradient over 10 min at a flow rate of 40 mL min^{-1} and detecting at 210−350 nm at room temperature. Mass spectra were recorded using electrospray positive and negative modes, alternate scans. The accurate mass measurements were performed on an Orbitrap mass spectrometer. ^{1}H and ^{13}C NMR spectra were recorded at 400, 500, or 600 MHz on Bruker instruments. The chemical shifts are expressed in ppm relative to tetramethylsilane.

(*R*)-3-(3-Cyclopropylphenyl)-4-((*R*)-3-(2-(5,6,7,8-tetrahydro-1,8-naphthyridin-2yl)ethyl)pyrrolidin-1-yl)butanoic Acid (8 Isomer 2 Isomer A Same as 30b). A solution of **19 Isomer 2 Isomer A** (250 mg, 0.559 mmol) in MeOH (20 mL) was treated with 2 M aq NaOH solution (0.559 mL, 1.12 mmol), and the reaction mixture was stirred at 20 °C for 72 h. The reaction mixture was then concentrated in vacuo and the residue was purified by reverse phase chromatography, eluting with MeCN−aqueous 10 mM ammonium bicarbonate solution. The appropriate fractions were combined and concentrated in vacuo to give **8 Isomer 2 Isomer A** (140 mg, 58%) as a solid, identified as (*R*)-3-(3-cyclopropylphenyl)-4-((*R*)-3-(2-(5,6,7,8-tetrahydro-1,8-naphthyridin-2-yl)ethyl)pyrrolidin-1-yl)-butanoic acid (**30b**): LCMS (system A) RT = 0.92 min, 100%, ES+ve *m*/*z* 434 (M + H)$^+$; ^{1}H NMR (CD_3OD, 400 MHz) 7.20−7.14 (1H, m), 7.10 (1H, d, *J* 7.3 Hz), 7.03−6.97 (2H, m), 6.91 (1H, d, *J* 7.3 Hz), 6.35 (1H, d, *J* 7.1 Hz), 3.42−3.32 (5H, m), 3.22−3.06 (3H, m), 2.78−2.62 (4H, m), 2.57−2.46 (3H, m), 2.33−2.22 (1H, m), 2.18−2.06 (1H, m), 1.91−1.81 (3H, m), 1.78−1.69 (2H, m), 1.67−1.56 (1H, m).

(*S*)-3-(3-Cyclopropylphenyl)-4-((*R*)-3-(2-(5,6,7,8-tetrahydro-1,8-naphthyridin-2-yl)ethyl)pyrrolidin-1-yl)butanoic Acid (8 Isomer 2 Isomer B same as 28b). A solution of **19 Isomer 2 Isomer B** (718 mg, 1.60 mmol) was hydrolyzed with 2 M aqueous NaOH solution (1.6 mL, 3.2 mmol) as described above to give **8 Isomer 2 Isomer B** (362 mg, 52%): LCMS (system A) RT = 0.92 min, 100%, ES+ve *m*/*z* 434 (M + H)$^+$; spectroscopic data identical to **28b** data, hence **8 Isomer 2 Isomer B** is (*S*)-3-(3-cyclopropylphenyl)-4-((*R*)-3-(2-(5,6,7,8-tetrahydro-1,8-naphthyridin-2-yl)ethyl)-pyrrolidin-1-yl)butanoic acid.

***tert*-Butyl 3-Ethynylpyrrolidine-1-carboxylate (11).** K_2CO_3 (2.77 g, 20.1 mmol) was added to a solution of *tert*-butyl 3-formylpyrrolidine-1-carboxylate (**9**) (2.0 g, 10 mmol) in MeOH (50 mL). After 5 min dimethyl (1-diazo-2-oxopropyl)phosphonate (**10**)

DOI: 10.1021/acs.jmedchem.8b00959
J. Med. Chem. XXXX, XXX, XXX−XXX

(1.93 g, 10.0 mmol) was added and the reaction mixture stirred at 20 °C for 18 h. The mixture was diluted with Et_2O (100 mL) and aqueous $NaHCO_3$ solution (50 mL). The organic phase was separated and concentrated in vacuo. The residue was purified by chromatography on a silica cartridge (20 g), eluting with EtOAc, and the appropriate fractions were combined and concentrated in vacuo to give **11** (1.74 g, 89%) as an oil: LCMS (system A) RT = 0.88 min, 100%, no mass ion was observed; ^{1}H NMR ($CDCl_3$, 400 MHz) 3.74−3.43 (2H, m), 3.42−3.24 (2H, m), 2.95 (1H, t, *J* 7 Hz), 2.21−2.12 (1H, m), 2.11 (1H, d, *J* 2 Hz), 2.02−1.90 (1H, m), 1.47 (9H, s).

***tert*-Butyl 7-((1-(*tert*-Butoxycarbonyl)pyrrolidin-3-yl)-ethynyl)-3,4-dihydro-1,8-naphthyridine-1(2*H*)-carboxylate (13).** A mixture of **11** (1.74 g, 8.91 mmol), *tert*-butyl 7-chloro-3,4-dihydro-1,8-naphthyridine-1(2*H*)-carboxylate (**12**) (2.395 g, 8.91 mmol), dicyclohexyl(2′,4′,6′-triisopropyl[1,1′-biphenyl]-2-yl)-phosphine (93 mg, 0.20 mmol), K_2CO_3 (3.69 g, 26.7 mmol), and $Pd_2(dba)_3$ (90 mg, 0.098 mmol) in DMA (25 mL) was heated to 100 °C for 4 h. The reaction mixture was concentrated in vacuo and partitioned between DCM (100 mL) and water (100 mL). The aqueous phase was separated and extracted with more DCM (100 mL), and the combined organic phases were concentrated in vacuo. The residue was purified by chromatography on a silica cartridge (100 g), eluting with a gradient of 0−50% EtOAc−cyclohexane. The appropriate fractions were combined and concentrated in vacuo to give **13** (1.7 g, 45%) as an oil: LCMS (system A) RT = 1.37 min, 90%, ES+ve *m*/*z* 428 $(M + H)^+$; ^{1}H NMR ($CDCl_3$, 400 MHz) 7.31 (1H, d, *J* 8 Hz), 7.04 (1H, d, *J* 8 Hz), 3.78−3.73 (2H, m), 3.72−3.48 (2H, m), 3.44−3.33 (2H, m), 3.22−3.13 (1H, m), 2.75 (2H, t, *J* 6.5 Hz), 2.27−2.17 (1H, m), 2.11−2.00 (1H, m), 1.93 (2H, quin, *J* 6.5 Hz), 1.54 (9H, s), 1.47 (9H, s).

***tert*-Butyl 7-(2-(1-(*tert*-Butoxycarbonyl)pyrrolidin-3-yl)-ethyl)-3,4-dihydro-1,8-naphthyridine-1(2*H*)-carboxylate (14) Isomer 1 and Isomer 2.** A solution of **13** (1.7 g, 4.0 mmol) in EtOH (20 mL) was hydrogenated over 10% Pd/C (846 mg) for 18 h. The catalyst was removed by through a Celite cartridge (10 g) and the filtrate was concentrated in vacuo. The residue was purified by column chromatography on silica (100 g) eluting with a gradient of 0−50% EtOAc−cyclohexane. The appropriate fractions were concentrated in vacuo to give (±)-**14** (1.46 g, 85%) as an oil: LCMS (system A) RT = 1.40 min, 94%, ES+ve *m*/*z* 432 $(M + H)^+$; ^{1}H NMR ($CDCl_3$, 400 MHz) 7.29 (1H, d, *J* 8 Hz), 6.80 (1H, d, *J* 8 Hz), 3.79−3.71 (2H, m), 3.64−3.37 (3H, m), 3.31−3.18 (1H, m), 2.98−2.85 (1H, m), 2.77−2.68 (4H, m), 2.25−2.11 (1H, m), 2.07−1.97 (1H, m), 1.92 (2H, quin, *J* 6.5 Hz), 1.87−1.76 (2H, m), 1.51 (9H, s), 1.46 (9H, s). Racemic **14** (1.46 g, 3.38 mmol) was resolved by preparative HPLC on a Chiralpak OJ column (250 mm × 20 mm), flow rate = 20 mL/min, collecting fractions of the first isomer, eluting between 11 and 17.5 min and the second isomer eluting between 22 and 30 min. The fractions were concentrated under reduced pressure to give **14** (Isomer 1, subsequently identified as the *R* enantiomer) (685 mg, 47%), analytical HPLC RT = 14.1 min, 94% on a Chiralpak OJ column (250 mm × 4.6 mm), eluting with 2% IPA-heptanes, flow rate = 1 mL/min, detecting at 215 nm, and **14** (Isomer 2, subsequently identified as the *S* enantiomer) (660 mg, 45%), analytical chiral HPLC RT = 20.2 min, 99%.

(*S*)-7-(2-(Pyrrolidin-3-yl)ethyl)-1,2,3,4-tetrahydro-1,8-naphthyridine, (*S*)-15. A solution of (*S*)-**21** (2.0 g, 6.0 mmol) in DCM (20 mL) was treated with a solution of 4 M HCl in 1,4-dioxane (6 mL), and the mixture was stirred for 16 h before it was concentrated. The residue was partitioned between DCM (50 mL) and aqueous saturated $NaHCO_3$ solution (50 mL). The organic phase was separated and concentrated in vacuo to give (*S*)-**15** (1.3 g, 93%) as a solid: LCMS (system A) RT = 0.70 min, 92%, ES+ve *m*/*z* 232 $(M + H)^+$; ^{1}H NMR (CD_3OD, 400 MHz) 7.14 (1H, d, *J* 7.3 Hz), 6.39 (1H, d, *J* 7.3 Hz), 3.42−3.35 (2H, m), 3.22−2.95 (3H, m), 2.71 (1H, t, *J* 6 Hz), 2.62−2.51 (3H, m), 2.18−2.02 (2H, m), 1.92−1.84 (2H, m), 1.78−1.70 (2H, m), 1.55−1.44 (1H, m).

(*R*)-7-(2-(Pyrrolidin-3-yl)ethyl)-1,2,3,4-tetrahydro-1,8-naphthyridine, (*R*)-15. A solution of (*R*)-*tert*-butyl 3-(2-(5,6,7,8-tetrahydro-1,8-naphthyridin-2-yl)ethyl)pyrrolidine-1-carboxylate (13.0 g, 39.2 mmol) in DCM (60 mL) was treated dropwise with a 4 M HCl solution in 1,4-dioxane (39.2 mL, 157 mmol), and the reaction mixture was stirred overnight. The solvent was removed in vacuo, and the residue was dissolved in MeOH and applied to a preconditioned SCX ion-exchange cartridge (70 g). The cartridge was washed with MeOH (5 CV) and then eluted with 2 M ammonia in MeOH (6 CV). The fractions were combined and concentrated in vacuo to afford (*R*)-**15** (8.5 g, 94%): LCMS (system A) RT = 0.74 min, 100%, ES+ve *m*/*z* 232 $(M + H)^+$; ^{1}H NMR spectrum same as for (*S*)-**15**. HRMS (ESI) calcd for $C_{14}H_{22}N_3$ $(M + H)^+$ 232.1808, found 232.1813.

7-(2-(Pyrrolidin-3-yl)ethyl)-1,2,3,4-tetrahydro-1,8-naphthyridine (15 Isomer 1). 14 (Isomer 1) (685 mg, 1.59 mmol) was dissolved in DCM (5 mL), and 4 M HCl in 1,4-dioxane (1 mL, 4.00 mmol) was added, and the reaction mixture stirred at 20 °C for 18 h. Further 4 M HCl in 1,4-dioxane (1 mL, 4.00 mmol) was added and the reaction mixture stirred for another 6 h. Water (10 mL) was then added followed by 2 M citric acid (pH ∼ 2), and the aqueous phase was separated and the pH adjusted to ∼12 with 2 M aqueous NaOH. DCM (10 mL) was added, and the organic phase was separated. The aqueous phase was extracted with further DCM (10 mL) and the combined organic phases were then concentrated in vacuo to give **15** (Isomer 1) (260 mg, 74%): LCMS (system B) RT = 0.42 min, ES+ve *m*/*z* 232 $(M + H)^+$; ^{1}H NMR ($CDCl_3$, 400 MHz) 7.06 (1H, d, *J* 7.5 Hz), 6.35 (1H, d, *J* 7.5 Hz), 4.77 (1H, br s), 3.40 (2H, td, *J* 5.5, 2.5 Hz), 3.22−3.11 (1H, m), 3.07−2.90 (1H, m), 2.69 (1H, t, *J* 6.5 Hz), 2.61−2.49 (3H, m), 2.08 (1H, dt, *J* 15, 7.5 Hz), 2.02−1.86 (5H, m), 1.78−1.69 (2H, m), 1.46−1.36 (1H, m).

15 Isomer 2 was similarly prepared from **14** (Isomer 2), and spectroscopic data were identical to those of its enantiomer.

(*E*)-Methyl 4-(3-(2-(5,6,7,8-tetrahydro-1,8-naphthyridin-2-yl)ethyl)pyrrolidin-1-yl)but-2-enoate (17). A solution of **15** (Isomer 1) (260 mg, 1.12 mmol) and DIPEA (0.235 mL, 1.35 mmol) in DCM (10 mL) was treated with (*E*)-methyl 4-bromocrotonate (**16**) (0.134 mL, 1.12 mmol), and the reaction mixture was stirred at 20 °C for 2 h. Water (20 mL) was added and the pH adjusted to ∼12 with 2 M aqueous NaOH solution. The aqueous phase was separated and extracted with further DCM (20 mL). The combined organic phases were concentrated in vacuo and purified by chromatography on an aminopropyl cartridge (20 g) eluting with a gradient of 0−50% EtOAc−cyclohexane. Appropriate fractions were concentrated in vacuo to give **17** (Isomer 1, subsequently identified as (*S*)-**17** (140 mg, 38%): LCMS (system A) RT = 1.08 min, 93%, ES+ve *m*/*z* 330 $(M + H)^+$; ^{1}H NMR ($CDCl_3$, 400 MHz) 7.04 (1H, d, *J* 8 Hz), 6.98 (1H, dt, *J* 16, 6 Hz), 6.33 (1H, d, *J* 7 Hz), 5.98 (1H, dt, *J* = 16, 2 Hz), 4.76 (1H, br. s), 3.74 (3H, s), 3.41−3.37 (2H, m), 3.22 (2H, td, *J* = 6, 2 Hz), 2.84 (1H, t, *J* 8 Hz), 2.71−2.65 (3H, m), 2.55−2.41 (3H, m), 2.22−2.11 (2H, m), 2.06−1.96 (1H, m), 1.93−1.86 (2H, m), 1.75−1.68 (2H, m), 1.49−1.40 (1H, m). Anal. chiral HPLC RT = 22 min on Chiralpak AD-H (250 mm × 4.6 mm) eluting with 15% EtOH (containing 0.2% isopropylamine)−heptane, flow rate = 1 mL/min, detecting at 215 nm.

Isomer 2 (*R*)-17 was similarly prepared, and spectroscopic data were identical to (*S*)-**17** data. Anal. chiral HPLC RT = 30 min on Chiralpak AD-H (250 mm × 4.6 mm) eluting with 15% EtOH (containing 0.2% isopropylamine)−heptane, flow rate = 1 mL/min, detecting at 215 nm.

(*S*,*E*)-Methyl 4-(3-(2-(5,6,7,8-Tetrahydro-1,8-naphthyridin-2-yl)ethyl)pyrrolidin-1-yl)but-2-enoate, (*S*)-17. This was obtained from (*S*)-**15** by alkylation to give (*S*)-**17** in 30% yield according to ref 30. Anal. chiral HPLC RT = 22 min, on a Chiralpak AD-H (250 mm × 4.6 mm) eluting with 15% EtOH (containing 0.2% isopropylamine)−heptane, flow rate = 1 mL/min, detecting at 215 nm.

(*R*,*E*)-Methyl 4-(3-(2-(5,6,7,8-Tetrahydro-1,8-naphthyridin-2-yl)ethyl)pyrrolidin-1-yl)but-2-enoate, (*R*)-17. This was similarly obtained to (*S*)-**17** from (*R*)-**15** by alkylation to give (*R*)-**17** according to ref 30.

3-(3-Cyclopropylphenyl)-4-(3-(2-(5,6,7,8-tetrahydro-1,8-naphthyridin-2- yl)ethyl)pyrrolidin-1-yl)butanoic Acid (19)

DOI: 10.1021/acs.jmedchem.8b00959
J. Med. Chem. XXXX, XXX, XXX−XXX

Isomer 1, Mixture of Isomers A and B. *(a) In the Absence of a Chiral Ligand.* (3-Cyclopropylphenyl)boronic acid (**18b**) (207 mg, 1.28 mmol) was added to a mixture of **17** (isomer 1) (140 mg, 0.425 mmol), 3.8 M aqueous KOH solution (47.7 mg, 0.850 mmol), and $[Rh(COD)Cl]_2$ (10.48 mg, 0.021 mmol) in 1,4-dioxane, and the solution was heated to 95 °C for 4 h. The reaction mixture was then concentrated in vacuo, and the residue was dissolved in DCM (20 mL) and water (20 mL). The aqueous phase was separated and further extracted with DCM (20 mL). The combined organic phases were concentrated in vacuo and the residue was purified by chromatography on a silica cartridge, eluting with a gradient of 0−10% MeOH−DCM. The appropriate fractions were combined and concentrated in vacuo to give **19 Isomer 1** (50 mg, 26%) as a 1:1 mixture of isomers **A** and **B** (diastereomers): LCMS (system A) RT = 1.42 min, 87%, ES+ve *m/z* 448 $(M + H)^+$;

(b) In the Presence of (R)-BINAP. A solution of **17** isomer 1 (1.95 g, 5.92 mmol) in 1,4-dioxane (45 mL) was added to a mixture of (3-cyclopropylphenyl)boronic acid (**18b**) (2.88 g, 17.8 mmol), (*R*)-BINAP (737 mg, 1.18 mmol), 3.8 M aqueous KOH (3.12 mL, 11.8 mmol), and $[Rh(COD)Cl]_2$ (292 mg, 0.592 mmol), and the mixture was heated to 95 °C for 4 h under nitrogen. The reaction mixture was allowed to cool to room temperature and concentrated in vacuo. The residue was partitioned between DCM (100 mL) and water (100 mL), and the aqueous phase was extracted with further DCM (100 mL). The combined organic phases were concentrated in vacuo and the residue was purified by chromatography on a silica (100 g) cartridge, eluting with a gradient of 0−25% MeOH−DCM. The appropriate fractions were concentrated in vacuo to give **19** (2.0 g, 75%) as a 23:77 mixture of diastereoisomers by HPLC on Chiralcel OJ (250 mm × 4.6 mm) column, eluting with 40% EtOH−heptane (containing 0.1% isopropylamine) isomer **A**, RT = 8.9 min, 23% and isomer **B**, RT = 16.2 min, 77%. The mixture was separated by preparative chiral HPLC on a Chiralcel OJ-H, column (250 mm × 30 mm), eluting with 30% EtOH−heptane (containing 0.2% isopropylamine), flow rate = 35 mL/min, detecting at 215 nm. Appropriate fractions were combined and concentrated under reduced pressure to give **19 Isomer 1 Isomer A** (250 mg, 12%), Anal. chiral HPLC RT = 8.9 min, 99%; LCMS (system A) RT = 1.44 min, ES+ve *m/z* 448 $(M + H)^+$; ^1H NMR ($CDCl_3$, 400 MHz) 7.20−7.14 (1H, m), 7.06 (1H, d, *J* 7.3 Hz), 7.00−6.96 (1H, m), 6.94−6.91 (1H, m), 6.91−6.87 (1H, m), 6.34 (1H, d, *J* 7.3 Hz), 4.72 (1H, br s), 3.58 (3H, s), 3.43−3.37 (2H, m), 3.33−3.24 (1H, m), 2.92−2.83 (2H, m), 2.75−2.66 (3H, m), 2.62−2.47 (5H, m), 2.42 (1H, dd, *J* 12, 5 Hz), 2.17−2.01 (2H, m), 2.00−1.83 (4H, m), 1.75−1.65 (2H, m), 1.44−1.33 (1H, m), 0.98−0.91 (2H, m), 0.71−0.66 (2H, m), and **19 Isomer 2 Isomer B** (718 mg, 36%), Anal. chiral HPLC RT = 16.2 min, 99%; LCMS (system A) RT = 1.44 min, ES+ve *m/z* 448 $(M + H)^+$; ^1H NMR ($CDCl_3$, 400 MHz) 7.16 (1H, t, *J* 8 Hz), 7.04 (1H, d, *J* 7.3 Hz), 6.96 (1H, d, *J* 8 Hz), 6.91 (1H, br s), 6.89 (1H, d, *J* 8 Hz), 6.33 (1H, d, *J* 7.3 Hz), 4.72 (1H, br s), 3.56 (3H, s), 3.41−3.36 (2H, m), 3.29−3.20 (1H, m), 2.87 (1H, dd, *J* 15, 6 Hz), 2.78−2.65 (5H, m), 2.54−2.45 (3H, m), 2.42−2.30 (2H, m), 2.20−2.06 (2H, m), 1.98−1.82 (4H, m), 1.73−1.63 (2H, m), 1.44−1.35 (1H, m), 0.96−0.90 (2H, m), 0.69−0.64 (2H, m).

(*S*)-*tert*-Butyl 3-(2-(5,6,7,8-Tetrahydro-1,8-naphthyridin-2-yl)ethyl)pyrrolidine-1-carboxylate (*S*)-21. A solution of (*S*)-*tert*-butyl 3-(2-(1,8-naphthyridin-2-yl)ethyl)pyrrolidine-1-carboxylate [(*S*)-**20**][30] (3.2 g, 9.77 mmol) in EtOH (50 mL) was hydrogenated over 10% Pd/C (600 mg) for 16 h. The catalyst was removed by filtration through a Celite cartridge (10 g) and washed with EtOH. The filtrate was concentrated under reduced pressure and the residue was purified by chromatography on a silica cartridge, eluting with 0−15% MeOH−DCM. Appropriate fractions were combined and evaporated to give (*S*)-**21**) (2.0 g, 62%) as a gum: LCMS (system A) RT = 1.24 min, 95%, ES+ve *m/z* 332 $(M + H)^+$; ^1H NMR (CD_3OD, 400 MHz) 7.05 (1H, d, *J* 7 Hz), 6.34 (1H, d, *J* 7.3 Hz), 4.74 (1H, br s), 3.63−3.35 (3H, m), 3.31−3.16 (1H, m), 2.97−2.82 (1H, m), 2.69 (2H, t, *J* 6 Hz), 2.60−2.51 (2H, m), 2.21−2.05 (1H, m), 2.04−1.95 (1H, m), 1.90 (2H, dt, *J* 12, 6 Hz), 1.80−1.63 (4H, m), 1.45 (9H, s). Anal. chiral HPLC RT = 40.1 min, 100%, on a Chiralpak AD column (250 mm × 4.6 mm) eluting with 3% EtOH−heptane, flow rate = 1 mL/min, detecting at 215 nm. The racemate had RT = 35.9 min, 50.4% and RT = 40.7 min, 49.6%.

(*S*)-Methyl 3-(3-Bromophenyl)-4-((*R*)-3-(2-(5,6,7,8-tetrahydro-1,8-naphthyridin-2-yl)ethyl)pyrrolidin-1-yl)butanoate (27a). (*R,E*)-Methyl 4-(3-(2-(5,6,7,8-tetrahydro-1,8-naphthyridin-2-yl)ethyl)pyrrolidin-1-yl)but-2-enoate [(*R*)-**17**] (40 g, 91 mmol), (3-bromophenyl)boronic acid (**18a**) (64.0 g, 319 mmol), 3.8 M aqueous KOH solution (47.9 mL, 182 mmol), (*R*)-BINAP (5.67 g, 9.11 mmol), and $[Rh(COD)Cl]_2$ (2.245 g, 4.55 mmol) in 1,4-dioxane (900 mL) were combined, deoxygenated with argon gas for 30 min, and then the solution was heated to 90 °C for 2 h. After 2 h the reaction mixture was concentrated under reduced pressure, the residue was dissolved in DCM (200 mL) and washed with 1 M HCl solution (1 L), and the phases were separated. The aqueous layer was basified with aqueous 1 M NaOH solution (1 L) and extracted with DCM (3 × 300 mL). The organic layer was dried (Na_2SO_4), filtered, and concentrated in vaccuo. The residue was dissolved in MeOH (100 mL), slurried with Celite (100 g), and purified by reverse-phase chromatography on a column (120 g), eluting with 40−50% water−MeCN to afford a diastereomeric mixture of the product (55 g) as yellow gum. The diastereomers were separated by chiral supercritical fluid chromatography (SFC) on Chiralcel OD-H (250 mm × 30 mm) column, eluting with 85% CO_2−15% (0.5% methanolic ammonia in IPA), flow rate 90 g/min, pressure 90 bar, detecting at 214 nm. The fractions were concentrated to provide **27a** (29.12 g, 66%) as the major isomer: LCMS (system A) RT = 1.45 min, 98%, ES+ve *m/z* 486, 488 $(M + H)^+$; ^1H NMR (DMSO-d_6, 400 MHz) 7.46 (1H, br s), 7.40−7.36 (1H, m), 7.27−7.22 (2H, m), 7.00 (1H, d, *J* 7.3 Hz), 6.26−6.21 (2H, m), 3.48 (3H, s), 3.25−3.13 (3H, m), 2.80 (1H, dd, *J* 15.5, 6 Hz), 2.71−2.52 (6H, m), 2.42−2.29 (4H, m), 2.07 (1H, t, *J* 8.5 Hz), 2.00−1.78 (2H, m), 1.78−1.69 (2H, m), 1.61−1.53 (2H, m), 1.34−1.21 (1H, m). Anal. chiral SFC RT = 7.12 min, 98.4% on a Chiralcel OJ-H (250 mm × 4.6 mm) column, eluting with 75% CO_2−25% (0.5% methanolic ammonia in IPA), flow rate 3 mL/min, pressure 100 bar at 27 °C.

(*S*)-*tert*-Butyl 3-(3-Morpholinophenyl)-4-((*R*)-3-(2-(5, 6, 7, 8-tetrahydro-1, 8-naphthyridin-2-yl)ethyl)pyrrolidin-1-yl)-butanoate (27c). A solution of (3-morpholinophenyl)boronic acid (6.42 g, 31.0 mmol) in aqueous 3.8 M KOH (8.16 mL, 31.0 mmol) was treated with a solution of (*R,E*)-*tert*-butyl 4-(3-(2-(1,8-naphthyridin-2-yl)ethyl)pyrrolidin-1-yl)but-2-enoate [(*R*)-**24** *tert*-butyl ester] (6.7 g, 15.5 mmol) in 1,4-dioxane (70 mL) and deoxygenated by evacuation under reduced pressure and nitrogen purging for 5 min. $[Rh(COD)Cl]_2$ (0.382 g, 0.775 mmol) and (*R*)-BINAP (0.965 g, 1.55 mmol) were added, and the mixture was deoxygenated for a further 5 min. The solution was heated at 90 °C for 60 min, cooled to room temperature, and then the reaction mixture was partitioned between DCM and water. The aqueous phase was extracted with more DCM and the combined DCM extracts were evaporated in vacuo. The residue (11.6 g) was purified by chromatography on an aminopropyl cartridge (50 g) eluting with a gradient of 0−50% EtOAc−cyclohexane over 40 min. The appropriate fractions were combined and evaporated in vacuo to give 5.61 g of brown oil. Analytical chiral HPLC on Chiralpak AD-H column (250 mm × 4.6 mm) eluting isocratically with 50% EtOH (containing 0.2% isopropylamine)−heptane, flow rate = 1.0 mL/min, detecting at 215 nm indicated a mixture of two diastereoisomers: RT = 6.99 min, 91% and RT = 12.2 min, 9%. The mixture was separated by preparative HPLC on a Chiralpak AD-H column (250 mm × 30 mm), eluting with 40% EtOH (containing 0.2% isopropylamine)−heptanes, flow rate = 30 mL/min, detecting at 230 nm, collecting fractions of the major component (RT = 6.5−10 min). The combined fractions were evaporated under reduced pressure to give (*S*)-*tert*-butyl 4-((*R*)-3-(2-(1, 8-naphthyridin-2-yl)ethyl)pyrrolidin-1-yl)-3-(3-morpholinophenyl)butanoate (**25c**) (4.18 g, 51%) as the major isomer: LCMS (system A) RT = 1.20 min, 94%, ES+ve *m/z* 531 $(M + H)^+$; $[\alpha]_D^{20}$ +10 (*c* 1.0 in EtOH); Anal. chiral HPLC RT = 7.2 min, >99.5% on Chiralpak AD-H. ^1H NMR ($CDCl_3$, 400 MHz) 9.07 (1H, dd, *J* 4, 2 Hz), 8.14 (1H, dd, *J* 8, 2 Hz), 8.08 (1H, d, *J* 8 Hz), 7.43

DOI: 10.1021/acs.jmedchem.8b00959
J. Med. Chem. XXXX, XXX, XXX−XXX

(1H, dd, *J* 8, 4 Hz), 7.37 (1H, d, *J* 8 Hz), 7.18 (1H, t, *J* 7.5 Hz), 6.78–6.71 (3H, m), 3.87–3.81 (4H, m), 3.25–3.10 (5H, m), 3.07–2.98 (2H, m), 2.85–2.68 (4H, m), 2.48–2.32 (3H, m), 2.27–2.12 (2H, m), 2.04–1.90 (2H, m), 1.52–1.40 (2H, m), 1.28 (9H, s).

Evaporation of the fractions with RT = 14–21 min gave the minor diastereoisomer (*R*)-*tert*-butyl 4-((*R*)-3-(2-(1, 8-naphthyridin-2-yl)-ethyl)pyrrolidin-1-yl)-3-(3-morpholinophenyl)butanoate **26c** (462 mg, 6%) as an oil. Anal. chiral HPLC RT = 12.2 min, 98.5%.

A solution of (*S*)-*tert*-butyl 4-((*R*)-3-(2-(1,8-naphthyridin-2-yl)-ethyl)pyrrolidin-1-yl)-3-(3-morpholinophenyl)butanoate (**25c**) (4.18 g, 7.88 mmol) was hydrogenated in EtOH (20 mL) over 10% Pd/C (838 mg) for 60 h. The catalyst was removed by filtration through a Celite cartridge (10 g) and washed with EtOH. The combined filtrate and washings were evaporated in vacuo to give **27c** (3.48 g, 83%) as an oil: LCMS (system A) RT = 1.36 min, 96%, ES+ve *m/z* 535 $(M + H)^+$; ^{1}H NMR (DMSO-d_6, 400 MHz) 7.12 (1H, t, *J* 8 Hz), 7.01 (1H, d, *J* 7.3 Hz), 6.81–6.72 (2H, m), 6.66 (1H, d, *J* 8 Hz), 6.24 (1H, d, *J* 7.3 Hz), 6.19 (1H, m), 3.77–3.68 (4H, m), 3.26–3.20 (2H, m), 3.12–3.02 (5H, m), 2.74–2.56 (6H, m), 2.43–2.29 (5H, m), 2.07 (1H, m), 2.03–1.83 (2H, m), 1.79–1.69 (2H, m), 1.63–1.54 (2H, m), 1.26 (9H, s), 1.35–1.20 (1H, m).

(*S*)-*tert*-Butyl 3-(3-(5-Methyl-1*H*-pyrazol-1-yl)phenyl)-4-((*R*)-3-(2-(5,6,7,8-tetrahydro-1,8-naphthyridin-2-yl)ethyl)-pyrrolidin-1-yl)butanoate (27g). Prepared from (*R*)-**24** *tert*-butyl ester and (3-(5-methyl-1*H*-pyrazol-1-yl)phenyl)boronic acid (**18g**) followed by hydrogenation over 10% Pd/C by the method described above for **27c**: LCMS (system A) RT = 1.40 min, 95%, ES+ve *m/z* 530 $(M + H)^+$; ^{1}H NMR ($CDCl_3$, 600 MHz) 7.57 (1H, d, *J* 1.5 Hz), 7.41–7.36 (1H, m), 7.32–7.27 (2H, m, 2H), 7.24 (1H, d, *J* 7.7 Hz), 7.04 (1H, d, *J* 7.3 Hz), 6.33 (1H, d, *J* 7.3 Hz), 6.19 (1H, d, *J* 1 Hz), 4.78 (1H, br s), 3.44–3.35 (2H, m), 3.31 (1H, tt, *J* 9, 6 Hz), 2.86 (1H, dd, *J* 15, 6 Hz), 2.78 (1H, t, *J* 8 Hz), 2.75–2.65 (4H, m), 2.55–2.42 (4H, m), 2.39–2.34 (1H, m), 2.33 (3H, s), 2.18–2.14 (1H, m), 2.14–2.07 (1H, m), 1.98–1.92 (1H, m), 1.90 (2H, dt, *J* 12, 6 Hz), 1.74–1.62 (2H, m), 1.44–1.36 (1H, m), 1.30 (9H, s); ^{13}C NMR ($CDCl_3$, 151 MHz) 171.8, 158.3, 155.7, 144.7, 139.9, 139.7, 138.7, 136.6, 128.8, 127.2, 124.1, 123.0, 113.1, 111.2, 106.7, 80.1, 62.4, 60.9, 54.0, 41.7, 41.6, 40.3, 37.3, 36.7, 35.7, 30.8, 28.0, 26.3, 21.5, 12.4. HRMS (ESI) calcd for $C_{32}H_{44}N_5O_2$ $(M + H)^+$ 530.3490, found 530.3479.

(*S*)-*tert*-Butyl 3-(3-(3,5-Dimethyl-1*H*-pyrazol-1-yl)-5-morpholinophenyl)-4-((*R*)-3-(2-(5,6,7,8-tetrahydro-1,8-naphthyridin-2-yl)ethyl)pyrrolidin-1-yl)butanoate (27ch). Prepared from (*R*,*E*)-**24** *tert*-butyl ester and 4-(3-(3,5-dimethyl-1*H*-pyrazol-1-yl)-5-(4,4,5,5-tetramethyl-1,3,2-dioxaborolan-2-yl)phenyl)-morpholine, the resulting mixture of diastereoisomers was separated by HPLC on a Chiralpak AD-H column (250 mm × 30 mm) eluting with 10% EtOH (containing 0.2% isopropylamine–heptane, flow rate = 40 mL/min, detecting at 215 nm, collecting fractions containing the major isomer (RT = 25–35 min). The fractions were concentrated under reduced pressure to give *tert*-butyl 4-(3-(2-(1,8-naphthyridin-2-yl)ethyl)pyrrolidin-1-yl)-3-(3-(3,5-dimethyl-1*H*-pyrazol-1-yl)-5-morpholinophenyl)butanoate **25ch** (134 mg). LCMS (system C) RT = 0.83 min, 100%, ES+ve *m/z* 625 $(M + H)^+$; IR ν_{max} (solid) 1719, 1602, 1149, 1122, 843 cm^{-1}; ^{1}H NMR ($CDCl_3$, 600 MHz) 9.07 (1H, dd, *J* 4, 2 Hz), 8.15 (1H, dd, *J* 8, 2 Hz), 8.09 (1H, d, *J* 8 Hz), 7.44 (1H, dd, *J* 8, 4 Hz), 7.37 (1H, d, *J* 8 Hz), 6.80 (1H, s), 6.78 (1H, br s), 6.72 (1H, s), 5.96 (1H, s), 3.88–3.79 (4H, m), 3.35–3.24 (1H, m), 3.21–3.16 (4H, m), 3.10–2.95 (2H, m), 2.82 (1H, dd, *J* 15, 6 Hz), 2.85–2.77 (1H, m), 2.77–2.73 (1H, m), 2.76–2.70 (1H, m), 2.56–2.47 (1H, m), 2.46–2.38 (1H, m), 2.43–2.35 (1H, m), 2.29–2.25 (4H, m), 2.27–2.20 (1H, m), 2.25–2.15 (1H, m), 2.03–1.98 (1H, m), 1.98–1.91 (2H, m), 1.44 (1H, s), 1.31 (9H, s); ^{13}C NMR ($CDCl_3$, 151 MHz) 179.1, 156.0, 153.3, 151.9, 148.7, 139.4, 137.0, 136.9, 136.6, 122.5, 121.4, 121.1, 115.3, 114.6, 110.6, 106.7, 66.8, 49.1, 42.0, 40.4, 37.3, 30.8, 28.0, 13.5, 12.4. HRMS (ESI) calcd for $C_{37}H_{49}N_6O_3$ $(M + H)^+$ 625.3861, found 625.3844. Anal. chiral HPLC RT = 17 min, >99.5% on a Chiralpak AD-H column (250 mm × 4.6 mm) eluting with 15% EtOH (containing 0.2% isopropylamine–heptane, flow rate = 1 mL/min, detecting at 215 nm. Hydrogenation of **25ch** (100 mg, 0.16 mmol) over Rh/C gave **27ch** (89 mg, 88%): LCMS (system A) RT = 1.42 min, 97%, ES+ve *m/z* 629 $(M + H)^+$; ^{1}H NMR (DMSO-d_6, 400 MHz) 6.99 (1H, d, *J* 7.3 Hz), 6.80 (1H, s), 6.77 (1H, s), 6.72 (1H, s), 6.22 (1H, *J* 7.3 Hz), 6.19 (1H, br), 6.02 (1H, s), 3.75–3.70 (4H, m), 3.25–3.20 (2H, m), 3.16–3.10 (4H, m), 2.78–2.56 (7H, m), 2.48–2.31 (5H, m), 2.24 (3H, s), 2.16 (3H, s), 2.11–2.03 (1H, m), 2.01–1.79 (2H, m), 1.78–1.70 (2H, m), 1.62–1.54 (2H, m), 1.34–1.26 (1H, m), 1.25 (9H, s). HRMS (ESI) calcd for $C_{37}H_{53}N_6O_3$ $(M + H)^+$ 629.4174, found 629.4167.

(*S*)-3-(3-Bromophenyl)-4-((*R*)-3-(2-(5,6,7,8-tetrahydro-1,8-naphthyridin-2-yl)ethyl)pyrrolidin-1-yl)butanoic Acid (28a). A solution of **27a** (104 mg, 0.214 mmol) in MeOH (3 mL) was stirred with aqueous 2 M NaOH solution (1 mL, 2 mmol) for 3.5 h. The reaction mixture was diluted with water (2 mL), and 2 M hydrochloric acid was added to pH 7 and then concentrated in vacuo. The residue was purified by MDAP (method B, HpH). Relevant fractions were combined and concentrated in vacuo to afford **28a** (27.3 mg, 27%): LCMS (system A) RT = 0.90 min, 98%, ES+ve *m/z* 472, 474 $(M + H)^+$; ^{1}H NMR (DMSO-d_6, 400 MHz) 7.45 (1H, s), 7.40–7.36 (1H, m), 7.30–7.24 (2H, m), 7.01 (1H, d, *J* 7 Hz), 6.31–6.22 (2H, m), 3.26–3.15 (4H, m), 2.86–2.72 (3H, m), 2.71–2.56 (4H, m), 2.56–2.46 (m, obscured by solvent), 2.45–2.30 (3H, m), 2.29–2.20 (1H, m), 2.07–1.95 (1H, m), 1.93–1.83 (1H, m), 1.78–1.69 (2H, m), 1.67–1.54 (2H, m), 1.38–1.26 (1H, m); HRMS (ESI) calcd for $[M + H^+]$ ($C_{24}H_{31}BrN_3O_2$) requires 472.1600, found 472.1602.

(*S*)-3-(3-Cyclopropylphenyl)-4-((*R*)-3-(2-(5,6,7,8-tetrahydro-1,8-naphthyridin-2-yl)ethyl)pyrrolidin-1-yl)butanoic Acid (28b). Prepared from (*R*)-**17**: LCMS (system A) RT = 0.92 min, 100%, ES+ve *m/z* 434 $(M + H)^+$; IR ν_{max} (solid) 3300–2500, 1672, 1599, 704 cm^{-1}; $[\alpha]_D^{25}$ +30 (*c* 1.00 in EtOH); ^{1}H NMR (CD_3OD, 600 MHz) 7.19 (1H, t, *J* 7.6 Hz), 7.12 (1H, d, *J* 7.3 Hz), 7.01 (1H, d, *J* 7.7 Hz), 6.99 (1H, s), 6.93 (1H, d, *J* = 7.9 Hz), 6.37 (1H, d, *J* 7.3 Hz), 3.51 (1H, dd, *J* 12.7, 9.4 Hz), 3.37–3.33 (3H, m), 3.33–3.31 (1H, m), 3.26 (2H, br. s), 3.16 (1H, dd, *J* 12.7, 3.9 Hz), 2.95 (1H, t, *J* 8.6 Hz), 2.79 (1H, dd, *J* 16.3, 10.5 Hz), 2.67 (2H, t, *J* 6.2 Hz), 2.57 (1H, dd, *J* 16.8, 3.2 Hz), 2.55–2.51 (2H, m), 2.30 (1H, spt, *J* 7.9 Hz), 2.21–2.13 (1H, m), 1.91–1.87 (1H, m), 1.87–1.82 (2H, m), 1.81–1.71 (2H, m), 1.65 (1H, dq, *J* = 12.9, 8.5 Hz), 0.99–0.87 (2H, m), 0.72–0.62 (2H, m); HRMS (ESI) calcd for $C_{27}H_{36}N_3O_2$ $(M + H)^+$ 434.2802, found 434.2795.

(*S*)-3-(3-Morpholinophenyl)-4-((*R*)-3-(2-(5,6,7,8-tetrahydro-1,8-naphthyridin-2-yl)ethyl)pyrrolidin-1-yl)butanoic Acid (28c). A solution of **27c** *tert*-butyl ester (3.48 g, 6.51 mmol) in DCM (30 mL) was treated with trifluoroacetic acid (20 mL) and stirred at room temperature for 1.5 h. The solvent was evaporated in vacuo, the residue was dissolved in EtOH (10 mL) and purified on a SCX-2 ion-exchange cartridge (70 g), eluting with ethanol (3CV) and then 2 M NH_3 in MeOH (3CV). The basic fractions were combined and evaporated in vacuo, and the residue (3.17 g) was further purified by reverse-phase chromatography on a C18 cartridge (120 g), eluting with a gradient of 15–40% MeCN (containing 0.1% aq NH_3–10 mM aq NH_4HCO_3 solution) over 10CV. The appropriate fractions were combined and evaporated in vacuo to give **28c** (2.1 g, 67%) as a white solid: LCMS (system A) RT = 0.77 min, 100%, ES+ve *m/z* 479 $(M + H)^+$; IR ν_{max} (neat) 3300–2500, 1673, 1598, 1118, 700 cm^{-1}; $[\alpha]_D^{25}$ +29 (*c* 1.02 in EtOH); ^{1}H NMR (CD_3OD, 600 MHz) 7.21 (1H, t, *J* 7.5 Hz), 7.13 (1H, d, *J* 7.5 Hz), 6.87–6.84 (2H, m), 6.74 (1H, d, *J* 7.5 Hz), 6.37 (1H, d, *J* 7.5 Hz), 3.84–3.80 (4H, m), 3.55 (1H, dd, *J* 12.5, 9.5 Hz), 3.39–3.35 (3H, m), 3.34–3.28 (m, obscured by solvent), 3.20 (1H, dd, *J* 12.5, 4 Hz), 3.16–3.12 (4H, m), 3.04–2.95 (1H, br), 2.81 (1H, dd, *J* 16.5, 10.5 Hz), 2.68 (2H, t, *J* 6 Hz), 2.63–2.52 (3H, m), 2.35–2.28 (1H, m), 2.24–2.17 (1H, m), 1.90–1.83 (2H, m), 1.82–1.73 (2H, m), 1.71–1.64 (1H, m); ^{13}C NMR (CD_3OD, 151 MHz) 180.3, 157.4, 157.3, 153.6, 144.8, 138.8, 131.0, 119.6, 116.0, 115.9, 115.8, 112.2, 68.1, 63.4, 59.9, 55.1, 50.7, 46.2, 42.5, 41.3, 38.2, 36.4, 34.7, 31.0, 27.5, 22.5. HRMS (ESI) calcd for $C_{28}H_{38}N_4O_3$ $(M + H)^+$ 479.3017, found 479.3012.

(*S*)-3-(3-Morpholinophenyl)-4-((*S*)-3-(2-(5,6,7,8-tetrahydro-1,8-naphthyridin-2-yl)ethyl)pyrrolidin-1-yl)butanoic Acid

DOI: 10.1021/acs.jmedchem.8b00959
J. Med. Chem. XXXX, XXX, XXX–XXX

(ent-28c). These are the data for the title compound prepared according to a similar route to that shown in Scheme 1. LCMS (system A) RT = 0.78 min, 100%, ES+ve *m/z* 479 $(M + H)^+$; ^{1}H NMR (CD_3OD, 400 MHz) 7.24 (1H, t, *J* 7.5 Hz), 7.14 (1H, d, *J* 7.3 Hz), 6.90−6.84 (2H, m), 6.77 (1H, d, *J* 7.5 Hz), 6.39 (1H, d, *J* 7.3 Hz), 3.86−3.80 (4H, m), 3.62−3.49 (2H, m), 3.42−3.34 (4H, m), 3.30−3.20 (2H, m), 3.18−3.12 (4H, m), 2.91−2.77 (2H, m), 2.71 (2H, t, *J* 6 Hz), 2.65−2.51 (3H, m), 2.42−2.30 (1H, m), 2.27−2.15 (1H, m), 1.92−1.83 (2H, m), 1.82−1.66 (3H, m).

(*S*)-3-(3-(1*H*-Pyrazol-1-yl)phenyl)-4-((*R*)-3-(2-(5,6,7,8-tetrahydro-1,8-naphthyridin-2-yl)ethyl)pyrrolidin-1-yl)butanoic Acid (28d). Prepared from (*R*)-**17**: LCMS (system A) RT = 0.82 min, 99%, ES+ve *m/z* 460 $(M + H)^+$; ^{1}H NMR (CD_3OD, 400 MHz) 8.23 (1H, d, *J* 2.5 Hz), 7.72 (1H, m), 7.68 (1H, m), 7.63 (1H, br d, *J* 8 Hz), 7.46 (1H, t, *J* 8 Hz), 7.25 (1H, br d, *J* 7.5 Hz), 7.15 (1H, d, *J* 7.5 Hz), 6.52 (1H, m), 6.38 (1H, d, *J* 7.5 Hz), 3.64−3.45 (2H, m), 3.39−3.32 (5H, m), 3.31−3.26 (1H, obscured by solvent), 3.15−3.06 (1H, m), 2.88 (1H, dd, *J* 16.5, 10 Hz), 2.71−2.61 (3H, m), 2.56 (2H, t, *J* 8 Hz), 2.40−2.28 (1H, m), 2.26−2.16 (1H, m), 1.90−1.61 (5H, m). HRMS (ESI) calcd for $C_{27}H_{34}N_5O_2$ $(M + H)^+$ 460.2707, found 460.2710. Anal. chiral HPLC RT = 17.2 min, 99.5% on a Chiralcel OJ-H column (250 mm × 4.6 mm) eluting with 30% EtOH (containing 0.2% isopropylamine)−heptane, flow rate = 1 mL/min, detecting at 215 nm.

(*S*)-3-(3-(3-Methyl-1*H*-pyrazol-1-yl)phenyl)-4-((*R*)-3-(2-(5,6,7,8-tetrahydro-1,8-naphthyridin-2-yl)ethyl)pyrrolidin-1-yl)butanoic Acid (28e). Prepared from (*R*)-**17**: LCMS (system A) RT = 0.90 min, 100%, ES+ve *m/z* 474 $(M + H)^+$; ^{1}H NMR (DMSO-d_6, 600 MHz) 8.35 (1H, d, *J* = 2.4 Hz), 7.65 (1H, t, *J* 1.5 Hz), 7.60 (1H, dd, *J* = 8, 1.5 Hz), 7.36 (1H, t, *J* 8 Hz), 7.12 (1H, d, *J* 8 Hz), 7.01 (1H, d, *J* 7.5 Hz), 6.31 (1H, d, *J* 2.5 Hz), 6.25 (1H, br s), 6.24 (1H, d, *J* 7.5 Hz), 3.28−3.24 (1H, m), 3.22 (2H, br dd, *J* 8, 3 Hz), 2.87 (1H, dd, *J* 12, 10 Hz), 2.84−2.80 (1H, m), 2.82−2.77 (1H, m), 2.73−2.67 (1H, m), 2.59 (2H, t, *J* 6 Hz), 2.57−2.53 (2H, m), 2.44 (1H, dd, *J* 16, 7 Hz), 2.40 (2H, t, *J* 8 Hz), 2.33−2.28 (1H, m), 2.27 (3H, s), 2.07−1.97 (1H, m), 1.94−1.85 (1H, m), 1.74 (2H, quin, *J* 6 Hz), 1.68−1.54 (2H, m), 1.39−1.30 (1H, m); ^{13}C NMR (DMSO-d_6, 151 MHz) 173.5, 157.2, 155.7, 149.4, 145.2, 139.7, 136.0, 129.3, 128.2, 124.5, 116.8, 115.9, 112.3, 109.8, 107.5, 61.6, 59.3, 53.2, 40.6, 40.5, 40.4, 36.5, 35.8, 34.9, 30.2, 25.9, 21.0, 13.4. HRMS (ESI) calcd for $C_{28}H_{36}N_5O_2$ $(M + H)^+$ 474.2864, found 474.2856. Anal. chiral HPLC RT = 18.5 min, 98.6% on a Chiralcel OD-H column (250 mm × 4.6 mm) eluting 50% EtOH (containing 0.2% isopropylamine)−heptane, flow rate = 1 mL/min, detecting at 215 nm.

(*S*)-3-(3-(4-Methyl-1*H*-pyrazol-1-yl)phenyl)-4-((*R*)-3-(2-(5,6,7,8-tetrahydro-1,8-naphthyridin-2-yl)ethyl)pyrrolidin-1-yl)butanoic Acid (28f). Prepared from (*R*)-**17**: LCMS (system A) RT = 0.86 min, 95%, ES+ve *m/z* 474 $(M + H)^+$; IR ν_{max} (neat): 3600−2200, 1672, 1590 cm^{-1}; ^{1}H NMR (CD_3OD, 600 MHz) 8.04 (1H, s), 7.64 (1H, s), 7.60 (1H, d, *J* 8 Hz), 7.55 (1H, s), 7.40 (1H, t, *J* 8 Hz), 7.24 (1H, d, *J* 8 Hz), 7.14 (1H, t, *J* 7 Hz), 6.39 (1H, t, *J* 7.5 Hz), 3.54−3.46 (2H, m), 3.38 (3H, m), 3.36 (m, obscured by solvent), 3.30−3.20 (3H, m), 2.95−2.74 (2H, m), 2.71 (2H, m), 2.67−2.62 (1H, m), 2.59−2.53 (2H, m), 2.37−2.28 (1H, m), 2.23−2.13 (1H, m), 2.19 (3H, s), 1.92−1.86 (2H, m), 1.85−1.63 (3H, m). HRMS (ESI) calcd for $C_{28}H_{36}N_5O_2$ $(M + H)^+$ 474.2864, found 474.2852.

(*S*)-3-(3-(5-Methyl-1*H*-pyrazol-1-yl)phenyl)-4-((*R*)-3-(2-(5,6,7,8-tetrahydro-1,8-naphthyridin-2-yl)ethyl)pyrrolidin-1-yl)butanoic Acid (28g). Prepared from **25g**: LCMS (system A) RT = 0.82 min, 100%, ES+ve *m/z* 474 $(M + H)^+$; IR ν_{max} (neat) 3300−2500, 1678, 1591 cm^{-1}; $[\alpha]_D^{25}$ +32 (*c* 0.96 in EtOH); ^{1}H NMR ($CDCl_3$, 600 MHz) 7.57 (1H, s), 7.42−7.39 (1H, m), 7.30 (1H, d, *J* 2 Hz), 7.29 (1H, s), 7.23 (1H, d, *J* 7.7 Hz), 7.13 (1H, d, *J* 7 Hz), 6.28 (1H, d, *J* 7.3 Hz), 6.20 (1H, s), 3.60−3.55 (1H, m), 3.57 (1H, br. s), 3.42 (2H, t, *J* 5 Hz), 3.01−2.95 (1H, m), 2.99−2.95 (1H, m), 2.76 (1H, d, *J* 9 Hz), 2.79 (1H, br. s), 2.73 (1H, s), 2.70 (2H, t, *J* 6 Hz), 2.52−2.47 (1H, m), 2.43 (1H, td, *J* 12.5, 6 Hz), 2.38−2.34 (3H, m), 2.13−2.08 (1H, m), 2.05−1.99 (1H, m), 2.01 (1H, br. s), 1.91 (2H, br. s), 1.91−1.87 (1H, m), 1.58−1.51 (1H, m), 1.44−1.37 (1H, m); ^{13}C NMR ($CDCl_3$, 151 MHz) 178.6, 154.6, 153.8, 146.4, 140.1, 139.8, 138.7, 138.4, 129.2, 126.5, 123.8, 122.8, 116.0, 109.9, 106.9, 64.4, 56.5, 54.6, 44.3, 41.1, 40.5, 37.4, 37.3, 34.3, 30.7, 26.0, 20.5, 12.5. HRMS (ESI) calcd for $C_{28}H_{36}N_5O_2$ $(M + H)^+$ 474.2864, found 474.2852.

(*S*)-3-(3-(3,5-Dimethyl-1*H*-pyrazol-1-yl)phenyl)-4-((*R*)-3-(2-(5,6,7,8-tetrahydro-1,8-naphthyridin-2-yl)ethyl)pyrrolidin-1-yl)butanoic Acid (28h). Prepared from (*R*)-**17**:[30] LCMS (system A) RT = 0.89 min, 100%, ES+ve *m/z* 488 $(M + H)^+$; ^{1}H NMR (DMSO-d_6, 600 MHz) 7.40 (1H, t, *J* 8 Hz), 7.34 (1H, s), 7.30 (1H, d, *J* 8.5 Hz), 7.25 (1H, d, *J* 8 Hz), 7.02 (1H, d, *J* 7.3 Hz), 6.32 (2H, br), 6.25 (1H, d, *J* 7.3 Hz), 6.05 (1H, s), 3.33−3.26 (2H, m), 3.25−3.21 (2H, m), 2.94−2.88 (1H, m), 2.86−2.79 (2H, m), 2.75−2.70 (1H, m), 2.67−2.57 (4H, m), 2.46 (1H, dd, *J* 16, 7.5 Hz), 2.40 (2H, t, *J* 8 Hz), 2.38−2.32 (1H, m), 2.27 (3H, s), 2.17 (3H, s), 2.07−1.98 (1H, m), 1.94−1.87 (1H, m), 1.76−1.71 (2H, m), 1.65−1.56 (2H, m), 1.39−1.32 (1H, m); HRMS (ESI) calcd for $C_{29}H_{38}N_5O_2$ $(M + H)^+$ 488.3020, found 488.3030. Anal. chiral HPLC RT = 12.5 min, 100% on a Chiralpak column (250 mm × 4.6 mm) eluting with 30% EtOH (containing 0.1% isopropylamine)−heptane, flow rate = 1 mL/min, detecting at 235 nm. For additional characterizing data on the corresponding hydrochloride see ref 30.

(*S*)-3-(3-(3-Methyl-1*H*-pyrazol-5-yl)phenyl)-4-((*R*)-3-(2-(5,6,7,8-tetrahydro-1,8-naphthyridin-2-yl)ethyl)pyrrolidin-1-yl)butanoic Acid (28j). A solution of (*S*)-methyl 3-(3-bromophenyl)-4-((*R*)-3-(2-(5,6,7,8-tetrahydro-1,8-naphthyridin-2-yl)ethyl)-pyrrolidin-1-yl)butanoate (**25a**) (51.2 mg, 0.105 mmol) and 3-methyl-5-(4,4,5,5-tetramethyl-1,3,2-dioxaborolan-2-yl)-1*H*-pyrazole (88 mg, 0.421 mmol) in EtOH (1.6 mL) was treated with K_3PO_4 (67.0 mg, 0.316 mmol) and water (0.4 mL) and chloro(dinorbonylphosphino)(2′-dimethylamino-1,1′-biphenyl-2-yl)palladium(II) (5.9 mg, 0.01 mmol), and the mixture was heated at 130 °C for 30 min under microwave irradiation. The reaction mixture was passed through a silica cartridge (2 g) and washed with MeOH. The filtrate was concentrated in vacuo, and the residue was purified by MDAP (method high pH). The appropriate fractions were combined and concentrated in vacuo to give **28j** (15.8 mg, 32%): LCMS (system A) RT = 0.83 min, 100%, ES+ve *m/z* 474 $(M + H)^+$; ^{1}H NMR (DMSO-d_6, 400 MHz) 7.61 (1H, s), 7.56 (1H, br d, *J* 7.5 Hz), 7.29 (1H, t, *J* 7.5 Hz), 7.14 (1H, br d, *J* 7.5 Hz), 7.01 (1H, d, *J* 7.5 Hz), 6.44 (1H, s), 6.32 (1H, br s), 6.25 (1H, d, *J* 7.5 Hz), 3.26−3.18 (4H, m), 2.93−2.88 (1H, m), 2.85−2.78 (2H, m), 2.76−2.70 (1H, m), 2.62−2.55 (4H, m), 2.55−2.51 (1H, m), 2.46−2.39 (3H, m), 2.37−2.32 (1H, m), 2.24 (3H, s), 2.07−1.98 (1H, m), 1.95−1.88 (1H, m), 1.77−1.70 (2H, m), 1.67−1.55 (2H, m), 1.39−1.31 (1H, m).

(*S*)-3-(3-(1,4-Dimethyl-1*H*-pyrazol-5-yl)phenyl)-4-((*R*)-3-(2-(5,6,7,8-tetrahydro-1,8-naphthyridin-2-yl)ethyl)pyrrolidin-1-yl)butanoic Acid (28k). Prepared from **25a** and 1,4-dimethyl-5-(4,4,5,5-tetramethyl-1,3,2-dioxaborolan-2-yl)-1*H*-pyrazole by the method described for **28j**: LCMS (system A) RT = 0.85 min, 98%, ES+ve *m/z* 488 $(M + H)^+$; ^{1}H NMR (DMSO-d_6, 400 MHz) 7.50 (1H, t, *J* 7.5 Hz), 7.43 (1H, br d, *J* 7.5 Hz), 7.39 (1H, br s), 7.34 (1H, s), 7.32 (1H, br d, *J* 7.5 Hz), 7.20 (1H, br d, *J* 7 Hz), 6.36 (1H, br d, *J* 7 Hz), 3.71 (3H, s), 3.66−2.93 (br obscured by water), 2.83 (1H, dd, *J* 16.5, 6 Hz), 2.66−2.62 (2H, m), 2.59 (1H, dd, *J* 16.5, 7.5 Hz), 2.55−2.45 (m, obscured by solvent), 2.24−2.15 (1H, m), 2.10−2.02 (1H, m), 1.98 (3H, s), 1.80−1.74 (2H, m), 1.70−1.63 (2H, m), 1.59−1.49 (1H, m). HRMS (ESI) calcd for $C_{29}H_{38}N_5O_2$ $(M + H)^+$ 488.3020, found 488.3028.

(*S*)-3-(3-(4*H*-1,2,4-Triazol-4-yl)phenyl)-4-((*R*)-3-(2-(5,6,7,8-tetrahydro-1,8-naphthyridin-2-yl)ethyl)pyrrolidin-1-yl)-butanoic Acid (28l). Prepared from (*R*)-**17**: LCMS (system C) RT = 0.34 min, 98%, ES+ve *m/z* 461 $(M + H)^+$; ^{1}H NMR ($CDCl_3$, 500 MHz) 8.49 (2H, s), 7.45 (1H, t, *J* 8 Hz), 7.34 (1H, d, *J* 8 Hz), 7.27 (1H, s), 7.20 (1H, d, *J* 8 Hz), 7.17 (1H, d, *J* 7 Hz), 6.27 (1H, br d, *J* 7 Hz), 3.67−3.60 (1H, m), 3.60−3.52 (1H, m), 3.45−3.38 (2H, m), 2.98−2.88 (2H, m), 2.80 (1H, t, *J* 12.5 Hz), 2.74−2.61 (4H, m), 2.48−2.40 (2H, m), 2.33−2.24 (1H, m), 2.13−1.81 (6H, m), 1.58−1.46 (1H, m), 1.45−1.34 (1H, m); ^{13}C NMR ($CDCl_3$, 126 MHz) 179.6, 154.1, 152.2, 148.5, 141.4, 139.0, 133.9, 130.3, 127.9, 121.5, 119.8, 116.5, 109.4, 64.1, 56.2, 54.9, 43.9, 40.9, 37.8, 37.4, 33.5, 30.8, 25.9, 20.1, 18.4. Anal. chiral HPLC RT = 13.5 min, 97% on a

DOI: 10.1021/acs.jmedchem.8b00959
J. Med. Chem. XXXX, XXX, XXX−XXX

Chiralpak ID column (250 mm × 4.6 mm) eluting with 50% EtOH (containing 0.2% isopropylamine)−heptane, flow rate = 1.0 mL/min, detecting at 215 nm. HRMS (ESI) calcd for $C_{26}H_{33}N_6O_2$ $(M + H)^+$ 461.2665, found 461.2664.

(*S*)-3-(3-(1*H*-1,2,4-Triazol-1-yl)phenyl)-4-((*R*)-3-(2-(5,6,7,8-tetrahydro-1,8-naphthyridin-2-yl)ethyl)pyrrolidin-1-yl)-butanoic Acid Sodium Salt (28m). Prepared from (*R*)-**17**: LCMS (system A) RT = 0.75 min, 100%, ES+ve *m/z* 461 $(M + H)^+$; ^{1}H NMR (DMSO-d_6, 400 MHz) 9.29 (1H, s), 8.23 (1H, s), 8.15 (1H, s), 7.77 (1H, m), 7.70 (1H, br d, *J* 8 Hz), 7.48 (1H, t, *J* 8 Hz), 7.32 (1H, d, *J* 8 Hz), 7.02 (1H, d, *J* 7.3 Hz), 6.32 (1H, br), 6.25 (1H, d, *J* 7.3 Hz), 3.36−3.29 (1H, m), 3.23 (3H, br), 2.94−2.81 (3H, m), 2.75−2.69 (1H, m), 2.68−2.56 (4H, m), 2.47−2.45 (m, obscured by solvent), 2.41 (2H, t, *J* 8 Hz), 2.37−2.32 (1H, m), 2.07−2.00 (1H, m), 1.96−1.86 (1H, m), 1.78−1.70 (2H, m), 1.66−1.56 (2H, m), 1.40−1.32 (1H, m).

(*S*)-3-(3-(3,5-Dimethyl-1*H*-1,2,4-triazol-1-yl)phenyl)-4-((*R*)-3-(2-(5,6,7,8-tetrahydro-1,8-naphthyridin-2-yl)ethyl)pyrrolidin-1-yl)butanoic Acid (28n). Prepared from (*R*)-**17**: LCMS (system A) RT = 0.75 min, 100%, ES+ve *m/z* 489 $(M + H)^+$; ^{1}H NMR (DMSO-d_6, 500 MHz) 7.47−7.42 (1H, m), 7.41 (1H, s), 7.38−7.31 (2H, m), 7.01 (1H, d, *J* 7 Hz), 6.28−6.21 (2H, m), 3.25−3.19 (2H, m), 2.40 (3H, s), 2.26 (3H, s), 2.05−1.94 (1H, m), 1.93−1.83 (1H, m), 1.78−1.69 (2H, m), 1.65−1.53 (2H, m), 1.38−1.28 (m, 1H). HRMS (ESI) calcd for $C_{28}H_{37}N_6O_2$ $(M + H)^+$ 489.2973, found 489.2989. Anal. chiral HPLC RT = 22.7 min, 99.5% on a Chiralcel OJ-H column (250 mm × 4.6 mm) eluting with 20% EtOH (containing 0.2% isopropylamine)−heptane, flow rate = 1 mL/min, detecting at 215 nm.

(*S*)-3-(3-(3-Methyl-4*H*-1,2,4-triazol-4-yl)phenyl)-4-((*R*)-3-(2-(5,6,7,8-tetrahydro-1,8-naphthyridin-2-yl)ethyl)pyrrolidin-1-yl)butanoic Acid (28o). Prepared from (*R*)-**17**: LCMS (system A) RT = 0.77 min, 92%, ES+ve *m/z* 475 $(M + H)^+$; ^{1}H NMR (DMSO-d_6, 500 MHz) 9.12 (1H, s), 7.69 (1H, s), 7.63 (1H, br d, *J* 7.5 Hz), 7.43 (1H, t, *J* 7.5 Hz), 7.25 (1H, br d, *J* 7.5 Hz), 7.00 (1H, br d, *J* 7.0 Hz), 6.28−6.21 (2H, m), 3.25−3.19 (2H, m), 2.36 (3H, s), 2.06−1.95 (1H, m), 1.94−1.83 (1H, m), 1.78−1.69 (2H, m), 1.66−1.53 (2H, m), 1.38−1.28 (1H, m). HRMS (ESI) calcd for C28H37N6O2 $(M + H)^+$ 475.2916, found 475.2819. Anal. chiral HPLC RT = 18.1 min, 99.4% on a Chiralcel OJ-H column (250 mm × 4.6 mm) eluting with 20% EtOH (containing 0.2% isopropylamine)-heptane, flow rate = 1 mL/min, detecting at 215 nm.

(*S*)-3-(3-(1*H*-1,2,3-Triazol-1-yl)phenyl)-4-((*R*)-3-(2-(5,6,7,8-tetrahydro-1,8-naphthyridin-2-yl)ethyl)pyrrolidin-1-yl)-butanoic Acid (28p). Prepared from (*R*)-**17**: LCMS (system C) RT = 0.37 min, 95%, ES+ve *m/z* 461 $(M + H)^+$; ^{1}H NMR (DMSO-d_6) MHz) 8.81 (1H, s), 7.96 (1H, s), 7.79 (1H, br s), 7.73 (1H, br d, *J* 7.5 Hz), 7.50 (1H, br t, *J* 7.5 Hz), 7.36 (1H, br d, *J* 7.5 Hz), 7.00 (1H, br d, *J* 7 Hz), 6.28−6.20 (2H, m), 3.22 (2H, br s), 2.39 (2H, br t, *J* 7.5 Hz), 2.32−2.23 (1H, m), 2.06−1.95 (1H, m), 1.94−1.83 (1H, m), 1.78−1.68 (2H, m), 1.66−1.53 (2H, m), 1.38−1.27 (1H, m). HRMS (ESI) calcd for $C_{26}H_{33}N_6O_2$ $(M + H)^+$ 461.2660, found 461.2657. Anal. chiral HPLC RT = 19.5 min, 98.8% on a Chiralcel AD-H column (4.6 mm × 250 mm) eluting with 20% EtOH (containing 0.2% isopropylamine)−heptane, flow rate = 1 mL/min, detecting at 215 nm.

Enriched 3-(3-(1*H*-Imidazol-1-yl)phenyl)-4-((*R*)-3-(2-(5,6,7,8-tetrahydro-1,8-naphthyridin-2-yl)ethyl)pyrrolidin-1-yl)-butanoic Acid (28q). Prepared from (*R*)-**17** to give a 63:37 mixture of diastereomers which were not separated: LCMS (system A) RT = 0.76 min, 100%, ES+ve *m/z* 460 $(M + H)^+$; ^{1}H NMR (DMSO-d_6, 500 MHz) 8.25 (1H, br s), 7.74 (1H, br s), 7.68−6.94 (m, 6H+), 6.40−6.15 (m, 1H+), 3.33−3.25 (1H, m), 3.22 (2H, br s), 2.42−2.34 (2H, m), 2.28−2.12 (1H, m), 2.04−1.95 (1H, m), 1.93−1.82 (1H, m), 1.78−1.69 (2H, m), 1.65−1.54 (2H, m), 1.38−1.27 (1H, m).

(*S*)-3-(3-(1,4-Dimethyl-1*H*-imidazol-2-yl)phenyl)-4-((*R*)-3-(2-(5,6,7,8-tetrahydro-1,8-naphthyridin-2-yl)ethyl)pyrrolidin-1-yl)butanoic Acid (28r). Prepared from (*R*)-**17**: LCMS (system A) RT = 0.81 min, 100%, ES+ve *m/z* 488 $(M + H)^+$; ^{1}H NMR (DMSO-d_6, 500 MHz) 7.48 (1H, s), 7.44 (1H, d, *J* 7.7 Hz), 7.35 (1H, t, *J* 7.6 Hz), 7.26 (1H, d, *J* 7.7 Hz), 7.01 (1H, d, *J* 6.6 Hz), 6.92 (1H, s), 6.32−6.21 (2H, m), 3.30−3.21 (4H, m), 3.18 (3H, s), 2.85−2.76 (2H, m), 2.75−2.63 (2H, m), 2.63−2.54 (3H, m), 2.46−2.30 (3H, m), 2.23 (1H, t, *J* 8.0 Hz), 2.12 (3H, s), 2.04−1.92 (1H, m), 1.92−1.82 (1H, m), 1.79−1.69 (2H, m), 1.67−1.53 (2H, m), 1.37−1.27 (1H, m). HRMS (ESI) calcd for $C_{29}H_{38}N_5O_2$ $(M + H)^+$ 488.3020, found 488.3025. Anal. chiral HPLC RT = 13.2 min, 99.5% on a Chiralcel OJ-H column (250 mm × 4.6 mm) eluting with 25% EtOH (containing 0.2% isopropylamine)−heptane (containing 0.2% isopropylamine), flow rate 1 mL/min, detecting at 215 nm.

(*S*)-3-(3-(2,4-Dimethyl-1*H*-imidazol-5-yl)phenyl)-4-((*R*)-3-(2-(5,6,7,8-tetrahydro-1,8-naphthyridin-2-yl)ethyl)pyrrolidin-1-yl)butanoic Acid Sodium Salt (28s). Prepared from (*R*)-**17** and purified by high pH reverse phase HPLC (method A): LCMS (system C) RT = 0.37 min, 100%, ES+ve *m/z* 488 $(M + H)^+$; ^{1}H NMR (DMSO-d_6, 400 MHz) 7.47−7.30 (2H, m), 7.30−7.23 (1H, m), 7.01 (1H, d, *J* 7.3 Hz), 6.25 (1H, d, *J* 7.3 Hz), 3.25−3.20 (3H, m), 2.90−2.67 (4H, m), 2.60 (2H, t, *J* 6 Hz), 2.55−2.52 (2H, m), 2.45−2.37 (3H, m), 2.35−2.27 (3H, m), 2.26 (3H, s), 2.08−1.99 (1H, m), 1.96−1.86 (1H, m), 1.77−1.70 (2H, m), 1.65−1.57 (2H, m), 1.39−1.29 (1H, m).

(*S*)-4-((*R*)-3-(2-(5,6,7,8-Tetrahydro-1,8-naphthyridin-2-yl)-ethyl)pyrrolidin-1-yl)-3-(3-(((*S*)-tetrahydrofuran-3-yl)oxy)-phenyl)butanoic Acid (28t). Prepared from (*R*)-**17**: LCMS (system A) RT = 0.83 min, 93%, ES+ve *m/z* 480 $(M + H)^+$; ^{1}H NMR (DMSO-d_6, 400 MHz) 7.19 (1H, t, *J* 8 Hz), 7.02 (1H, d, *J* 7 Hz), 6.84−6.71 (3H, m), 6.30 (2H, m), 5.00 (1H, m), 3.93−3.71 (5H, m), 3.29−3.11 (4H, m), 2.89−2.66 (5H, m), 2.64−2.57 (2H, m), 2.45−2.16 (5H, m), 2.05−1.85 (3H, m), 1.80−1.70 (2H, m), 1.68−1.55 (2H, m), 1.41−1.30 (1H, m). Anal. chiral SFC RT = 6.91 min, 97.5%, on a Chiralpak AD-H column (250 mm × 4.6 mm) eluting with 60% CO_2−40% (0.5% diethylamine in EtOH), flow rate 4 g/min, pressure 100 bar.

(*S*)-4-((*R*)-3-(2-(5,6,7,8-Tetrahydro-1,8-naphthyridin-2-yl)-ethyl)pyrrolidin-1-yl)-3-(3-(((*R*)-tetrahydrofuran-3-yl)oxy)-phenyl)butanoic Acid (28u). Prepared from (*R*)-**17**: LCMS (system C) RT = 0.47 min, 96%, ES+ve *m/z* 480 $(M + H)^+$; ^{1}H NMR ($CDCl_3$ + D_2O, 400 MHz) 7.21 (1H, br t, *J* 8 Hz), 7.12 (1H, br d, *J* 7.5 Hz), 6.80 (1H, br d, *J* 8 Hz), 6.74−6.68 (2H, m), 6.28 (1H, d, *J* 7.5 Hz), 4.94−4.89 (1H, m), 4.74−4.65 (3H, m), 4.03−3.87 (4H, m), 3.47−3.38 (3H, m), 3.02−2.93 (2H, m), 2.78−2.67 (5H, m), 2.52−2.40 (2H, m), 2.27−1.98 (4H, m), 1.94−1.81 (3H, m), 1.62−1.52 (1H, m), 1.48−1.38 (1H, m). Anal. chiral SFC RT = 3.45 min, 98.9%, on a Chiralpak AS-H column (250 mm × 4.6 mm), eluting with 50% CO_2−50% (0.5% isopropylamine in isopropanol), flow rate 4 g/min, pressure 100 bar.

(*S*)-3-(3-(Oxetan-3-yloxy)phenyl)-4-((*R*)-3-(2-(5,6,7,8-tetrahydro-1,8-naphthyridin-2-yl)ethyl)pyrrolidin-1-yl)butanoic Acid (28v). Prepared from (*R*)-**17**: LCMS (system C) RT = 0.44 min, 100%, ES+ve *m/z* 466 $(M + H)^+$; ^{1}H NMR (DMSO-d_6, 400 MHz) 7.19 (1H, t, *J* 8 Hz), 7.02 (1H, d, *J* 8 Hz), 6.84 (1H, d, *J* 8 Hz), 6.67 (1H, br s), 6.57 (1H, dd, *J* 8, 2 Hz), 6.27−6.22 (2H, m), 5.25 (1H, quint, *J* 6 Hz), 4.91 (2H, t, *J* 7 Hz), 4.54−4.49 (2H, m), 3.26−3.11 (3H, m), 2.86−2.64 (4H, m), 2.60 (2H, t, *J* 6 Hz), 2.57−2.45 (m, obscured by solvent), 2.43−2.27 (4H, m), 2.07−1.97 (1H, m), 1.95−1.85 (1H, m), 1.78−1.71 (2H, m), 1.65−1.55 (2H, m), 1.39−1.29 (1H, m). Anal. chiral SFC RT = 7.46 min, 99%, on a Chiralpak AD-H column (250 mm × 4.6 mm), eluting with 60% CO_2, 40% (0.5% diethylamine in EtOH), flow rate 4.0 g/min, pressure 100 bar.

(*S*)-4-((*R*)-3-(2-(5,6,7,8-Tetrahydro-1,8-naphthyridin-2-yl)-ethyl)pyrrolidin-1-yl)-3-(3-((tetrahydro-2*H*-pyran-4-yl)oxy)-phenyl)butanoic Acid (28w). A solution of *tert*-butyl (*S*)-4-((*R*)-3-(2-(5,6,7,8-tetrahydro-1,8-naphthyridin-2-yl)ethyl)pyrrolidin-1-yl)-3-(3-((tetrahydro-2*H*-pyran-4-yl)oxy)phenyl)butanoate (**27w** *tert*-butyl ester) (prepared from (*R*)-**24** *tert*-butyl ester) (190.9 mg, 0.347 mmol) in 2-methyltetrahydrofuran (2 mL) was treated with conc HCl (0.145 mL, 1.74 mmol), and the mixture was stirred rapidly at 40 °C for 18 h. The reaction mixture was diluted with water, and the phases were separated. The organic phase was extracted with water, and the aqueous phases were combined. The pH of the combined aqueous phases was adjusted to pH 7.5 with aqueous 2 M NaOH, and the solution was extracted with DCM. The organic phase was then

DOI: 10.1021/acs.jmedchem.8b00959
J. Med. Chem. XXXX, XXX, XXX−XXX

washed with brine, dried ($MgSO_4$), and evaporated in vacuo. The residue (100.7 mg) was purified by MDAP (method A). The required fractions were combined and evaporated in vacuo to give **28w** (66 mg, 39%) as an off-white foam: LCMS (system A) RT = 0.85 min, 100%, ES+ve *m/z* 494 $(M + H)^+$; ^1H NMR ($CDCl_3$, 400 MHz) 7.24−7.16 (2H, m), 6.80−6.74 (3H, m), 6.29 (1H, d, *J* 7 Hz), 4.51−4.44 (1H, m), 4.02−3.95 (2H, m), 3.62−3.54 (2H, m), 3.50−3.34 (3H, m), 3.15−3.05 (1H, m), 3.02−2.93 (1H, m), 2.79−2.67 (6H, m), 2.56−2.46 (1H, m), 2.28−2.16 (1H, m), 2.16−2.06 (1H, m), 2.06−1.97 (2H, m), 1.96−1.73 (6H, m), 1.71−1.60 (1H, m), 1.58−1.47 (1H, m).

(3*S*)-4-((*R*)-3-(2-(5,6,7,8-Tetrahydro-1,8-naphthyridin-2-yl)ethyl)pyrrolidin-1-yl)-3-(3-(tetrahydrofuran-3-yl)phenyl)butanoic Acids (28x Isomer 1 and 28x Isomer 2). Prepared from (*R*)-**17**. **28x Isomer 1**: LCMS (system A) RT = 0.84 min, 100%, ES +ve *m/z* 464 $(M + H)^+$; ^1H NMR (DMSO-d_6, 600 MHz) 7.22 (1H, t, *J* 7.5 Hz), 7.14 (1H, s), 7.10 (1H, br d, *J* 7.5 Hz), 7.07 (1H, br d, *J* 7.5 Hz), 7.02 (1H, br d, *J* 7 Hz), 6.30−6.20 (2H, m), 4.04−3.99 (1H, m), 3.96−3.90 (1H, m), 3.82−3.75 (1H, m), 3.52 (1H, br t, *J* 8 Hz), 3.37−3.30 (1H, m), 3.26−3.21 (2H, m), 3.20−3.14 (1H, m), 2.91−2.83 (1H, m), 2.82−2.74 (2H, m), 2.74−2.68 (1H, m), 2.62−2.57 (2H, m), 2.60−2.53 (1H, m), 2.52−2.47 (1H, m), 2.43−2.38 (2H, m), 2.41−2.36 (1H, m), 2.36−2.31 (1H, m), 2.31−2.24 (1H, m), 2.08−1.99 (1H, m), 1.95−1.85 (2H, m), 1.78−1.71 (2H, m), 1.67−1.55 (2H, m), 1.40−1.30 (1H, m); ^{13}C NMR (DMSO-d_6, 151 MHz) 173.6, 157.1, 155.7, 143.7, 142.5, 136.0, 128.4, 126.3, 125.2, 125.1, 112.3, 109.8, 73.8, 67.6, 61.8, 59.2, 53.1, 44.1, 40.9, 40.6, 40.1, 36.5, 35.7, 34.8, 33.9, 30.1, 25.9, 21.0.

Prepared from (*R*)-**17**. **28x Isomer 2**: LCMS (system A) RT = 0.84 min, 100%, ES+ve *m/z* 464 $(M + H)^+$; ^1H NMR (DMSO-d_6, 600 MHz) 7.24−7.19 (1H, m), 7.13 (1H, s), 7.10 (1H, d, *J* 7.5 Hz), 7.07 (1H, d, *J* 7.5 Hz), 7.02 (1H, d, *J* 7.0 Hz), 6.27−6.23 (2H, m), 4.01 (1H, t, *J* 8 Hz), 3.93 (1H, td, *J* 8, 4.5 Hz), 3.78 (1H, q, *J* 8 Hz), 3.52 (2H, t, *J* 8 Hz), 3.33 (1H, quin, *J* 8 Hz), 3.25−3.21 (2H, m), 3.20−3.14 (1H, m), 2.86 (1H, dd, *J* 12, 10 Hz), 2.81−2.74 (2H, m), 2.73−2.67 (1H, m), 2.60 (2H, t, *J* 6 Hz), 2.56 (1H, td, *J* 9, 5.5 Hz), 2.49−2.47 (1H, m), 2.43−2.35 (3H, m), 2.33 (1H, dd, *J* 9, 7 Hz), 2.28 (1H, dtd, *J* 12, 8, 4.5 Hz), 2.07−1.98 (1H, m), 1.94−1.86 (2H, m), 1.74 (2H, quin, *J* 6 Hz), 1.67−1.54 (2H, m), 1.39−1.30 (1H, m); ^{13}C NMR (DMSO-d_6, 151 MHz) 173.6, 157.2, 155.7, 143.8, 142.5, 136.0, 128.4, 126.3, 125.1, 125.1, 112.3, 109.8, 73.8, 67.6, 61.9, 59.2, 53.1, 44.2, 40.9, 40.6, 40.2, 36.5, 35.7, 34.9, 33.9, 30.1, 25.9, 21.0.

(*S*)-4-((*R*)-3-(2-(5,6,7,8-Tetrahydro-1,8-naphthyridin-2-yl)ethyl)pyrrolidin-1-yl)-3-(3-(tetrahydro-2*H*-pyran-4-yl)phenyl)butanoic Acid (28y). Prepared from (*R*)-**17**: LCMS (system A) RT = 0.90 min, 98%, ES+ve *m/z* 478 $(M + H)^+$; ^1H NMR (DMSO-d_6, 600 MHz) 7.20 (1H, t, *J* 8 Hz), 7.11 (1H, s), 7.07 (1H, d, *J* 8 Hz), 7.06−7.03 (1H, m), 7.01 (1H, d, *J* 7.3 Hz), 6.26−6.23 (2H, m), 3.93 (2H, dt, *J* 11, 3 Hz), 3.44−3.38 (2H, m), 3.24−3.21 1H, (m, 1H), 3.21−3.14 (1H, m), 2.85 (1H, dd, *J* 12, 10 Hz), 2.78−2.67(4H, m), 2.63−2.51 (3H, m), 2.45−2.28 (4H, m), 2.06−1.97 (1H, m), 1.93−1.84 (1H, m), 1.76−1.71 (2H, m), 1.68−1.55 (6H, m), 1.34 (1H, br dd, *J* 12, 8 Hz); ^{13}C NMR (DMSO-d_6, 151 MHz) 173.7, 157.2, 155.7, 145.8, 143.8, 136.0, 128.2, 125.8, 124.9, 124.5, 112.2, 109.8, 67.3, 61.9, 59.3, 56.0, 53.2, 41.1, 40.6, 40.6, 40.0, 36.5, 35.7, 34.9, 33.5, 33.5, 30.1, 25.9, 21.0. HRMS (ESI) calcd for $C_{29}H_{40}N_3O_3$ 478.3064 $(M + H)^+$, found 478.3058. Anal. chiral HPLC RT = 7.5 min, 99.5% on a Chiralpak AD-H column (250 mm × 4.6 mm) eluting 50% EtOH (containing 0.2% isopropylamine)−heptane, flow rate = 1.0 mL/min, detecting at 215 nm.

(*S*)-3-(3-Cyclopropyl-5-morpholinophenyl)-4-((*R*)-3-(2-(5,6,7,8-tetrahydro-1,8-naphthyridin-2-yl)ethyl)pyrrolidin-1-yl)butanoic Acid (28bc). Prepared from (*R*)-**17**: LCMS (system A) RT = 0.95 min, 94%, ES+ve *m/z* 519 $(M + H)^+$; ^1H NMR (DMSO-d_6, 600 MHz) 7.01 (1H, d, *J* 7.3 Hz), 6.56 (1H, s), 6.43 (1H, s), 6.40 (1H, s), 6.27−6.24 (2H, m), 3.74−3.69 (4H, m), 3.26−3.21 (m, obscured by water), 3.09−3.04 (4H, m), 2.89 (1H, t, *J* 11 Hz), 2.81−2.70 (3H, m), 2.63−2.56 (3H, m), 2.54−2.46 (m, obscured by solvent), 2.41 (2H, t, *J* 8 Hz), 2.38−2.32 (2H, m), 2.07−2.00 (1H, m), 1.95−1.88 (1H, m), 1.84−1.79 (1H, m), 1.78−1.73 (2H, m), 1.67−1.57 (2H, m), 1.40−1.32 (1H, m), 0.90−0.85 (2H, m), 0.66−0.62 (2H, m); ^{13}C NMR (DMSO-d_6, 151 MHz) 173.7, 157.2, 155.7, 151.1, 144.3, 144.2, 136.0, 115.5, 112.3, 111.5, 110.2, 109.8, 66.1, 61.9, 59.1, 53.1, 48.6, 41.5, 40.6, 40.4, 36.5, 35.7, 34.8, 30.1, 25.9, 21.0, 15.4, 9.0. HRMS (ESI) calcd for $C_{31}H_{43}N_4O_3$ 519.3335 $(M + H)^+$, found 519.3333. Anal. chiral HPLC RT = 17.0 min, 99.5% on a Chiralpak AD-H column (250 mm × 4.6 mm) eluting with 40% EtOH (containing 0.2% isopropylamine)−heptane, flow rate = 1 mL/min, detecting at 215 nm.

(*S*)-3-(3-(3,5-Dimethyl-1*H*-pyrazol-1-yl)-5-morpholinophenyl)-4-((*R*)-3-(2-(5,6,7,8-tetrahydro-1,8-naphthyridin-2-yl)ethyl)pyrrolidin-1-yl)butanoic Acid (28ch). Prepared from (*R*)-**26ch**: LCMS (system A) RT = 0.85 min, 98%, ES+ve *m/z* 573 $(M + H)^+$; IR i_{max} (neat) 3300−2500, 1678, 1595, 1118, 725 cm^{-1}; ^1H NMR (DMSO-d_6, 600 MHz) 7.02 (1H, d, *J* 7.3 Hz), 6.86 (1H, s), 6.79 (1H, m), 6.75 (1H, s), 6.25 (1H, s), 6.26 (1H, d, *J* 7.3 Hz), 6.03 (1H, s), 3.76−3.71 (4H, m), 3.27−3.20 (4H, m), 3.18−3.13 (4H, m), 2.96−2.88 (1H, m), 2.83−2.78 (2H, m), 2.75−2.68 (1H, m), 2.63−2.54 (3H, m), 2.45−2.38 (2H, m), 2.36−2.32 (1H, m), 2.26 (3H, s), 2.16 (3H, s), 2.10−1.98 (1H, m), 1.94−1.87 (1H, m), 1.76−1.71 (2H, m), 1.67−1.55 (2H, m), 1.39−1.32 (1H, m); ^{13}C NMR (DMSO-d_6, 151 MHz) 173.7, 157.6, 156.3, 151.7, 147.6, 145.3, 140.7, 139.5, 136.5, 114.3, 113.2, 112.8, 110.3, 109.3, 107.2, 66.4, 62.1, 59.7, 53.7, 48.6, 41.3, 41.1, 40.8, 37.0, 36.3, 35.3, 30.5, 26.5, 21.4, 13.6, 12.5. HRMS (ESI) calcd for $C_{33}H_{45}N_6O_3$ 573.3548 $(M + H)^+$, found 573.3534.

(*R*)-3-(3-Morpholinophenyl)-4-((*R*)-3-(2-(5,6,7,8-tetrahydro-1,8-naphthyridin-2-yl)ethyl)pyrrolidin-1-yl)butanoic Acid (30c). Similarly prepared to **28c** from **26c**. LCMS (system A) RT = 0.79 min, 100%, ES+ve *m/z* 479 $(M + H)^+$; ^1H NMR (CD_3OD, 400 MHz) 7.23 (1H, t, *J* 7.5 Hz), 7.14 (1H, d, *J* 7.3 Hz), 6.90−6.84 (2H, m), 6.77 (1H, d, *J* 7.5 Hz), 6.39 (1H, d, *J* 7.3 Hz), 3.86−3.80 (4H, m), 3.61−3.49 (2H, m), 3.43−3.34 (4H, m), 3.30−3.20 (2H, m), 3.19−3.12 (4H, m), 2.91−2.77 (2H, m), 2.70 (2H, t, *J* 6 Hz), 2.66−2.51 (3H, m), 2.42−2.30 (1H, m), 2.26−2.15 (1H, m), 1.92−1.83 (2H, m), 1.82−1.66 (3H, m).

(*S*)-3-(3-Morpholinophenyl)-4-((*R*)-3-(2-(5,6,7,8-tetrahydro-1,8-naphthyridin-2-yl)ethyl)pyrrolidin-1-yl)butanoic Acid (ent-30c). These are the data for the title compound prepared according to a similar route to that shown in Scheme 1. LCMS (system A) RT = 0.79 min, 100%, ES+ve *m/z* 479 $(M + H)^+$; ^1H NMR (CD_3OD, 600 MHz) 7.21 (1H, t, *J* 7.8 Hz), 7.13 (1H, d, *J* 7.3 Hz), 6.87−6.82 (2H, m), 6.74 (1H, d, *J* 7.5 Hz), 6.37 (1H, d, *J* 7.3 Hz), 3.84−3.77 (4H, m), 3.54 (1H, dd, *J* 12.7, 9.4 Hz), 3.40−3.37 (1H, m), 3.37−3.34 (2H, m), 3.34−3.30 (1H, m), 3.32−3.27 (2H, m), 3.20 (1H, dd, *J* = 12.7, 3.8 Hz), 3.15−3.10 (4H, m), 3.00 (1H, br s), 2.80 (1H, dd, *J* 16.4, 10.5 Hz), 2.68 (2H, t, *J* 6.2 Hz), 2.59 (1H, dd, *J* 16.3, 2.4 Hz), 2.54 (2H, t, *J* 7.3 Hz), 2.32 (1H, spt, *J* 7.9 Hz), 2.19 (1H, dq, *J* 13.1, 6.6 Hz), 1.89−1.83 (2H, m), 1.82−1.72 (2H, m), 1.66 (1H, dq, *J* 13.0, 8.6 Hz); ^{13}C NMR (CD_3OD, 151 MHz) 180.3, 157.4, 157.3, 153.6, 144.8, 138.8, 131.0, 119.6, 116.0, 115.9, 115.8, 112.2, 68.1, 63.4, 59.9, 55.1, 50.7, 46.2, 42.5, 41.3, 38.2, 36.4, 34.7, 31.0, 27.5, 22.5.

(*R*)-3-(3-(3,5-Dimethyl-1*H*-pyrazol-1-yl)phenyl)-4-((*R*)-3-(2-(5,6,7,8-tetrahydro-1,8-naphthyridin-2-yl)ethyl)pyrrolidin-1-yl)butanoic Acid (30h). Similarly prepared to **28h** from **26h** via the following sequence. A solution of (*R*)-*tert*-butyl 4-((*R*)-3-(2-(1,8-naphthyridin-2-yl)ethyl)pyrrolidin-1-yl)-3-(3-(3,5-dimethyl-1*H*-pyrazol-1-yl)phenyl)butanoate[30] (60 mg, 0.111 mmol) in EtOH (5 mL) was hydrogenated over 5% Pd/C (24 mg, 0.011 mmol) for 18 h. The catalyst was removed by passing through a Celite cartridge (10 g) and the filtrate was concentrated in vacuo to give (*R*)-*tert*-butyl 3-(3-(3,5-dimethyl-1*H*-pyrazol-1-yl)phenyl)-4-((*R*)-3-(2-(5,6,7,8-tetrahydro-1,8-naphthyridin-2-yl)ethyl)pyrrolidin-1-yl)butanoate (51 mg, 84%) as a colorless gum: LCMS (system A) RT = 1.44 min, 81%, ES+ve *m/z* 544 (M + H)+; ^1H NMR (CDCl3, 400 MHz) 7.30−7.38 (m, 1H), 7.24−7.29 (m, 2H), 7.20 (d, J = 7.81 Hz, 1H), 7.04 (d, J = 7.30 Hz, 1H), 6.31 (d, J = 7.30 Hz, 1H), 5.97 (s, 1H), 3.35−3.41 (m, 2H), 3.26−3.33 (m, 1H), 2.79−2.88 (m, 2H), 2.56−2.71 (m, 5H), 2.38−2.55 (m, 5H), 2.29 (s, 3H), 2.27 (s, 3H), 2.00−2.13 (m, 2H), 1.84−1.98 (m, 3H), 1.64−1.72 (m, 2H), 1.30 (s, 9H).

DOI: 10.1021/acs.jmedchem.8b00959
J. Med. Chem. XXXX, XXX, XXX−XXX

A solution (*R*)-*tert*-butyl 3-(3-(3,5-dimethyl-1*H*-pyrazol-1-yl)-phenyl)-4-((*R*)-3-(2-(5,6,7,8-tetrahydro-1,8-naphthyridin-2-yl)ethyl)-pyrrolidin-1-yl)butanoate (51 mg, 0.094 mmol) in MeOH (5 mL) was stirred with 37% aqueous HCl (0.2 mL, 2.435 mmol) for 18 h. The solvent was removed in vacuo and the residue dissolved in H_2O (1 mL) and purified by MDAP (method A). Relevant fractions were combined and concentrated in vacuo to afford (*R*)-3-(3-(3,5-dimethyl-1*H*-pyrazol-1-yl)phenyl)-4-((*R*)-3-(2-(5,6,7,8-tetrahydro-1,8-naphthyridin-2-yl)ethyl)pyrrolidin-1-yl)butanoic acid (25 mg, 55%): LCMS (system A) RT = 0.85 min, 98%, ES+ve *m*/*z* 488 $(M + H)^+$; ^{1}H NMR (CD_3OD; 400 MHz) 7.51 (1H, t, *J* 8 Hz), 7.41−7.33 (3H, m), 7.16 (1H, d, *J* 7.3 Hz, 1H), 6.41 (1H, d, *J* 7.3 Hz), 6.09 (1H, s), 3.68−3.36 (6H, m), 2.98−2.82 (2H, m), 2.74−2.63 (3H, m), 2.62−2.53 (2H, m), 2.44−2.33 (1H, m), 2.30 (3H, s), 2.27 (3H, s), 2.39−2.18 (1H, m), 1.92−1.84 (2H, m), 1.84−1.68 (3H, m). Anal. chiral HPLC RT = 9.36 min, 100% on a Chiralpak column (250 mm × 4.6 mm) eluting with 30% EtOH (containing 0.1% isopropylamine)−heptane, flow rate = 1 mL/min, detecting at 235 nm.

4-(3-Cyclopropylphenyl)morpholine (32). 4-(3-Bromophenyl)morpholine (**31**) (2.3 g, 9.5 mmol) was dissolved in THF (10 mL), and the solution was added to cyclopropylmagnesium bromide (22.8 mL of a 0.5 M solution in THF, 11.4 mmol). $PdCl_2$(dppf)−CH_2Cl_2 (270 mg, 0.32 mmol) was added, and the mixture was heated to 60 °C for 3 h, cooled to room temperature, and partitioned between water (50 mL) and DCM (50 mL). The organic layer was separated, and then the aqueous layer was extracted with DCM (2 × 10 mL). The combined organic layers were evaporated under reduced pressure and the residue was purified by chromatography on a silica cartridge (100 g), eluting with 0−50% EtOAc−cyclohexane (10 CV). The appropriate fractions were combined an evaporated under reduced pressure to give **32** (1.7 g, 88%) as an oil: LCMS (system A) RT = 1.08 min, 93%, ES+ve *m*/*z* 204 $(M + H)^+$; ^{1}H NMR (CD_3OD, 400 MHz) 7.11 (1H, t, *J* 8 Hz), 6.73 (1H, d, *J* 8 Hz), 6.70 (1H, s), 6.56 (1H, d, *J* 8 Hz), 3.85−3.78 (4H, m), 3.13−3.05 (4H, m), 1.90−1.80 (1H, m), 0.93−0.87 (2H, m), 0.67−0.59 (2H, m).

4-(3-Cyclopropyl-5-(4,4,5,5-tetramethyl-1,3,2-dioxaborolan-2-yl)phenyl)morpholine (33). A mixture of **32** (1.0 g, 4.9 mmol), bispinacolatodiboron (750 mg, 3.0 mmol), 4,4′-di-*tert*-butyl-2,2′-bipyridine (80 mg, 0.3 mmol), and $[Ir(COD)OMe]_2$ (98 mg, 0.15 mmol) was dissolved in TMBE (8 mL) and heated in a microwave oven for 1 h at 80 °C. The reaction mixture was adsorbed onto Florisil and purified by chromatography on a silica cartridge (100 g), eluting with 0−50% EtOAc in cyclohexane (10CV). The appropriate fractions were combined and evaporated under reduced pressure to give **33** (845 mg, 52%) as a white solid: LCMS (system A) RT = 1.31 min, 57%, ES+ve *m*/*z* 330 $(M + H)^+$ for the ester; and RT = 0.74 min, 43%, ES+ve *m*/*z* 248 $(M + H)^+$ (for the boronic acid **18bc** resulting from hydrolysis of the boronic ester **33** in the LCMS mobile phase); ^{1}H NMR (CD_3OD, 400 MHz) 7.12 (1H, d, *J* 2 Hz), 6.96 (1H, s), 6.82 (1H, s), 3.83−3.77 (4H, m), 3.12−3.06 (4H, m), 1.90−1.82 (1H, m), 1.32 (12H, s), 0.94−0.87 (2H, m), 0.68−0.63 (2H, m). HRMS (ESI) calcd for $C_{13}H_{19}BNO_3$ 248.1452 $(M + H)^+$, found 248.1447 (for boronic acid **18bc**).

1-(3,5-Dibromophenyl)-3,5-dimethyl-1*H*-pyrazole (34). Sulfuric acid (6.82 mL, 61.4 mmol) and sodium nitrite (638 mg, 9.25 mmol) in water (3 mL) were slowly added to a stirred solution of 3,5-dibromoaniline (2.11 g, 8.41 mmol) in MeCN (50 mL), cooled to 0 °C in an ice bath, and the reaction mixture was stirred at 0 °C for 72 h before adding L-ascorbic acid (1.629 g, 9.25 mmol) in water (5 mL). The mixture was stirred overnight at room temperature, and then pentane-2,4-dione (1.72 mL, 16.8 mmol) was added in one charge. The mixture was stirred at room temperature for 72 h and for 5 h at 80 °C, before it was partitioned between EtOAc (200 mL) and water (100 mL). The organic layer was washed with 2 M HCl (50 mL) and water (50 mL). The organic solution was dried (Na_2SO_4) and concentrated in vacuo. The residue was purified by chromatography on silica eluting with a gradient of 0−10% EtOAc−hexane. The appropriate fractions were combined and evaporated in vacuo to give **34** (1.75 g, 62%) as a yellow solid: LCMS (system A) RT = 1.35 min, 99%, ES+ve *m*/*z* 329, 331, 333 $(M + H)^+$; ^{1}H NMR (DMSO-d_6, 400 MHz) 7.83 (1H, t, *J* 2 Hz), 7.75 (2H, m), 6.11 (1H, s), 2.34 (3H, s), 2.17 (3H, s).

4-(3-Bromo-5-(3,5-dimethyl-1*H*-pyrazol-1-yl)phenyl)-morpholine (35). A solution of **34** (8.2 g, 25 mmol) in toluene (250 mL) was treated with morpholine (2.38 g, 27 mmol), $Pd_2(dba)_3$ (4.71 g, 5.14 mmol), sodium *tert*-butoxide (2.39 g, 25 mmol), and 2,2′-bis(diphenylphosphino)-1,1′-binaphthalene (5.04 g, 8.1 mmol). The mixture was heated to reflux for 2 h and then passed through a pad of Celite. The filtrate was washed with water (200 mL). The organic phase was passed through a phase separator and concentrated in vacuo. The residue was purified by chromatography on a silica cartridge (325 g) eluting with a gradient of 0−100% EtOAc−cyclohexane (14CV) to give **35** (3.5 g, 33%): LCMS (system A) RT = 1.15 min, ES+ve *m*/*z* 336, 338 $(M + H)^+$.

4-(3-(3,5-Dimethyl-1*H*-pyrazol-1-yl)-5-(4,4,5,5-tetramethyl-1,3,2-dioxaborolan-2-yl)phenyl)morpholine (36). A solution of **35** (10 g, 29.7 mmol) in 1,4-dioxane (200 mL) was treated at room temperature with bis(pinacolato)diboron (8.31 g, 32.7 mmol), potassium acetate (7.30 g, 74.4 mmol), XPhos (681 mg, 1.43 mmol), and $Pd_2(dba)_3$ (409 mg, 0.446 mmol) in one charge. The reaction mixture was deoxygenated three times with argon and then stirred at 110 °C for 1 h. The reaction mixture was concentrated in vaccuo and the residue was dissolved in DCM (300 mL) and filtered on a Celite pad. The pad was washed with DCM (100 mL), and the combined filtrate and washing were washed with water (400 mL) and brine (200 mL). The organic layer was dried (Na_2SO_4) and concentrated in vaccuo. The residue was purified by chromatography on silica eluting with a gradient of 0−50% EtOAc−hexane, and the appropriate fractions were combined and evaporated in vacuo to give an oil, which was triturated with cold pentane (2 × 50 mL). The resulting solid was collected by filtration, washed with cold pentane (50 mL) to give **36** (4.2 g, 36%) as an off-white solid: MS ES+ve *m*/*z* 384 $(M + H)^+$ (for ester **36**) and 302 $(M + H)^+$ (for the boronic acid **18ch**); ^{1}H NMR (CD_3OD, 400 MHz) 7.38 (1H, d, *J* 2.5 Hz), 7.20 (1H, d, *J* 2.5 Hz), 7.07 (1H, d, *J* 2.5 Hz), 6.05 (1H, s), 3.90−3.78 (4H, m), 3.22−3.19 (4H, m), 2.26 (3H, s), 2.24 (3H, s), 1.35 (12H, s). HRMS (ESI) calcd for calcd for $C_{15}H_{21}BN_3O_3$ 302.1670 (boronic acid **18ch**), found 302.1674.

Molecular Modeling. An $\alpha_v\beta_6$ homology model was generated using Molecular Operating Environment[61] (Chemical Computing Group) and the $\alpha_v\beta_3$ X-ray structure 1L5G[30] as template. During lead optimization, compounds were modeled into the binding site using Maestro[62] and Glide (Schrödinger software) and preferred docking poses were selected using criteria of favorable protein−ligand interactions, acceptable ligand geometry, good shape and surface complementarity with the $\alpha_v\beta_6$ receptor.

Pharmacokinetic Studies. All animal studies were ethically reviewed and carried out in accordance with Animals (Scientific Procedures) Act 1986 and the GSK Policy on the Care, Welfare and Treatment of Animals. Comprehensive experimental details for the studies described here are provided in the Supporting Information.

■ ASSOCIATED CONTENT

Supporting Information

The Supporting Information is available free of charge on the ACS Publications website at DOI: 10.1021/acs.jmedchem.8b00959.

(i) Biological data with standard deviations and *n*-numbers and SMILES of final compounds; (ii) further synthetic experimental procedures; (iii) a table of test compound purities; (iv) the LC/MS trace showing the purity of **28h**; (v) the DMPK experimental procedures; and (vi) files containing the details of the homology models used (PDF)

Molecular formula strings and some data (CSV)

Coordinates information for 4UM9 used for modeling (PDB)

DOI: 10.1021/acs.jmedchem.8b00959
J. Med. Chem. XXXX, XXX, XXX−XXX

Coordinates information for GSK3008348 used for modeling (PDB)

AUTHOR INFORMATION

Corresponding Author

*E-mail: simon.jf.macdonald@gsk.com. Phone: (+44)1438 790495. Fax: (+44)1438 768302.

ORCID

Panayiotis A. Procopiou: 0000-0001-5907-116X

Simon J. F. Macdonald: 0000-0002-4859-8246

Notes

The authors declare the following competing financial interest(s): Most of the authors are shareholders in GlaxoSmithKline.

ACKNOWLEDGMENTS

We thank Pan Procopiou for preparing the first draft of this paper, Sean Lynn and Stephen Richards for running the 600 MHz ^{1}H NMR spectra, Bill J. Leavens for collecting the HRMS data, Eric Hortense for the analytical HPLC on chiral stationary phase, Steve Jackson and Andy Knaggs for separation of diastereomers by preparative chiral HPLC, Ian B. Campbell, Daniel Clare, Eric Tse, Hans Cook, Benoit Rhone, Kayleigh Mercer, Richard Hatley, and Heather Barnett for synthetic assistance, Peter Marshall for the MALDI studies, Gianpaolo Bravi for modeling studies, and Tim Ritchie for assistance in preparing the selectivity bar charts. We also thank GVK Bio, a CRO in India who provided many intermediates for this work.

ABBREVIATIONS USED

BINAP, 2,2′-bis(diphenylphosphino)-1,1′-binaphthyl; IPF, idiopathic pulmonary fibrosis; $PdCl_2(dppf)\cdot CH_2Cl_2$, [1,1′-bis(diphenylphosphino)ferrocene]dichloropalladium(II), complex with dichloromethane; ICH, The International Conference on Harmonisation; IPA, isopropyl alcohol; $[Ir(COD)OMe]_2$, -di-μ-methoxobis(1,5-cyclooctadiene)diiridium(I); $Pd_2(dba)_3$, tris(dibenzylideneacetone)dipalladium(0);; LAP, latency associated peptide; LBF, liver blood flow; MDCK-MDR1, Madin−Darby canine kidney cells transfected with the human MDR1 gene;; MIDAS, metal ion dependent adhesion site; phosphSMAD2 or pSMAD2, phosphorylated intracellular signaling molecule Mothers Against Decapentaplegic homolog 2; RGD, arginine−glycine−aspartic acid; $[Rh(COD)Cl]_2$, 1,5-cyclooctadienerhodium(I) chloride dimer; SD, standard deviation; SDL, specificity determining loop; TBME, *tert*-butyl methyl ether; TGFβ1, transforming growth factor β1; XPhos, 2-dicyclohexylphosphino-2′,4′,6′-triisopropylbiphenyl

REFERENCES

(1) Buendía-Roldán, I.; Mejía, M.; Navarro, C.; Selman, M. Idiopathic pulmonary fibrosis: clinical behavior and aging associated comorbidites. *Respiratory Medicine* **2017**, *129*, 46−52.

(2) Hutchinson, J.; Fogarty, A.; Hubbard, R.; McKeever, T. Global incidence and mortality of idiopathic pulmonary fibrosis: a systematic review. *Eur. Respir. J.* **2015**, *46*, 795−806.

(3) Richeldi, L.; Collard, H. R.; Jones, M. G. Idiopathic pulmonary fibrosis. *Lancet* **2017**, *389*, 1941−1952.

(4) Datta, A.; Scotton, C. J.; Chambers, R. C. Novel therapeutic approaches for pulmonary fibrosis. *Br. J. Pharmacol.* **2011**, *163*, 141−172.

(5) Weill, D.; Benden, C.; Corris, P. A.; Dark, J. H.; Davis, R. D.; Keshavjee, S.; Lederer, D. J.; Mulligan, M. J.; Patterson, G. A.; Singer, L. G.; Snell, G. I.; Verleden, G. M.; Zamora, M. R.; Glanville, A. R. A consensus document for the selection of lung transplant candidates: 2014-an update from the pulmonary transplantation council of the international society for heart and lung transplantation. *J. Heart Lung Transpl.* **2015**, *34*, 1−15.

(6) Raghu, G.; Richeldi, L. Current approaches to the management of idiopathic pulmonary fibrosis. *Respiratory Medicine* **2017**, *129*, 24−30.

(7) Maher, T. M.; Inoue, Y.; Case, A. H.; Sakamoto, W.; Stowasser, S.; Wuyts, W. A. M30 Effect of dose reductions and/or interruptions on the efficacy of nintedanib in patients with idiopathic pulmonary fibrosis (IPF): subgroup analysis of the Inpulsis trials. *Thorax* **2017**, *72*, A253.

(8) Nanthakumar, C. B.; Hatley, R. J. D.; Lemma, S.; Gauldie, J.; Marshall, R. P.; Macdonald, S. J. F. Dissecting fibrosis: therapeutic insights from the small-molecule toolbox. *Nat. Rev. Drug Discovery* **2015**, *14*, 693−720.

(9) Barczyk, M.; Carracedo, S.; Gullberg, D. Integrins. *Cell Tissue Res.* **2010**, *339*, 269−280.

(10) Ley, K.; Rivera-Nieves, J.; Sandborn, W. J.; Shattil, S. Integrin-based therapeutics: biological basis, clinical use and new drugs. *Nat. Rev. Drug Discovery* **2016**, *15*, 173−183.

(11) Miller, L. M.; Pritchard, J. M.; Macdonald, S. J. F.; Jamieson, C.; Watson, A. J. B. Emergence of small-molecule non-RGD-mimetic inhibitors for RGD integrins. *J. Med. Chem.* **2017**, *60*, 3241−3251.

(12) Hatley, R. J. D.; Macdonald, S. J. F.; Slack, R. J.; Le, J.; Ludbrook, S. B.; Lukey, P. T. An av-RGD integrin inhibitor toolbox: drug discovery insight, challenges and opportunities. *Angew. Chem., Int. Ed.* **2018**, *57*, 3298−3321.

(13) Bandyopadhyay, A.; Raghavan, S. Defining the role of integrin $\alpha_v\beta_6$ in cancer. *Curr. Drug Targets* **2009**, *10*, 645−652.

(14) Prabhu, S.; Harris, F.; Lea, R.; Snape, T. J. Small-molecule clinical trial candidates for the treatment of glioma. *Drug Discovery Today* **2014**, *19*, 1298−1308.

(15) Sheldrake, H. M.; Patterson, L. H. Strategies to inhibit tumor associated integrin receptors: rationale for dual and multi-antagonists. *J. Med. Chem.* **2014**, *57*, 6301−6315.

(16) Cirkel, G. A.; Kerklaan, B. M.; Vanhoutte, F.; Der Aa, A. V.; Lorenzon, F.; Namour, F.; Pujuguet, P.; Darquenne, S.; De Vos, F. Y. F.; Snijders, T. J.; Voest, E. E.; Schellens, J. H. M.; Lolkema, M. P. A dose escalating phase I study of GLPG0187, a broad spectrum integrin receptor antagonist, in adult patients with progressive high-grade glioma and other advanced solid malignancies. *Invest. New Drugs* **2016**, *34*, 184−192.

(17) Hutchinson, J. H.; Halczenko, W.; Brashear, K. M.; Breslin, M. J.; Coleman, P. J.; Duong, L. T.; Fernandez-Metzler, C.; Gentile, M. A.; Fisher, J. E.; Hartman, G. D.; Huff, J. R.; Kimmel, D. B.; Leu, C.-T.; Meissner, R. S.; Merkle, K.; Nagy, R.; Pennypacker, B.; Perkins, J. J.; Prueksaritanont, T.; Rodan, G. A.; Varga, S. L.; Wesolowski, G. A.; Zartman, A. E.; Rodan, S. B.; Duggan, M. E. Nonpeptide $\alpha_v\beta_3$ antagonists. 8. In vitro and in vivo evaluation of a potent $\alpha_v\beta_3$ antagonist for the prevention and treatment of osteoporosis. *J. Med. Chem.* **2003**, *46*, 4790−4798.

(18) Meissner, R. S.; Perkins, J. J.; Duong, L. T.; Hartman, G. D.; Hoffman, W. F.; Huff, J. R.; Ihle, N. C.; Leu, C.-T.; Nagy, R. M.; Naylor-Olsen, A.; Rodan, G. A.; Rodan, S. B.; Whitman, D. B.; Wesolowski, G. A.; Duggan, M. E. Nonpeptide $\alpha_v\beta_3$ antagonists. Part 2: constrained glycyl amides derived from RGD tripeptide. *Bioorg. Med. Chem. Lett.* **2002**, *12*, 25−29.

(19) Coleman, P. J.; Askew, B. C.; Hutchinson, J. H.; Whitman, D. B.; Perkins, J. J.; Hartman, G. D.; Rodan, G. A.; Leu, C.-T.; Prueksaritanont, T.; Fernandez-Metzler, C.; Merkle, K. M.; Lynch, R.; Lynch, J. J.; Rodan, S. B.; Duggan, M. E. Non-peptide $\alpha_v\beta_3$ antagonists. Part 4: potent and orally bioavailable chain-shortened RGD mimetics. *Bioorg. Med. Chem. Lett.* **2002**, *12*, 2463−2465.

(20) Sheppard, D. The role of integrins in pulmonary fibrosis. *Eur. Respir. Rev.* **2008**, *17*, 157−162.

(21) Horan, G. S.; Wood, S.; Ona, V.; Li, D. J.; Lukashev, M. E.; Weinreb, P. H.; Simon, K. J.; Hahm, K.; Allaire, N. E.; Rinaldi, N. J.;

DOI: 10.1021/acs.jmedchem.8b00959
J. Med. Chem. XXXX, XXX, XXX−XXX

Goyal, J.; Feghali-Bostwick, C. A.; Matteson, E. L.; O'Hara, C.; Lafyatis, R.; Davis, G. S.; Huang, X.; Sheppard, D.; Violette, S. M. Partial inhibition of integrin $\alpha_v\beta_6$ prevents pulmonary fibrosis without exacerbating inflammation. *Am. J. Respir. Crit. Care Med.* **2008**, *177*, 56−65.
(22) Tatler, A. L.; Jenkins, G. TGFβ activation and lung fibrosis. *Proc. Am. Thorac. Soc.* **2012**, *9*, 130−136.
(23) Weinreb, P. H.; Simon, K. J.; Rayhorn, P.; Yang, W. J.; Leone, D. R.; Dolinski, B. M.; Pearse, B. R.; Yokota, Y.; Kawakatsu, H.; Atakilit, A.; Sheppard, D.; Violette, S. M. Function-blocking integrin $\alpha_v\beta_6$ monoclonal antibodies: distinct ligand-mimetic and non-ligand-mimetic classes. *J. Biol. Chem.* **2004**, *279*, 17875−17997.
(24) Miller, W. H.; Manley, P. J.; Cousins, R. D.; Erhard, K. F.; Heerding, D. A.; Kwon, C.; Ross, S. T.; Samanen, J. M.; Takata, D. T.; Uzinskas, I. N.; Yuan, C. C.; Haltiwanger, R. C.; Gress, C. J.; Lark, M. W.; Hwang, S. M.; James, I. E.; Rieman, D. J.; Willette, R. N.; Yue, T. L.; Azzarano, L. M.; Salyers, K. L.; Smith, B. R.; Ward, K. W.; Johanson, K. O.; Huffman, W. F. Phenylbutyrates as potent, orally bioavailable vitronectin receptor (integrin $\alpha_v\beta_3$) antagonists. *Bioorg. Med. Chem. Lett.* **2003**, *13*, 1483−1486.
(25) Adams, J.; Anderson, E. C.; Blackham, E. E.; Chiu, Y. W. R.; Clarke, T.; Eccles, N.; Gill, L. A.; Haye, J. J.; Haywood, H. T.; Hoenig, C. R.; Kausas, M.; Le, J.; Russell, H. L.; Smedley, C.; Tipping, W. J.; Tongue, T.; Wood, C. C.; Yeung, J.; Rowedder, J. E.; Fray, M. J.; McInally, T.; Macdonald, S. J. F. Structure activity relationships of αv integrin antagonists for pulmonary fibrosis by variation in aryl substituents. *ACS Med. Chem. Lett.* **2014**, *5*, 1207−1212.
(26) Maden, C. H.; Fairman, D.; Chalker, M.; Costa, M. J.; Fahy, W. A.; Garman, N.; Lukey, P. T.; Mant, T.; Parry, S.; Simpson, J. K.; slack, R. J.; Kendrick, S.; Marshall, R. P. Safety, tolerability and pharmacokinetics of GSK3008348, a novel integrin avb6 inhibitor in healthy participants. *Eur. J. Clin. Pharmacol.* **2018**, *74*, 701−709.
(27) Ohira, S. Methanolysis of dimethyl (1-diazo-2-oxopropyl)-phosphonate: generation of dimethyl (diazomethyl)phosphonate and reaction with carbonyl compounds. *Synth. Commun.* **1989**, *19*, 561−564.
(28) Davies, A. J.; Brands, K. M. J.; Cowden, C. J.; Dolling, U.-H.; Lieberman, D. R. An efficient one-pot synthesis of annulated pyridines utilising a directed *ortho*-metallation/transmetallation approach. *Tetrahedron Lett.* **2004**, *45*, 1721−1724.
(29) Procopiou, P. A.; Barrett, T. N.; Copley, R. C. B.; Tame, C. J. Determination of Absolute Configuration of two $\alpha_v\beta_6$ integrin inhibitors for the treatment of idiopathic pulmonary fibrosis and investigations on the asymmetric 1,4- addition of arylboronic acids to crotonate esters bearing a C4-oxygen substituent. *Tetrahedron: Asymmetry* **2017**, *28*, 1384−1393.
(30) Anderson, N. A.; Campbell, I. B.; Fallon, B. J.; Lynn, S. M.; Macdonald, S. J. F.; Pritchard, J. M.; Procopiou, P. A.; Sollis, S. L.; Thorp, L. R. Synthesis and determination of absolute configuration of a non-peptidic $\alpha_v\beta_6$ integrin antagonist for the treatment of idiopathic pulmonary fibrosis. *Org. Biomol. Chem.* **2016**, *14*, 5992−6009.
(31) Anderson, N. A.; Fallon, B. J.; Valverde, E.; Macdonald, S. J. F.; Pritchard, J. M.; Suckling, C. J.; Watson, A. J. B. Asymmetric rhodium-catalysed addition of arylboronic acids to acyclic unsaturated esters containing a basic γ-amino group. *Synlett* **2012**, *23*, 2817−2821.
(32) Trost, B. M.; Fullerton, T. J. New synthetic reactions. Allylic alkylation. *J. Am. Chem. Soc.* **1973**, *95*, 292−294.
(33) Schnyder, A.; Indolese, A. F.; Studer, M.; Blaser, H.-U. A new generation of air stable, highly active Pd complexes for C-C and C-N coupling reactions with aryl chlorides. *Angew. Chem., Int. Ed.* **2002**, *41*, 3668−3671.
(34) Maleczka, R. E., Jr.; Shi, F.; Holmes, D.; Smith, M. R., III. C-H Activation-borylation-oxidation: a one-pot unified route to meta-substituted phenols bearing ortho-/para-directing groups. *J. Am. Chem. Soc.* **2003**, *125*, 7792−7793.
(35) Cooper, A. E.; Ferguson, D.; Grime, K. Optimisation of DMPK by the inhaled route: challenges and approaches. *Curr. Drug Metab.* **2012**, *13*, 457−473.
(36) Allen, A.; Bareille, P. J.; Rousell, V. M. Fluticoasone furoate, a novel inhaled corticosteroid, demonstrates prolonged absorption kinetics in man compared with inhaled fluticasone propionate. *Clin. Pharmacokinet.* **2013**, *52*, 37−42.
(37) Procopiou, P. A.; Barrett, V. J.; Bevan, N. J.; Biggadike, K.; Box, P. C.; Butchers, P. R.; Coe, D. M.; Conroy, R.; Emmons, A.; Ford, A. J.; Holmes, D. S.; Horsley, H.; Kerr, F.; Li-Kwai-Cheung, A.-M.; Looker, B. E.; Mann, I. S.; McLay, I. M.; Morrison, V. S.; Mutch, P. J.; Smith, C. E.; Tomlin, P. Synthesis and structure−activity relationships of long-acting β2 adrenergic receptor agonists incorporating metabolic inactivation: An antedrug approach. *J. Med. Chem.* **2010**, *53*, 4522−4530.
(38) Rowedder, J. E.; Ludbrook, S. B.; Slack, R. J. Determining the true selectivity profile of á$_v$ integrin ligands using radioligand binding: applying an old solution to a new problem. *SLAS Discovery* **2017**, *22*, 962−973.
(39) The minimum discriminatory difference for the $\alpha_v\beta_6$ cell adhesion assay based on 95% confidence limits is just over 0.4.
(40) Gillie, D. J.; Novick, S. J.; Donovan, B. T.; Payne, L. A.; Townsend, C. Development of a high-throughput electrophysiological assay for the human ether-à-go-go related potassium channel hERG. *J. Pharmacol. Toxicol. Methods* **2013**, *67*, 33−44.
(41) Danker, T.; Möller, C. Early identification of hERG liability in drug discovery programs by automated patch clamp. *Front. Pharmacol.* **2014**, *5*, 1−11.
(42) Young, R. J.; Green, D. V. S.; Luscombe, C. N.; Hill, A. P. Getting physical in drug discovery II: the impact of chromatographic hydrophobicity measurements and aromaticity. *Drug Discovery Today* **2011**, *16*, 822−830.
(43) Waring, M. J. Lipophilicity in drug discovery. *Expert Opin. Drug Discovery* **2010**, *5*, 235−248.
(44) Ritchie, T. J.; Macdonald, S. J. F.; Peace, S.; Pickett, S. D.; Luscombe, C. N. The developability of heteroaromatic and heteroaliphatic rings − do some have a better pedigree as potential drug molecules than others? *MedChemComm* **2012**, 3, 1062−1069.
(45) Anderson, N. A.; Fallon, B. J.; Pritchard, J. M. Naphthyridine Derivatives Useful as Alpha V Beta 6 Integrin Antagonists. WO 154725, 2014.
(46) Anderson, N. A.; Campbell-Crawford, M. H. J.; Hancock, A. P.; Lemma, S.; Pritchard, J. M.; Procopiou, P. A.; Sollis, S. L. Preparation of Naphthyridines as Integrin Antagonists. WO 162570, 2017.
(47) Anderson, N. A.; Campbell, I. B.; Campbell-Crawford, M. H. J.; Hancock, A. P.; Lemma, S.; Macdonald, S. J. F.; Pritchard, J. M.; Procopiou, P. A. Naphthyridine Derivatives as Alpha V Beta 6 Integrin Antagonists for the Treatment of Fibrotic Diseases. WO 046230, 2016.
(48) Ritchie, T. J.; Macdonald, S. J. F. Heterocyclic replacements for benzene: Maximising ADME benefits by considering individual ring isomers. *Eur. J. Med. Chem.* **2016**, *124*, 1057−1068.
(49) Dong, X.; Zhao, B.; Iacob, R. E.; Zhu, J.; Koksal, A. C.; Lu, C.; Engen, J. R.; Springer, T. A. Force interacts with macromolecular structure in activation of TGF-β. *Nature* **2017**, *542*, 55−59.
(50) Xiong, J. P.; Stehle, T.; Zhang, R.; Joachimiak, A.; Frech, M.; Goodman, S. L.; Arnaout, M. A. Crystal structure of the extracellular segment of integrin alpha V beta 3 in complex with an Arg-Gly-Asp ligand. *Science* **2002**, *296*, 151−155.
(51) Dong, X.; Hudson, N. E.; Lu, C.; Springer, T. A. Structural determinants of integrin β-subunit specificity for latent TGF-β. *Nat. Struct. Mol. Biol.* **2014**, *21*, 1091−1097.
(52) Hall, E. R.; Bibby, L. I.; Slack, R. J. Characterisation of a novel, high affinity and selective $\alpha_v\beta_6$ integrin RGD-mimetic ligand. *Biochem. Pharmacol.* **2016**, *117*, 88−96.
(53) Slack, R. J.; Hafeji, M.; Rogers, R.; Ludbrook, S. B.; Marshall, J. F.; Flint, D. J.; Pyne, S.; Denyer, J. C. Pharmacological characterization of the $\alpha_v\beta_6$ integrin binding and internalization kinetics of the foot-and-mouth disease virus derived peptide A20FMDV2. *Pharmacology* **2016**, *97*, 114−125.
(54) John, A. E.; Graves, R. H.; Pun, T. K.; Vitulli, G.; Forty, E. J.; Mercer, P. F.; Morrell, J. L.; Barrett, J. W.; Hafeji, M.; Bibby, L. I.;

DOI: 10.1021/acs.jmedchem.8b00959
J. Med. Chem. XXXX, XXX, XXX−XXX

Gower, E.; Morrison, V. S.; Boyce, S. H.; Man, Y.; Anderson, N. A.; Fallon, B. J.; Pritchard, J. M.; Sollis, S. L.; Le, J.; Gudmann, N. S.; Leeming, D. J.; Flint, D. J.; Pyne, S.; Maher, T. M.; Fisher, A. J.; Chambers, R. C.; Lukey, P. T.; Marshall, R. P.; Jenkins, G. R.; Macdonald, S. J. F.; Slack, R. J. Discovery of a novel, inhaled small molecule $\alpha v\beta 6$ integrin inhibitor for idiopathic pulmonary fibrosis. *Sci. Transl. Med.*, submitted 2018.

(55) Slack, R. J.; John, A.; Forty, E.; Mercer, P.; Graves, R.; Pun, T.; Vitulli, G.; Gower, E.; Morrison, V.; Ludbrook, S.; Nanthakumar, C.; Anderson, N.; Procopiou, P.; Pritchard, J.; Budd, D.; Flint, D.; Pyne, S.; Denyer, J.; Marshall, J.; Fisher, A.; Chambers, R.; Jenkins, G.; Lukey, P.; Macdonald, S. J. F.; Marshall, R. P. P112 Discovery of a novel, high affinity, small molecule $\alpha v\beta 6$ inhibitor for the treatment of idiopathic pulmonary fibrosis. *QMJ* **2016**, *109*, S60.

(56) Gower, E.; Wilkinson, A.; Morrison, V.; Nanthakumar, C.; Slack, R. J. P109 High affinity engagement of the $\alpha v\beta 6$ integrin induces degradation: novel mechanisms for sustained inhibition of pro-fibrotic TGFβ activation. *QJM* **2016**, *109*, S59.

(57) Smith, D. A.; Di, L.; Kerns, E. H. The effect of plasma protein binding on in vivo efficacy: misconceptions in drug discovery. *Nat. Rev. Drug Discovery* **2010**, *9*, 929−939.

(58) It is now well established that P-gp is expressed and functionally active in human lung at both bronchial and alveolar epithelia levels. It has the potential to influence the kinetics of pulmonary absorption of its substrates, and the physicochemical relationships determining the significance of P-gp to absorption in the lung are different from those operative in the intestine. See the following: Price, D. F.; Luscombe, C. N.; Eddershaw, P. J.; Edwards, C. D.; Gumbleton, M. The differential absorption of a series of P-glycoprotein substrates in isolated perfused lungs from Mdr1a/1b genetic knockout mice can be attributed to distinct physico-chemical properties: an insight into predicting transporter-mediated, pulmonary specific disposition. *Pharm. Res.* **2017**, *34*, 2498−2516.

(59) *Assessment and Control of DNA Reactive (Mutagenic) Impurities in Pharmaceuticals to Limit Potential Carcinogenic Risk. Guidance for industry*; ICH Harmonised Guideline M7(R1); ICH, March 2018.

(60) *Guidance for Industry: Genotoxicity Testing and Data Interpretation for Pharmaceuticals Intended for Human Use*; ICH Harmonised Tripartite Guideline S2 (R1); ICH, November 2011.

(61) *Molecular Operating Environment (MOE)*, version 2013.08; Chemical Computing Group Inc. (1010 Sherbooke St. West, Suite No. 910, Montreal, QC, Canada, H3A 2R7), 2017.

(62) Friesner, R. A.; Murphy, R. B.; Repasky, M. P.; Frye, L. L.; Greenwood, J. R.; Halgren, T. A.; Sanschagrin, P. C.; Mainz, D. T. Extra precision Glide: docking and scoring incorporating a model of hydrophobic enclosure for protein-ligand complexes. *J. Med. Chem.* **2006**, *49*, 6177−6196.

DOI: 10.1021/acs.jmedchem.8b00959
J. Med. Chem. XXXX, XXX, XXX−XXX